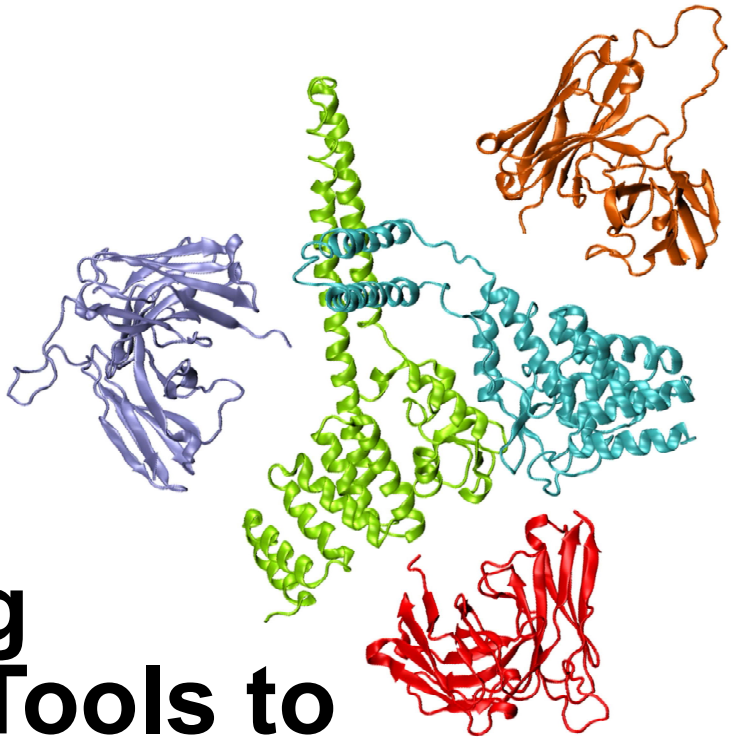

Developing Synthetic Tools to Image and Modulate the Activity of Carboxyl terminus of Hsc70-Interacting Protein (CHIP)

Mariana Cristina De Sá Cardoso Dos Santos
Mestrado em Bioquímica
Departamento de Química e Bioquímica
2015

Orientadores
Ted Hupp, Chair in Experimental Cancer Research,
University of Edinburgh

Kathryn Ball, Personal Chair of Biochemistry and Cell Signalling,
University of Edinburgh

Coorientador
Lucília Saraiva, Professora Auxiliar, Faculdade de Farmácia

U.PORTO

INSTITUTO DE CIÊNCIAS BIOMÉDICAS ABEL SALAZAR
UNIVERSIDADE DO PORTO

U.PORTO

FACULDADE DE CIÊNCIAS
UNIVERSIDADE DO PORTO

Todas as correções determinadas pelo júri, e só essas, foram efetuadas.

O Presidente do Júri,

Porto, _____/_____/_____

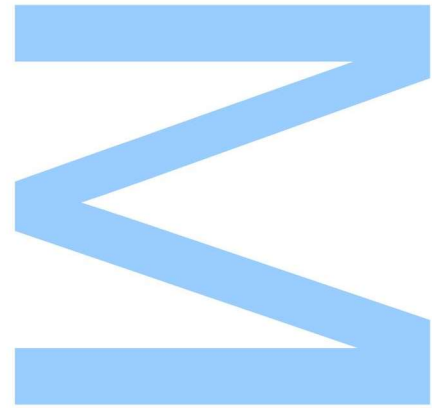

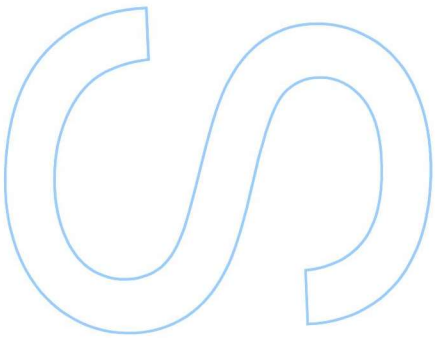

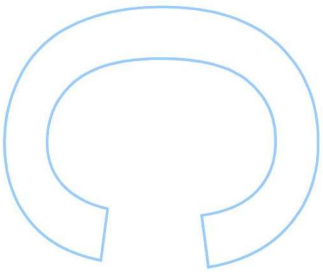

The experimental work described in this thesis has been carried out at the Edinburgh Cancer Research Centre (ECRC) of the Institute of Genetics and Molecular Medicine at the University of Edinburgh in the framework of the ERASMUS+ programme.

The image presented in the cover includes the crystal structure of the CHIP U-box E3 ubiquitin ligase (PDB ID:2C2L) (Zhang et al., 2005) and the structures of the scFv 7A, 7G and 11F predicted by homology from the primary structure sequence using the *Raptor X* web server (Kallberg et al., 2012). The image was compiled and coloured using the graphic software *Visual Molecular Dynamics* (VMD) (Humphrey et al., 1996).

ACKNOWLEDGMENTS

This thesis would not have been possible without the help and support of a lot of people. Near or far all the people I will mention next played a part on getting me through the amazing year that made this work come to life.

First of all I would like to thank my supervisors in Edinburgh, Ted Hupp and Kathryn Ball. I cannot thank you enough for accepting me in your group and giving me an opportunity, when I was just a student with very little lab experience; for supporting me and my work throughout the amazing nine months I spent in Edinburgh. I want to thank Ted for your inspirational and never ending enthusiasm for science and your ideas and advice. To Kathryn, a simple thank you would be too little to express how grateful I am for all that you've taught me, for all your invaluable help, guidance and support in this amazing journey. You always had a kind word and a hundred new ideas to make up for the ones that didn't work.

I would also like to thank everyone in the TRH/KLB lab; your support, friendship and help made the time I spent in the lab so fun and enjoyable that it didn't even feel like work. You all made feel welcome and helped me grown as a researcher and as a person. It was an honour to meet and work with such a special and brilliant group of people. I'd like to direct a special mention to Euan Murray for all his help with the Phage Display technology. And a very big thank you to Jia and Jonas, my partners on 'Team CHIP' and 'Team α-synuclein' respectively; thank you for your patience and all you've taught me, for always being willing to discuss my results and sharing your time, knowledge, opinions (and snacks) with me and for being such amazing friends.

My next thank you goes to my friend Lutske. You were my biggest supporter and friend in my first few months in Edinburgh and there is no way I'll ever be able to thank you for your support and incredible colourfulness that made my days so much better, when our situation was not ideal.

I'd like to dedicate a special mention to all my Erasmus friends, particularly Beccy, Marta, Francesca and Massimo, with whom I learned so much and had so much fun.

Now it's time to thank all those who helped me, even though they were far away. My first thank you is for my supervisor in Portugal, Professor Lucília Saraiva for all her help and support and for always believing in me and my work and also her research group from the Faculty of Pharmacy at the University of Porto who always made me feel welcome and part of the fold whenever I went back to Portugal.

Next, I want to thank my friends that I missed so much but from whom I never felt distant because as promised you always kept in touch and kept me updated on all that was going on back home. Ivânia, Paivinha, Fátima, Mariana, Ana Rita, Tânia, Abigail,

Sofia and my fellow Erasmus adventurers Fernando and Pedro, thank you all for your support and friendship that from so many miles away carried me through these months I spent in Edinburgh. You were always willing to congratulate me on my victories and comfort me on my setbacks and share yours with me and for that I am so very thankful. I'd like to direct a special thank you to Marina who besides all that was mentioned above also helped me through the writing of this work, pushing me to write, even when I didn't feel like it, and always do my best.

Last but definitely not less important I would like to thank my family. You were and always are my biggest supporters. Your love and the confidence you have in me always makes me want to fight and work harder to be great and one day make a difference. Everything I am, I owe it to you for all the great experiences that you provided me with and everything you taught me. I would like to direct a special thank you to my parents and my brother who were the ones who truly made this possible, for always being there, for loving me and always lifting me up to help me overcome all the obstacles that came my way during this last year and always.

ABSTRACT

The C-terminus of the Hsc70 Interacting Protein (CHIP) is a 35kDa homodimeric quality control E3 Ubiquitin ligase that occupies a very central position in the maintenance of cell homeostasis due to its role in the preservation of the integrity of the proteome. CHIP acts as the bridge between the chaperones network and the ubiquitin/proteasome pathway due to its functions as both a co-chaperone for heat shock proteins and as an E3 ligase.

Although CHIP's role in several pathologies such as Alzheimer's, Parkinson and Cancer has been established little is still known about this protein and the mechanisms that regulate it are not yet well understood.

In this study, a canine scFv antibody library was screened against wild type CHIP and the CHIP TPR mutant K30A with the goal of selecting scFvs that could then be used to image and modulate CHIP's activity.

Four different clones were selected by Phage Display technology, purified and characterized according to their affinity for the targets and their activity was tested in *in vitro* ubiquitination assays. The scFv fragments were shown to inhibit CHIP's ubiquitination of α-synuclein but not CHIP's autoubiquitination or p53 ubiquitination, suggesting that different intrinsic mechanics may be at play. Additionally, CHIP appeared to induce the formation of α-synuclein gel-excluding bands which have been predicted to be either α-synuclein aggregates or refolded α-synuclein.

This project has shown that scFvs can be an interesting biological tool that can not only be used to design new detection strategies or for possible future therapeutic applications but also to produce a better understanding of the molecular dynamics and mechanisms that regulate CHIP through the modulation of its activity.

Keywords: CHIP; Phage Display; ScFv; Ubiquitination; α-synuclein

RESUMO

C-terminus of the Hsc70 Interacting Protein (CHIP) é uma enzima E3 homodimérica de 35kDa com uma função relevante na manutenção da homeostasia celular devido ao seu envolvimento na preservação da integridade do proteassoma. A CHIP funciona como ponte entre a rede de chaperones e a via proteolítica dependente de ubiquitina/proteassoma devido às suas funções como co-chaperone de proteinas de choque térmico (Hsp) e como ligase de ubiquitina E3.

Apesar do envolvimento da CHIP em várias patologias como a Doença de Alzheimer, Parkinson ou cancro já ser bem reconhecido, ainda são desconhecidos muitos dos mecanismos moleculares que determinam e regulam a atividade desta proteína.

Neste estudo, uma biblioteca canina de anticorpos scFv foi rastreada contra a CHIP e a sua mutante K30A, com o objetivo de selecionar scFvs que pudessem ser usados para a deteção e modulação da atividade da CHIP.

Quatro scFv clones diferentes foram selecionados através da tecnologia de *Phage Display*, purificados e caracterizados de acordo com a sua afinidade para os alvos. Adicionalmente a sua atividade *in vitro* foi testada recorrendo-se a ensaios de ubiquitinação.

Os resultados obtidos demonstraram que estes fragmentos scFv eram capazes de inibir a ubiquitinação da α-sinucleina pela CHIP, mas não a auto-ubiquitinação da CHIP ou a ubiquitinção da p53. Estes resultados sugerem o envolvimento de diferentes mecanismos nestes processos de ubiquitinação pela CHIP.

Adicionalmente demonstrou-se também que a CHIP parece induzir a formação de bandas de α-sinucleína que ficam retidas no gel de concentração, as quais poderão ser agregados ou ‘refolded’ α-sinucleína.

Neste projeto foi possivel mostrar que os anticorpos scFv podem ser uma ferramenta biológica relevante não só para desenhar novas estratégias de deteção ou possíveis terapias, mas também para estudar as dinâmicas moleculares e os mecanismos que regulam a CHIP através da modulação da sua atividade.

Palavras-Chave: CHIP; ‘Phage Display’; ScFv; Ubiquitinação; α-sinucleína

CONTENTS

TABLES

FIGURES

ABBREVIATIONS

AAV - Adeno-associated virus

ABL - Abelson murine leukemia viral oncogene homolog 1

BAG - BCL2-Associated Athanogene

BiTE - Bispecific T-cell Engager

BSA - Bovine Serum Albumine

CD19 - Cluster of Differentiation 19

Cdk5 - Cell division protein kinase 5

CDR Complementary Determining Region

CFTR - Cystic fibrosis transmembrane conductance regulator

C_H - Constant Variable Chain

CHIP - Carboxyl-terminus of Hsc70-Interacting Protein

C_L – Constant Light Chain

CXCR2 - C-X-C chemokine receptor type 2

ECL - Enhanced chemiluminescence

EGFR – Epidermal Growth Factor Receptor

ELISA - Enzyme Linked Imunnosorbent Assay

EMMPRIN - Extracellular Matrix Metalloproteinase Inducer

ER – Endoplasmic Reticulum

ERAD – ER Associated Degradation

ERK – Extracellular-signal Regulated Kinases

Fab - Fragment Antigen Binding

Fc - fragment crystallisable

Fv - Fragment Variable

GRP78 – Glucose Regulated Protein 78

HECT - homologous to E6-associated protein carboxyl terminus

HER2 - human epidermal growth factor receptor 2

HIF-1 - Hypoxia-Inducible Factor-1

HRP - Horseradish Peroxidase

Hsc – Heat Shock cognate

Hsp - Heat shock protein

IPTG - Isopropyl β-D-1-thiogalactopyranoside

IRF 1 - Interferon Regulatory factor 1

LB - Lysogeny broth

mAbs - Monoclonal Antibodies

MT1-MMP - Membrane-Type 1 Matrix Metalloproteinase

Pael-R - Parkin-associated endothelin receptor-like receptor

PBS - Phosphate-Buffered Saline

PBST - Phosphate-Buffered Saline/Tween

PCR - Polymerase Chain Reaction

PEG – Polyethylene Glycol

PTEN - Phosphatase and Tensin homolog

rAb – Recombinant Antibody

RING – Really Interesting New Protein

RIT - Recombinant Immunotoxin

RNAi - Interference RNA

SCF - S-phase kinase-associated protein 1, Cullin, F-box containing complex

scFv - Single Chain Fragment Variable

ScFv - single chain variable fragment

siRNA – silencing RNA

tAIF - Truncated Apoptosis-inducing factor

TPR - tetratricopeptide repeat

V_H - Variable Heavy Chain

V_HH - camelid heavy-chain antibody

V_L - Variable Light Chain

V-NAR - variable region of new or nurse shark antigen receptor

WT – Wild Type

I. INTRODUCTION

1. The Rise of Recombinant Antibodies

As a fundamental part of the immune system, antibodies, also known as immunoglobulins (Igs), are an effective security system against pathogenic organisms or toxins that threaten our body due to their ability to correctly find almost any target antigen and elicit a neutralization response from the host organism (Murphy et al., 2012). As such they are the best "search engines" to detect very small amounts of target molecules, which makes them one of the most used tools in research laboratories all over the world. Besides their broad use in research techniques, new recombinant technologies have facilitated antibody engineering, potentiating their use in diagnostics and as therapeutics for cancer, infectious and inflammatory diseases (Chames et al., 2009).

1.1. General Antibody Structure

IgG is a bivalent, Y-shaped antibody, with a well-established structure (Figure 1) and the most abundant antibody in human serum. It is also the most common format for antibodies in diagnostics and therapeutics. The variable regions determine the specificity, diversity and affinity of the antigen binding while the constant domains mediate the antibody structure, half-life and effector functions. Within each variable domain of the light and heavy chains are three hypervariable regions, also known as complementary determining regions (CDRs), which form loops and exhibit high sequence variability, being predominantly responsible for antigen recognition. The rest of the V_L and V_H domains, denominated framework regions, are less variable and act as a platform to support the CDR loops (Murphy et al., 2012).

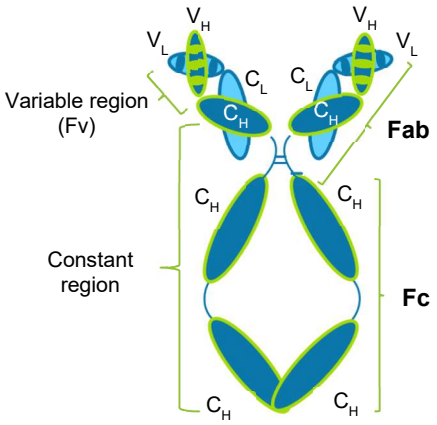

Figure 1. Basic Structure of the IgG molecule.

IgG structure comprises two large heavy chains and two smaller light chains. Each light chain presents one variable domain (V_L) and one constant domain (C_L) while the heavy chains contain one variable domain (V_H) and three constant domains (C_H). The constant region is coloured blue and the variable regions are designed with stripes representing the CDRs.

However this structure is sometimes unattractive for certain applications, due to the effects induced by the Fc domain. For example, unwanted activation of the effector functions can lead to cytokine release mediated toxicity and a long serum half-life is particularly undesirable in imaging applications, where rapid clearance is required in order to improve contrast (Holliger and Hudson, 2005).

Smaller antibody fragments were then generated to overcome the limitations of monoclonal antibodies (mAbs). Initially, this was accomplished by removing the Fc domain using proteolytic treatments with enzymes such as papain or pepsin, yielding Fab and $F(ab')_2$ fragments, respectively (Porter, 1959; Nisonoff et al., 1960). Inbar and colleagues were able to obtain a Fv fragment by peptic digestion of a mouse IgA-myeloma (Inbar et al., 1972) however the development of general procedures for Fv isolation was met with limited success (Kakimoto and Onoue, 1974; Sharon and Givol, 1976; Lin and Putnam, 1978; Reth et al., 1979; Sen and Beychok, 1986) and Fab antibodies persisted as the smallest fragment used for biomedical purposes. Later, advances in recombinant DNA technology and antibody engineering led the way to the development of a large variety of recombinant antibody (rAb) fragments with unlimited potential for research, diagnostics and therapy.

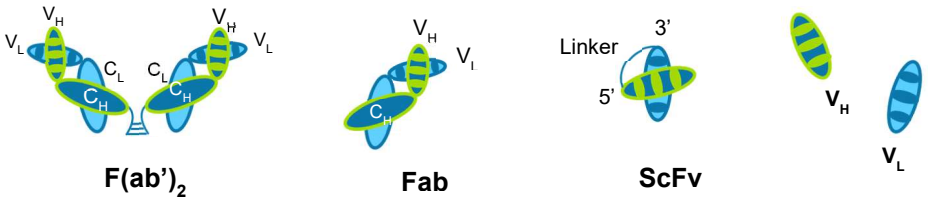

Figure 2. Schematic representation of proteolysis and engineered rAb fragments.

Among these fragments can be included Fab, scFv (single chain variable fragment), V-domain molecules (Figure 2) as well as camelid V_HH and shark V-NAR fragments. Compared to mAbs, these minimized antibodies can retain target specificity while presenting several advantages such as a smaller size and reduced immunogenicity, since they lack the Fc domain; better tissue penetration, rapid blood clearance and lower retention time in nontarget tissue, which can be quite beneficial for the purposes of radiotherapy and diagnostics. These and other properties can be tailored and manipulated to better suit the future application of the fragments (Holliger and Hudson, 2005). The rAb fragments can also be easily and cost-effectively cloned and expressed in large quantities in bacterial (Skerra and Pluckthun, 1988), plant (Galeffi et al., 2006), insect (Choo et al., 2002), mammalian and yeast cells (Ho et al., 2006), which makes them more economically viable.

1.2. ScFvs and derived multimeric complexes

ScFv fragments represent the smallest functional V_H-V_L domains capable of high-affinity binding to the antigen and were first developed by Huston and co-workers (Huston

et al., 1988) and immediately followed by Whitlow and his team (Bird et al., 1988). Nowadays, scFvs are the most popular rAb fragment due to their versatility.

Antibodies in the format of scFv are proteins with a molecular weight varying from 26 to 30 kDa that have the ability to bind to the target with identical affinity to that of the parental mAb (Bird et al., 1988) and consist of one V_H and one V_L chain connected by a flexible peptide linker (Maynard and Georgiou, 2000; Monnier et al., 2013).

Currently, the most used linkers include sections of glycine and serine residues for flexibility and Glutamic acid and lysine charged residues to improve solubility (Whitlow et al., 1993). Generally, these sequences are 15 to 20 amino acids long, as scFvs joined by a linker with less than 12 amino acids cannot fold into a functional Fv domain (Holliger et al., 1993) and should maintain an hydrophilic nature to keep them from interposing within or between the variable domains during folding of the scFv (Argos, 1990). The variable regions can be associated in either V_L-linker-V_H or V_H-linker-V_L orientation, but the latter is the most common. This factor deserves some attention as the orientation can impact scFv stability, binding to the antigen (Desplancq et al., 1994) and expression efficiency (Merk et al., 1999).

As scFv fragments are small and bind monovalently to their target they often present low functional affinity (also termed avidity) and a short *in vivo* half-life (Fitch et al., 1999; Mayer et al., 1999). While these properties can be useful for some imaging diagnostic techniques, for example, they can compromise the success of these molecules as therapeutics agents as these may require higher retention times on the target antigen or engagement of multiple receptors in order to activate signal transduction and/or apoptosis (Teeling et al., 2004; Linsley, 2005). In order to overcome this problem while maintaining optimal size for tissue penetration, scFv antibodies are engineered into different types of multimeric complexes for greater binding avidities and better pharmacokinetic properties (Goel et al., 2000; May et al., 2012).

Among the above mentioned complexes it is possible to find minibodies, diabodies, triabodies, tetrabodies and bispecific scFv fragments (Figure 3).

Diabodies, triabodies and tetrabodies are noncovalent molecules that assemble due to short linker lengths. ScFv fragments with linkers of three to twelve amino acids will have the tendency to dimerize, as the V_H chain will associate with the V_L chain of another scFv forming a diabody (~60kDa) (Holliger et al., 1993). Decreasing the linker length to three or less amino acids will induce the scFv association into triabodies (~90kDa) (Iliades et al., 1997) or tetrabodies (~120kDa) (Dolezal et al., 2003).

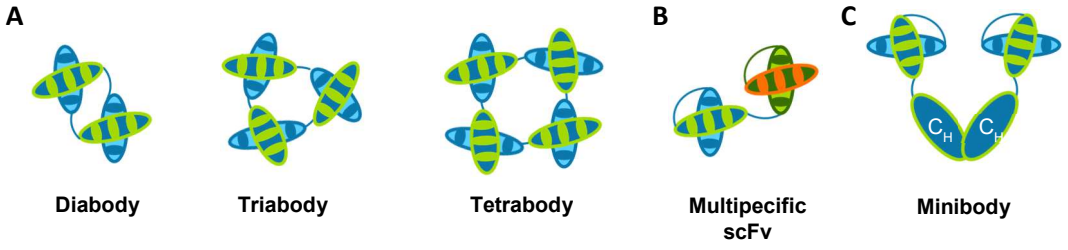

Figure 3. Multimeric formats of scFv.

Several complexes with tailored valences and specificities can be engineered using scFvs as building blocks. Here are represented examples of several categories of multimeric scFv formats. **A**. Diabodies, triabodies and tetrabodies can be obtained by assembling two, three or four, respectively, scFvs, for an increase in valency. There is also the possibility of engineering these antibody formats for increased specificity (bispecific, trispecific and tetraspecific) by combining scFvs selected for different antigens. **B**. Multi- or bispecif scFvs combine scFvs with different antigenic targets. **C.** Minibody assembled by combining scFvs with two IgG's constant domains.

Multispecific scFv antibodies can be developed by combining two or more scFvs with different antigenic targets, enhancing target selectivity and allowing the interaction with multiple epitopes within the same molecule or in different targets (Neri et al., 1995; Coloma and Morrison, 1997).

Minibodies consist of multivalent antibody fragments that have been covalently linked to self-assembling proteins, for example, amphiphilic helix bundles and leucine zippers (Pack and Pluckthun, 1992), IgG constant domains (Hu et al., 1996) or Fc-regions (Li et al., 2000); tetravalent molecules were achieved by covalent linkage with homomultimers such as streptavidin (Kipriyanov et al., 1995; Kipriyanov et al., 1996; Cloutier et al., 2000) or the multimerization domain of p53 (Rheinnecker et al., 1996; Liu et al., 2007) and assessed for pretargeted immunotherapy (Schultz et al., 2000; Goshorn et al., 2001; Lin et al., 2006) and biotinylated drug delivery (Wang et al., 2007).

ScFvs were also engineered into bifunctional fragments through conjugation or attachment to toxins (Chaudhary et al., 1989) and radionuclides (Kuan et al., 1999) mostly for cancer therapy, liposomes (Laukkanen et al., 1994) and enzymes (Sharma et al., 2005) for improved drug delivery, quantum dots (Wang et al., 2008) for imaging, viruses (Nakamura et al., 2004) for gene therapy, and cytokines (Halin et al., 2002) or chemokines (Guo et al., 2004) for immunotherapy.

1.3. From the bench to the frontline: current applications of scFvs

The improvement of methodologies that allow for the development of scFv antibodies and the advantages they present over conventional mAbs has potentiated the use of these fragments in very different, and sometimes complimentary, applications that

range from research to therapeutics and *in vivo* imaging. The contribution of scFvs and its development to these areas and recent examples will be detailed below.

ScFv fragments have become an increasingly useful tool in the study of protein functions and their molecular mechanisms, particularly when only a domain of the protein needs to be studied.

RNAi technology has been used routinely for the purpose of studying protein function but as it down regulates the expression of the whole protein it is unhelpful when the aim is to focus on specific domains. Moreover, the use of this technology *in vivo* has elicited several problems regarding delivery to the target tissue and consequently off-target toxicity issues (Aagaard and Rossi, 2007). ScFvs, on the other hand, can be selected specifically for different protein domains and for different epitopes in those domains as was the case of a study that reported the development of scFv fragments that targeted different epitopes of the G-protein coupled receptor CXCR2 as allosteric antagonists and showed ligand-dependent differences in functional assays (Rossant et al., 2014).

These antibody fragments are also becoming a strategic tool to study the importance of individual domains in the understanding of the general mechanism of action of a protein and its loss of function. Murphy and colleagues engineered a scFv capable of inhibiting the activity of MT1-MMP, a pericellular protease involved in tumour cell invasion and angiogenesis, by binding to a non-catalytic domain. Also this study presents a potential novel approach to inhibit proteinases by targeting sites outside the catalytic domain (Basu et al., 2012). Another study dissected the activity of Pax6, a homeodomain transcription factor, in the migration of oligodendrocyte precursor cells, using a scFv against the extracellular domain of Pax6 that lead to loss of function (Di Lullo et al., 2011). A plasmid carrying the scFv was electroporated in the neural tube and the scFv was able to neutralize the extracellular domain emphasizing its involvement in the process being studied.

A recent report elucidated the role of EMMPRIN (extracellular matrix metalloproteinase inducer) down-regulation in the promotion of apoptosis through the mitochondrial pathway by intracellular acidosis via intracellular expression of a scFv using a chimeric adenoviral vector (Thammasit et al., 2015). This highlights another advantage of scFvs against RNAi technology as scFvs can be delivered by a viral vector, avoiding the need for multiple administrations and ensuring maintenance of antibody concentration to sustain silencing.

As has been shown scFvs can be used to study protein and domain functions in both *in vitro* and *in vivo* studies. Moreover studies of this nature can also lead to new therapeutic targets and reveal molecules with therapeutic potential.

Therapy is perhaps the leading driver for the great improvements registered in scFv development, in the last few years, especially cancer therapy.

ScFvs present several properties that are important in cancer therapy such as the ability to specifically recognize markers expressed in tumour cells and a reduced size for better and more even tissue penetration. A smaller size also means faster clearance rate and while that can be beneficial when scFvs are coupled with drugs or toxins, allowing for a lower exposure for healthy tissue, it also compromises the ability of the scFv to concentrate in the tumour when they're not conjugated. As was already discussed above, this problem was overcome by engineering multimeric scFv complexes.

ScFv-based tumour therapy involves targeting specific markers in cancer cells and neutralizing the protein, delivering a therapeutic entity such as a toxin, a drug or siRNA, or initiate an immune response.

A scFv derived format that has seen great approval and development in the area of cancer immunotherapy are BiTEs (Bispecific T-cell Engagers) (Figure 4). Recently the first BiTE fragment, Blinatumomab (Amgen), was approved by the FDA for the treatment of refractory Philadelphia chromosome–negative acute lymphoblastic leukemia. This antibody redirects unstimulated primary human T cells towards CD19-positive lymphoma cells but presents the disadvantage of requiring continuous IV infusion due to its low molecular weight. Concurrently some more bispecific antibodies are now undergoing clinical trials, several are also BiTEs, and the group also includes tetravalent bispecific antibodies that should not require such a frequent administration as blinatumomab (Sheridan, 2015; Wu et al., 2015).

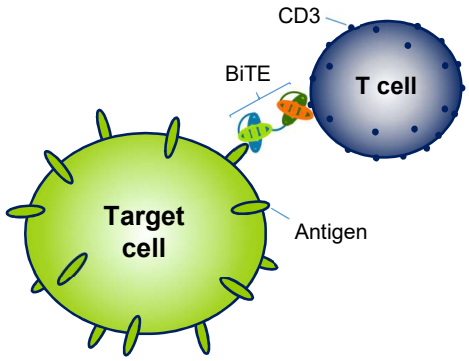

Figure 4. BiTE.

BiTEs are bispecific diabodies, in which one of the scFv fragments is specific for CD3, the signal transduction element of the T-cell receptor (TCR), while the other engages with a protein found at the surface of target cells. This forms a link between the target cell and the T cell which will release cytotoxic proteins, despite the absence of MHC I or co-stimulatory molecules, triggering apoptosis of the target cell. This imitates physiological events registered during T cell attacks (Wu et al., 2015).

Another area being developed in scFv-mediated cancer therapy are recombinant immunotoxins (RITs) in which scFv are used to direct cytotoxic drugs to cancer cells. This is achieved by replacing the cell binding domain of Pseudomonas exotoxin A with a scFv specific for the desired antigen (Liu et al., 2012). Several immunotoxins are currently undergoing clinical trials such as SSP1 which is being evaluated in combination with chemotherapy for treatment of malignant pleural mesothelioma (Hassan et al., 2014) and moxetumomab pasudotox for advanced hairy cell leukemia (Kreitman et al., 2012) which is in a phase III clinical trial. At the same time more immunotoxins are being investigated

as novel EGFR-specific immunotoxins using scFvs derived from already approved mAb therapies (panitumumab and cetuximab) (Niesen et al., 2015) .

Neurodegenerative diseases have also applied scFvs to attempt to generate therapies which was possible because scFvs are capable of crossing the blood brain barrier, even when they are administered peripherally, and can be overexpressed *in vivo*, allowing for prolonged therapy without repeated injections (Robert and Wark, 2012).

For example, in Alzheimer's disease, anti-Aβ scFv, overexpressed via AAV (adeno-associated virus) delivered by intracranial injection, have been shown to reduce amyloid plaques in mice and were still detectable in the brain without causing neurotoxicity (Ryan et al., 2010). Less invasive administration routes were also studied, namely intramuscular (Wang et al., 2010; Yang et al., 2013) and intranasal (Cattepoel et al., 2011); both were successful and lead to reduction of Aβ accumulation. A more recent study reported scFvs that bind toxic oligomeric but not monomeric or fibrillar tau and were capable of detecting it in earlier stages than usual, demonstrating potential for biomarker development (Tian et al., 2015). Another study demonstrated the *in vivo* effects of a pan-amyloid specific scFv antibody that mitigated memory deficits and brain amyloid load in mice with Alzheimer' Disease (Zhao et al., 2014).

In vivo imaging is another area that was has been improved by the use of scFvs especially regarding diagnostic applications such as tumour detection. The low molecular weight of scFvs allows them to be coupled to radionuclei, quantum dots and nanoparticles while maintaining the necessary properties for *in vivo* imaging. Among these properties are high affinity for the target, deep tissue penetration and a fast clearance rate. As such the scFv format provides an ideal non-invasive tool to detect and analyse the expression of a specific target *in vivo*.

For example, a scFv fragment specific for GRP78, a protein important for cell proliferation and angiogenesis, was linked to quantum dots and delivered in a xenograft mouse model. The complex quantum dot-scFv allowed for easy visualization of the target *in vivo*. Additionally it was also able to inhibit breast tumour growth (Xu et al., 2012).

Quantum dots were also conjugated to anti-tumour scFvs specific for the oncomarkers, HER1/EGFR and HER2/neu, forming self-assembling fluorescent complexes with the target that enabled visualization of cancer cells *in vitro* (Zdobnova et al., 2012).

Magnetic resonance imaging is an emerging field in the application of scFv fragments as it sensitivity has been shown to improve by linking scFv antibodies with supramagnetic iron oxide nanoparticles (SPIONs). In tumour imaging, these particles

provide a clearer contrast between healthy and cancer cells due to different uptake levels and adding scFv allows targeting of specific cells (Vigor et al., 2010).

Another promising imaging modality that has already adopted the scFv format is Photoaccoustic which also employs iron oxide nanoparticles. In this case, the nanoparticles were conjugated with an anti-HER2 scFv and used to image HER2-positive tumours (Kanazaki et al., 2015).

Since they were introduced, scFvs have become progressively more applicable in research laboratories, diagnostic and therapeutic applications. As this format of fragments continues to evolve and its uses become more widely acknowledged it is expected that it will also become more relevant in the progress of all the areas mentioned above, but more particularly in therapy.

2. Engineering scFv by Phage Display Technology

Conventionally, scFv antibodies were produced from hybridoma cells acquired from immunized animals by amplification of the VH and VL domains from mRNA and connecting them by a polylinker followed by insertion in the choice vector (Huston et al., 1988). However, lately, this technology has been surpassed by *in vitro* molecular displaying technologies due to their adaptability to high throughput formats not to mention the ease of manipulation to optimize scFv properties in order to produce a pool of varied and highly functional antibodies (Bradbury et al., 2011).

Three different molecular displays from which scFv can be selected and affinity matured have been reported, namely phage-display (McCafferty et al., 1990), ribosome display (Hanes and Pluckthun, 1997) and cell surface display (Francisco et al., 1993; Boder and Wittrup, 1997). All three formats share the same basic principle as molecular display libraries, created by cloning a diverse collection of rAb genes, are screened for target antigen binding and the resulting enriched pools are amplified after each round of selection with the target. After a few selection rounds the polyclonal pools are screened for antigen reactivity.

2.1. Molecular Display Libraries

Antibody diversity results from somatic recombination in B lymphocytes through a combination of three different gene segments, V, D and J. Depending on the source of the variable region genes, four different types of molecular display libraries can be built.

Immune libraries derive from immunoglobulin genes of lymphocytes from immunized animals (Clackson et al., 1991) or naturally immunized (Jacobin et al., 2002) or infected, humans (Burton et al., 1991). These libraries have been constructed from various species, besides humans, including mouse, chicken, rabbit and camel (Hoogenboom et al., 1998). Despite being antigen-specific and enriched in affinity matured clones they also present several disadvantages such as the need to create a new library for each antigen, the time required for immunizations and the unpredictability of the immune response (Azzazy and Highsmith, 2002).

Naïve, synthetic and semi-synthetic libraries are 'single pot' repertories, resulting from non-immunized donors and are antigen independent, consequently they represent a source of antibodies against a diverse assortment of antigens including self, toxic and non-immunogenic antigens (Marks et al., 1991; Griffiths et al., 1993; Vaughan et al., 1996).

Naïve libraries offer the possibility to select antibodies of desired specificity and high affinity without immunization being necessary (Burton et al., 1991). Genes responsible for the variable domain are obtained through B-cell mRNA amplification using oligonucleotides specific for the V_L and V_H families. The heavy and light chains are then randomly combined and cloned to create a combinatorial scFv library. This procedure gives access to germline antibodies, this is, antibodies that have yet to be exposed to antigens, however the frequency of those antibodies is dependent on the source of the B-cells (Marks et al., 1991).

Synthetic libraries result from *in vitro* assembly of V, D and J gene segments. Assembly of V-genes artificially allows for introduction of diversity using PCR techniques and degenerate primers to randomize CDR regions (Hoogenboom and Winter, 1992). The heavy chain CDR3 has been the main target of these modifications in synthetic repertoires. Examples of synthetic libraries include the Tomlinson I and J libraries (de Wildt et al., 2000; Goletz et al., 2002) and the human combinatorial antibody libraries (HuCAL) for scFv (HuCAL-scFv) (Knappik et al., 2000) and Fab fragments (HuCAL-Fab1, HuCAL GOLD, HuCAL PLATINUM) (Rauchenberger et al., 2003; Rothe et al., 2008; Prassler et al., 2011)

Semi-synthetic libraries combine elements of both natural and synthetic origin in order to increase natural diversity while introducing synthetic functional diversity. These libraries are typically created by amplifying natural naïve CDR1 and CD2 regions and synthetically randomizing CD3 regions, by shuffling natural CDR regions or by combinatorial mutation of certain amino acids in the V_H and V_L chains of the CDR3 region (Barbas et al., 1992). It has also been reported a synthetic library that combined synthetic CDR1 and CDR2 regions and a natural CDR3 (Hoet et al., 2005).

All these three libraries are amenable to high throughput screening and capable of generating and selecting thousands of antibodies specific to different epitopes on the same target.

2.2. Phage Display

Phage-display is the oldest and most frequently used system for molecular display. This technique was first implemented in 1985, when Smith and colleagues showed that foreign DNA fragments could be fused to the gene encoding the phage minor coat protein, pIII, of a nonlytic filamentous bacteriophage and consequently expressed in the form of a fusion protein at the surface of the phage without affecting the its infectivity (Smith, 1985). Later, a team of researchers based in Cambridge successfully applied this technology to the production of scFv antibodies by showing that these fragments could be displayed at the surface of the virion as functional proteins capable of binding to antigens (McCafferty et al., 1990).

The phage of choice is M13, a flexible rod like shaped filamentous phage with a 6000 to 8000 bases circular genome surrounded by a coat of five different proteins. One end of the phage displays by five copies of each of the two minor coat proteins, pIII and pVI while the other end presents three to five copies of pVII and pIX; the rest of the phage particle is covered with several thousand copies of the coat protein pVIII. (Smith and Petrenko, 1997).

The most commonly used coat proteins for phage display are pIII and pVIII. The pIII protein is involved in phage-host interactions during infection and is 460 amino acids long while pVIII protein has only 50 amino acids (Crissman and Smith, 1984; Smith, 1985). As these proteins have an important role in viral packaging and infectivity displaying large foreign peptides on every copy of selected coat protein could interfere with these functions limiting the performance of the phage display technology.

This obstacle could be overcome by expressing the foreign fragment only in a portion of the coat protein and different solutions were engineered to achieve this goal. In some phage display systems instead of introducing the DNA encoding the scFv library directly into the phage genome, the library is inserted as a gene cassette encoding scFv-pIII fusion proteins. This way the phage will retain the wild type pIII protein copy ensuring that only some pIII coat proteins display scFvs (Smith and Petrenko, 1997).

Another option is to insert the fusion coat protein in a phagemid (a plasmid with both phage and *E. coli* derived origins of replication), while the WT coat protein and the remaining genes essential for phage assembly are delivered by a helper phage with a deficient packaging signal. Co-infection of the bacteria by the phagemid and the helper

phage produces hybrid virions with the phagemid genome and displaying only limited copies of the fusion coat protein (Vieira and Messing, 1987; Mead and Kemper, 1988). During phage assembly WT pIII competes with the fusion protein for integration into the phage particle however since in a wild type phage there is only three to five copies of pIII coat protein, the majority of phagemid particles will only display zero or one copy of the fusion protein per phage. This is the reason why higher affinity antibodies are more often selected from phagemid than phage libraries, as there is no avidity (O'Connell et al., 2002).

The selection of scFv from phage display libraries is achieved by multiple rounds of probing against the desired antigen interspaced with washing steps to remove nonspecific phage clones. Typically, several rounds of panning with progressively increased washing stringency in between are performed to enrich the resulting phage pools with the highest affinity binders (Figure 5). This process is denominated biopanning and it is generally performed against a target immobilized onto a solid support as microtiter plate wells (Schofield et al., 2007), immunotubes (Weisser et al., 2007) or columns (McWhirter et al., 2006). Additionally, the phage library can be incubated with biotinylated antigen and then the antigen-phage complex is captured using a streptavidin surface (Winter et al., 1994). This approach could be beneficial for proteins that suffer conformational changes due to immobilization or so as not to limit the epitopes exposed to the panning.

In order to retrieve the phage particles that express scFv fragments capable of binding to the target protein an elution step is performed. Several elution strategies have been used including low (Smith, 1985) or high (Parmley and Smith, 1988) pH buffers, proteolytic cleavage (Ward et al., 1996), competition with free antigen (Oldenburg et al., 1992) and even ultrasound (Lunder et al., 2008).

The eluted phages retain their infective capacity and can therefore be propagated by infecting new bacterial hosts, to yield an amplified library, already more specific for the target protein, that can serve as input for the next affinity panning round. Usually only two to three rounds of panning are necessary however this can vary depending on the target protein. The eluate from the final round of panning are propagated and subjected to further analysis to isolate clones of interest.

Phage display of scFvs presents several advantages over other techniques. High stability of the phages allows storage at 4ºC for several years (Burritt et al., 1996) and makes phage display amenable to obtain binders for a specific conformation, structure, folding or enzymatic activity of the target protein (Forrer et al., 1999). Additionally, scFv production can be achieved swiftly and economically just by infecting *E.coli.*

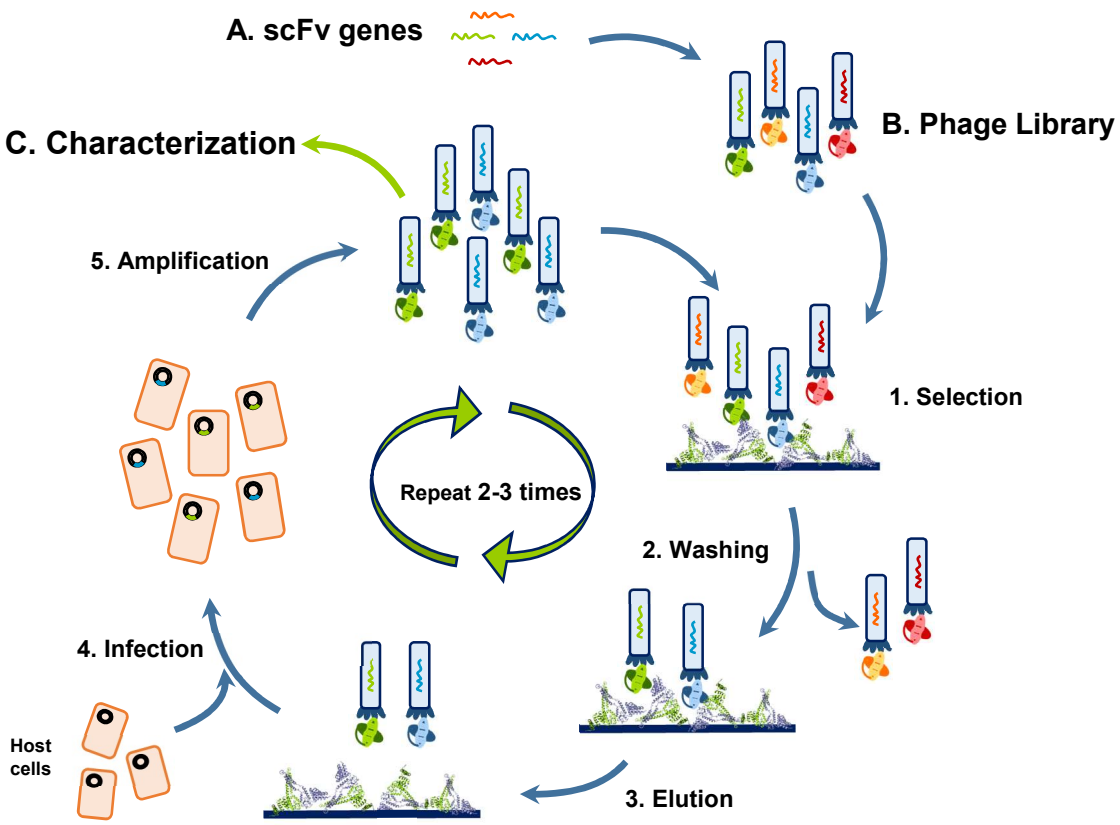

Figure 5. Phage Display Cycle.

A library of gene variants of antibody fragments (A) is expressed on the surface of M13 phage (B) and incubated with an immobilized antigen to select based on the expressed epitopes antigen binding scFv (1). After extensive washing to remove unbound and low affinity phage particles (2), the remaining bound phage particles are eluted (3). The selected phage are used to infect host cells (4) which are then grown (5) originating a "new" library enriched with variants of antibody fragments capable of high affinity interaction with the desired antigen (polyclonal pool). This cycle is usually repeated from two or three times to increase the pool of high affinity antibodies. The use of phage display results in selection of high affinity antibodies, that can be expressed and characterized (C) (Smith, 1985).

Recent improvements in this technique include the development of a high-throughput phage-display screening in array format using a protein chip carrying recombinant phage particles that aims to facilitate antibody identification and characterization (Diez et al., 2015); an industrialized platform to generate high affinity antibodies for transcription factors and epigenetic antigens through an optimized automated phage display and antigen expression pipeline capable of producing a great number of sequenced Fabs with high affinity stability and good expression in *E. coli* (Hornsby et al., 2015); and generation of scFv fragments capable of revealing structural differences of amyloid-β fibrils resulting from variations in the acidity of the environment during the fibrillogenesis process (Droste et al., 2015).

In summary, phage display technology has seen great improvements since it was first developed in 1985 in order to accommodate the new applications and demands of today's science. This technique has been particularly useful in the high throughput development of new scFv fragments which in turn have been widely used in basic research

and immunotherapy, as has been described before. Considering the evolution this technique has achieved and seeing as it is still extensively employed, new developments are to be expected and new applications unveiled.

2.3. Alternative Molecular Display Systems

Even though phage display is the most commonly used molecular display system, Ribosome and Cell Surface display also have to be considered as two well-established techniques which also have their advantages.

Ribosome display doesn't require cell growth or transformation as it is a fully *in vitro* transcription/translation system. The concept involves the translation of the scFv encoding nucleic acids to form a complex that is then incubated with the target protein to select specific binders (Figure 6). This system can overcome the limitations of cell-based displays such as the expression bias and generate larger libraries than phage or cell surface display constituting a powerful alternative to the remaining molecular display systems (Hanes and Pluckthun, 1997).

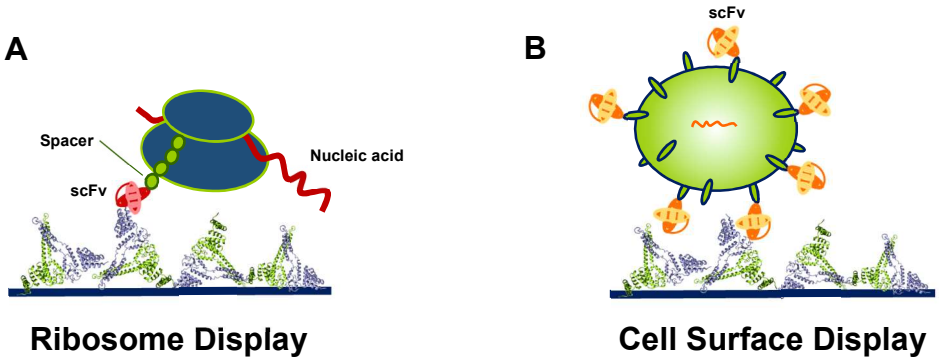

Figure 6. Alternative Molecular Display Systems.

A. **Ribosome Display**. mRNA molecules are incubated with a stoichiometric amount of ribosome and once the translated antibody fragment emerges from the ribosome, the lack the stop codons will lead to the formation of a protein-ribosome-mRNA complex. The presence of a spacer region at the 3' terminal of the DNA library ensures the fusion to the ribosome while allowing the protein to fold correctly. The complexes are then incubated with the immobilized target to probe for binding. Elution is achieved by destruction of the complex or competitive elution with free ligands. The eluted mRNA is subjected to reverse transcription-PCR in order to obtain DNA for the next round of panning (Hanes and Pluckthun, 1997). **B. Cell Surface Display.** The protein of interest is expressed at the surface of the cell fused with one of its surface proteins and high-affinity binders can be selected and quantified, according to scFv expression and antigen binding, by flow cytometry using both fluorescently labelled antigens and anti-epitope tagged reagents (Boder and Wittrup, 1997).

In the cell surface display system, thousands of copies of the scFv are anchored to proteins such as the Lpp-OmpA chimera on the membrane of E.coli (Francisco et al., 1993) or the α-agglutinin adhesion receptor on the cell wall of yeast (Boder and Wittrup, 1997) and consequently displayed on the surface of the cells and selected with Fluorescent Activated Cell Sorting (FACS) technology. This selection technique allows for

a swift and quantitative screening and ensures that tightly bound clones will be recovered. The most popular format is yeast display but *E. coli* and *Bacillus thuringiensis* (Du et al., 2005).

3. CHIPping Away at the Unknown

The Carboxy-terminus of Hsc-70 Interacting Protein (CHIP) is a 35kDa homodimeric quality control E3 ligase. CHIP is highly expressed in tissues with high metabolic rates such as the heart, the adult striated muscle and the brain. Intracellularly, it is known for being present in both the cytoplasm (Ballinger et al., 1999) and the nucleus under different conditions (Meacham et al., 2001)

Evolutionarily, CHIP's amino acid sequence is well-conserved across several species, sharing a particularly high similarity with that of mouse (~98%) and its ubiquitination domain, the U-box, is the least altered region of the sequence. This protein was first described in 1999 when it was discovered during an assay that aimed to identify TPR-containing proteins in the heart by screening a phage library of human heart cDNA against a fragment of cytochrome 40 (Ballinger et al., 1999).

Fifteen years later, even though several CHIP interactors and substrates have been identified and its relevance in physiology and disease has been widely studied, little is still known about its molecular mechanistics and regulation.

3.1. Unravelling CHIP's Structure and Activity

The maintenance of normal cellular functions rests heavily on the integrity of the cell's proteome; to this end, the cell possesses a set of pathways responsible for monitoring and maintaining the health of its proteins. Central to these pathways are the molecular chaperones that can promote the folding of misfolded protein, and if that's not possible target them to the ubiquitin-proteasome system (UPS) which is responsible for the degradation of proteins usually marked with ubiquitin tags.

The addition of ubiquitin to the target proteins is accomplish through a process known as ubiquitination, which requires a succession of biochemical reactions catalysed by three different groups of enzymes (Figure 7). CHIP belongs to the group of the E3 ubiquitin ligases.

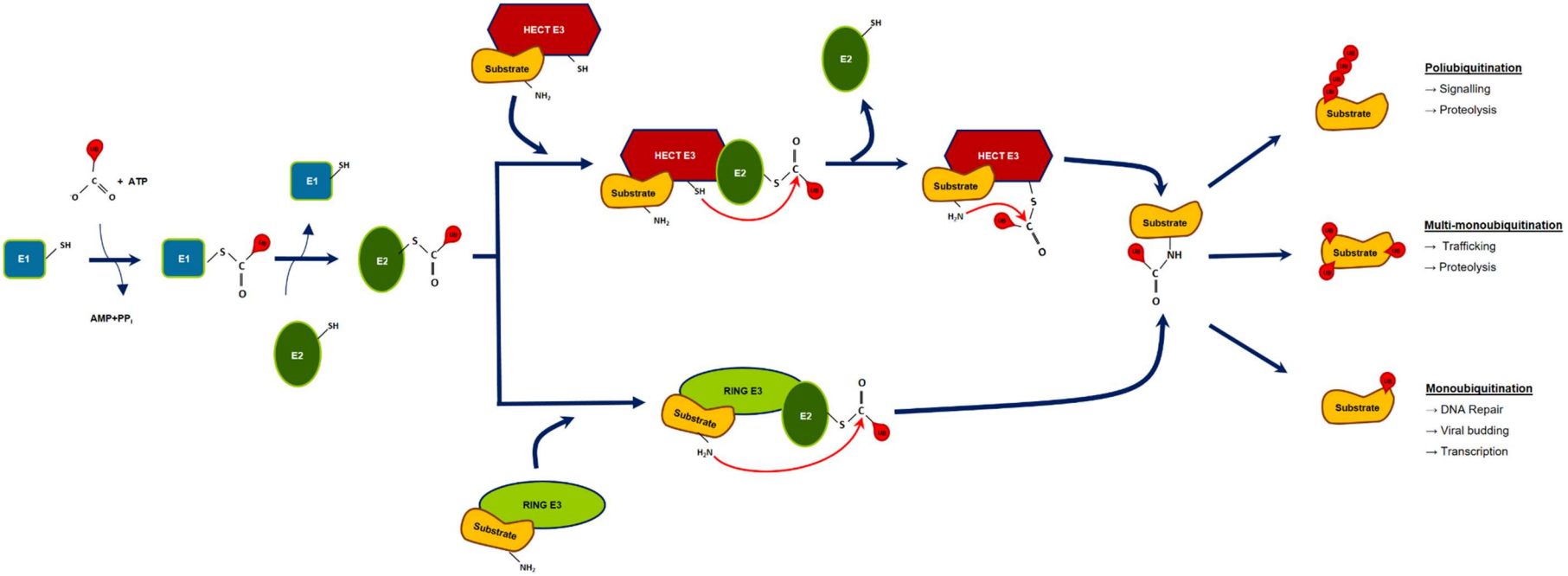

Figure 7. Ubiquitination Pathway

Protein ubiquitination involves three classes of enzymes. First, the C-terminus of ubiquitin (UB) is linked by a thioester bond to the active site cysteine of a ubiquitin-activating enzyme E1, generating an Ub-E1 complex. This reaction is ATP-dependent and activates ubiquitin. Afterwards ubiquitin is transferred to the active site cysteine of an ubiquitin-conjugating enzyme (E2), forming an E2-Ub thioester, and releasing E1. E3 ubiquitin ligases interact both with the complex E2-Ub and the substrate by catalysing the final transfer of ubiquitin by two different mechanisms, depending on the type of ligase and are the main source of specificity in the ubiquitin system. HECT-type E3s act as covalent intermediates as ubiquitin is initially transferred to the active site cysteine of E3 and only then conjugated to the substrate. Instead RING and U-box E3s facilitate the transference of ubiquitin directly from the complex E2-Ub to the substrate. Ubiquitination reactions occur mostly on primary amines in Lysines, and, less often, a free N-terminus, resulting in stable peptide bonds with the C-terminus of ubiquitin. This process can occur once (monoubiquitination) or multiple times on different Lysine residues of the protein (multi-monoubiquitination). Additionally, ubiquitin can also be transferred to one of the Lysines or the N-terminal methionine of other ubiquitin molecules already attached to the substrate originating poly-ubiquitin chains. The type of ubiquitination influences the fate and function of the modified protein as monoubiquitination often leads to involvement in processes as DNA repair, protein trafficking, and transcription (Ramanathan and Ye, 2012) while multi-monoubiquitination can also redirect proteins for proteasomal degradation (Dimova et al., 2012; Shabek et al., 2012). Regarding polyubiquitination, K11-linked chains are integral to proteasomal targeting of anaphase-promoting complex/cyclosome (APC/C) substrates (Wickliffe et al., 2011)meanwhile linkage through K48 and other lysines chains of four or more ubiquitin molecules efficiently target proteins for proteasomal degradation (Xu et al., 2009; Kim et al., 2011). Linear and K63-linked ubiquitin chains are associated with non-degradation events of NF-κB signaling (Schmukle and Walczak, 2012) and are also implicated in DNA repair and targeting of endocytic proteins for lysosomal degradation (Ramaekers and Wouters, 2011; Clague et al., 2012).

In fact, CHIP plays an important role in the ubiquitin-proteasome scheme as a bridge between the molecular chaperone system and the degradation pathway due to its functions as both a quality control E3 ubiquitin ligase and a co-chaperone of several heat shock proteins (Hsp) (McDonough and Patterson, 2003).

CHIP's structure is intimately associated with its activity. Each monomer (34.5kDa) displays two specialized domains, which impact CHIP's activity in a different but complementary manner, joined by a central coiled-coil region. The amino terminus contains three tetratricopeptide repeats (TPR), responsible for the interactions with chaperones, and the carboxyl terminus displays a U-box domain that grants CHIP its E3 ubiquitin ligase activity (Figure 8) (Zhang et al., 2005).

The U-box, positioned at the C-terminus, is structurally similar to RING finger domains, the main difference resting on the fact that U-boxes are stabilized by hydrogen bonds instead of zinc binding (Aravind and Koonin, 2000). CHIP's U-box (residues 232-298) contains a pair of β-hairpins running into a short α-helix followed by a third hairpin and concluding in in a C-terminal α-helix (Zhang et al., 2005). This region acts as a scaffold or an adaptor, positioning the substrate in proximity with the E2-ubiquitin complex, as opposed to the HECT ubiquitin ligases, that form transient thioester links with the ubiquitin molecule and transfer it to the substrate (Passmore and Barford, 2004).

The TPR domain (residues 26-131) includes three TPRs, each of which consists of two antiparallel α-helices separated by a turn to form a 'knob and hole' structure (Zhang et al., 2005) with a hydrophobic surface that facilitates protein:protein interactions (Das et al., 1998). This domain is primarily responsible for CHIP's interactions with the Hsc/Hsp proteins.

Initially it was believed that TPR domains were mostly rigid, invariable structures, even upon ligand binding. Nevertheless recent structural and dynamic studies have suggested otherwise and added that binding to the TPR domain can actually lead to large conformation changes in the protein as a whole (Parashar et al., 2013).

This possibility has already started to be investigated for CHIP. A study conducted using Hydrogen/Deuterium Exchange coupled with Mass Spectrometry (HDX-MS) demonstrated that the TPR domain in CHIP is not only loosely folded but also that the first sixty amino acids are intrinsically disordered. Also it was revealed a high degree of flexibility in the TPR domain which decreased upon Hsp70 or Hsp70 peptide binding (Graf et al., 2010).

These results above were supported by a recent publication that additionally looked at a CHIP TPR mutant (CHIP-K30A), in which the lysine in position 30 was replaced by an alanine, a residue that encourages helix formation. This protein had only been studied as a non-chaperone binding mutant of CHIP with decreased catalytic activity. However it was revealed that, when compared with wild type CHIP, the mutant presents a TPR domain with reduced flexibility, equivalent to the decrease seen for the ligand-bound TPR domain. Additionally molecular dynamics studies were conducted and it was shown that the mutation affected not only TPR movements but also the U-box's. This observation lead the way to a new mechanism of regulation for CHIP and established the K30A mutant as a useful tool to study the effect of TPR stabilization in the absence of a ligand (Narayan et al., 2015).

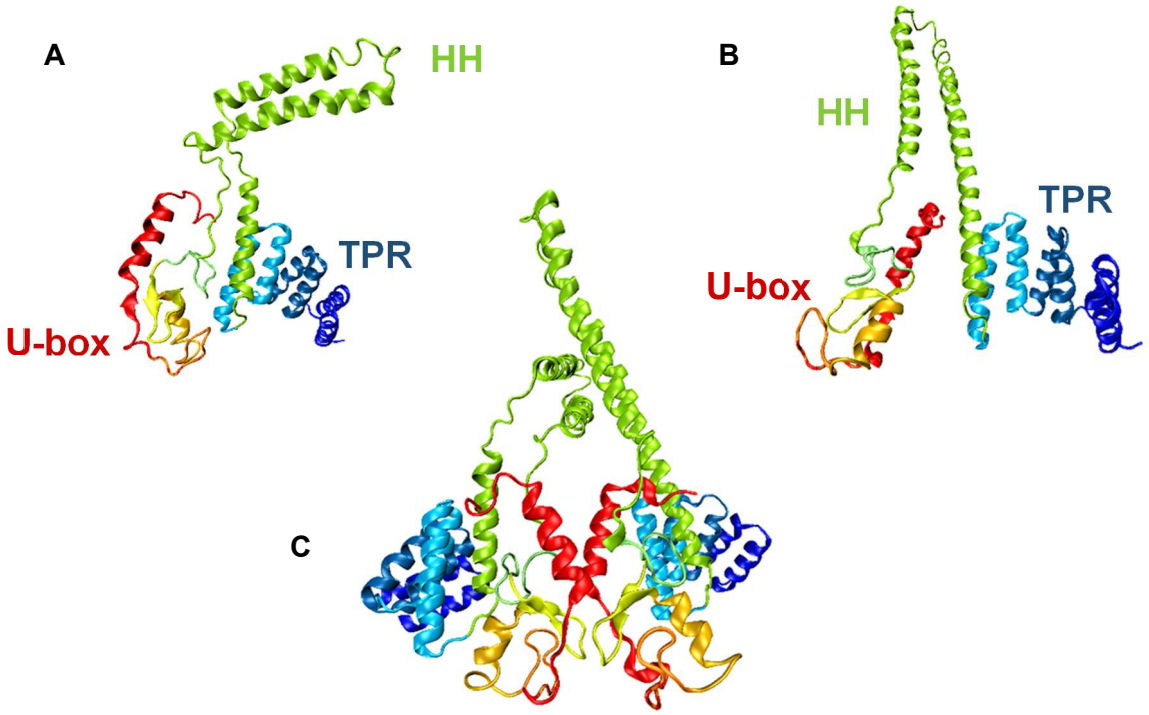

Figure 8. Representation of CHIP's structure.

(A) Structure of the CHIP protomer that presents the 'broken' coiled coil domain (CC) indicating the tetratricopeptide repeat domain (TPR) and the U-box domain. (B) As in (A) but for the protomer that maintains a straight coiled coil domain. (C) The two protomer assembled. These images were obtained from PDB file 2C2L (Zhang et al., 2005) using the graphic software *Visual Molecular Dynamics* (VMD) (Humphrey et al., 1996) coloured according to the different secondary structure motifs

The TPR and the U-box domains are brought together by a charged coiled-coil domain (helix 7 and 8), essential for the coupling of CHIP's inactive monomers and consequently its function. as enzymatic activity of CHIP is dependent on its dimerization (Nikolay et al., 2004). When CHIP dimerizes, the two protomers adopt significantly different conformations forming an asymmetric dimer. The assembly of CHIP's two monomers involves the interaction of the U-box domain and the central helical domain of

each monomer. However helix 7 adopts distinct conformations in the two monomers; in one remains a straight α-helix while in the other it breaks forming two perpendicular α-helices. This, along with a dislocation in the U-boxes and the helical domains symmetry axes leads to structural arrangements that positions the TPR domain of one of the protomers in front of its U-box domain, blocking it. For this reason CHIP displays a "half-of-sites" activity (Zhang et al., 2005).

CHIP is predominantly responsible for the ubiquitination of chaperone-bound substrates by binding to C-terminal of Hsp/c70 and Hsp 90 with its TPR domain in order to facilitate ubiquitination via its catalytic U-box by the 26S proteasome. Chaperone clients usually include chaperone activated signalling proteins and proteins prone to aggregation that are subjected to chaperone assisted quality control (Connell et al., 2001; Jiang et al., 2001).

In order to perform its role as ubiquitin ligase, CHIP depends on the interaction with E2 proteins. CHIP has been shown to interact with UbcH5 to produce Lys-48-linked polyubiquitination and with E2 complex Ubc13-Uev1A to generate Lys-63-linked polyubiquitination. This suggests the product formed in CHIP-mediated ubiquitination reactions is dependent on which E2 is involved (Xu et al., 2008). Another study identified a set of other seven other E2 enzymes that bind and function with CHIP *in vitro* to produce all types of ubiquitination events. This study also confirmed that CHIP requires the SPA motif in loop 7 of E2 for recognition and binding (Soss et al., 2011). Different ubiquitination patterns have also been described depending on the E2 present but also due to small changes in the substrate, as ubiquitination assays showed that the distribution of multiple ubiquitination chain types is different for Hsp70 versus Hsc70, even though these proteins present highly sequence homology and similar structure (Soss et al., 2015).

Additionally, CHIP has also been shown to interact with other E3 ligases to facilitate their ubiquitination activity, functioning as an E4 ligase. So far this function of CHIP has been demonstrated for Parkin, considered the culprit for a juvenile form of Parkinson (Imai et al., 2002), and for the complex SCF^{Skp2} (Nie et al., 2008).

3.2. Regulation

CHIP is regulated at different levels and new insights about possible mechanisms have been in study lately.

Few studies have been dedicated to studying CHIP's transcriptional regulation under physiological and pathological contexts. Still, it is to be expected that in case of a massive accumulation of misfolded proteins, quick adjustments of the levels of Hsp70

chaperones and its co chaperones would be required so as to maintain homeostasis. The levels of CHIP and/or Hsp70 mRNA are in fact upregulated and have, *in vivo* and *in vitro*, protective effect under stress conditions such as heat shock, pathological polyQ overexpression (Miller et al., 2005; Dikshit and Jana, 2007) and oxidative stress (Stankowski et al., 2011). A decrease in CHIP's mRNA and protein levels has been observed in breast cancer (Kajiro et al., 2009; Patani et al., 2010), colorectal (Ruckova et al., 2012; Wang et al., 2014b) and gastric cancer (Gan et al., 2012) and correlated greatly with prognosis. These results are in agreement with evidence showing that CHIP acts as tumoral suppressor.

The one example of CHIP posttranscriptional regulation that has been reported so far is in the context of bone morphogenesis as translational repression of CHIP by miR-764-5p was deemed essential for adequate osteoblast differentiation (Guo et al., 2012).

Posttranslational modifications (PTM) of CHIP have also been investigated however only ubiquitin modifications have been reported. CHIP undergoes a regulatory ubiquitination in cells and *in vitro* which doesn't promote its turnover but instead facilitates substrate targeting for proteasomal degradation (Jiang et al., 2001; McDonough and Patterson, 2003). For instance, Ataxin 3, an ubiquitin-interacting motif containing deubiquitinase, provides chain editing activity for CHIP by binding and deubiquitinating CHIP upon completion of substrate ubiquitination however this activity is dependent on E2 Ube2w ubiquitination of CHIP (Scaglione et al., 2011). Additionally it has also been reported that CHIP undergoes extensive autoubiquitination however the extension of this process seems to be dependent on the E2 enzyme present in the reaction (Soss et al., 2011; Soss et al., 2015). Until recently no direct evidence of other PTMs had been found. It had only been proposed that CHIP had functional phosphorylation sites (Dephoure et al., 2008) and interacted with protein kinases such as ERK5 and Lim Kinase 1 (LIMK1) (Lim et al., 2007; Woo et al., 2010). However recently a study reporter that Cdk5 phosphorylates CHIP at Ser20, promoting tAIF-mediated neuronal death (Kim et al., 2015).

Moreover substrate PTM and conformation changes also have roles in functional regulation of CHIP. For instance, under stress conditions, Abl phosphorylation of MST1 kinase inhibits its degradation by CHIP allowing it to bind to FOXO3 and trigger neuronal cell death (Xiao et al., 2011). Also Landré and colleagues reported that IRF-1 (interferon regulatory factor-1) ubiquitination by CHIP was inhibited when IRF-1 adopted a DNA bound conformation as it obstructed the E3 docking site (Landre et al., 2013).

The activity of CHIP is also regulated by its interactions with other proteins. This regulation occurs by varied mechanisms including: competition with substrate binding (eg. S100 proteins) (Shimamoto et al., 2013); competition with chaperone binding (eg. Xap2)

(Lees et al., 2003); conformational modification of the chaperone complex (eg.HspBP1) (Alberti et al., 2004); interference with CHIP:E2 interaction (eg. BAG2) (Arndt et al., 2005); facilitation of chaperone binding (eg. BAG1/3) (Demand et al., 2001; Dai et al., 2005) and of the interaction with the E2 (eg. S5a) (Kim et al., 2009).

It has also been proposed a chaperone-mediated allosteric model of CHIP regulation. An *in vitro* study, carried out using wild type and a U-box mutant (P269A) CHIP without E3 ligase activity, suggested that CHIP-Hsc70 binding is dependent on allosteric interactions between the U-box and the TPR domains. The increased binding efficiency of TPR to Hsc70 by the U-box mutation raised the possibility that the U-box contributes to TPR domain folding, induced during binding to Hsc70 (Matsumura et al., 2013). In line with this allosteric model, recent publication reported that changes in the TPR domain flexibility, secondary structure and motion also impact the U-box, as a TPR mutant with a less flexible conformation also showed decreased catalytic activity. Furthermore this study suggested that Hsp70 can modulate CHIP's ubiquitination activity on native proteins, through the TPR domain, on top of its function as a targeting signal for CHIP in the chaperones and protein control pathways (Narayan et al., 2015).

3.3. Two ends of the same CHIP: physiology and disease

In view of CHIP's position as hub between the ubiquitin/proteasome system and the chaperones' pathway it is not difficult to conceive its involvement in numerous cellular processes and the important role it presents in the regulation of a great number of proteins. Thus CHIP's significance in several physiological and disease related processes has been avidly studied.

Currently, CHIP is well established as an E3 ubiquitin ligase and as such, one of its main physiological functions is to ensure the maintenance of protein quality under both normal and stress situations. Denatured proteins or nascent polypeptides are recognized by chaperones, due to their exposed hydrophobic surfaces, and failure to refold them triggers degradation. As CHIP associates closely with chaperones it gains access to a whole portfolio of clients.

Several publications have linked CHIP to the ER associated degradation pathway (ERAD). First it was shown that CHIP was necessary for proper biogenesis of CFTR (Cystic fibrosis transmembrane conductance regulator) as it promoted degradation of misfolded receptors. Consequently CHIP became a possible target for strategies that aim to rescue misfolded but potentially functional receptors from ERAD without affecting pro-folding activities (Matsumura et al., 2013). Then Donelly and co-workers identified CHIP

as a promoter for HSP70/90/40 mediated ER degradation of the NaCl cotransporter (NCC) which due to its complex topology is not processed efficiently and is prone to suffer ERAD (Donnelly et al., 2013). More recently CHIP was reported as an E3 ligase for nicotinic acetylcholine receptor α3 subunit and UBXN2A was identified as an adaptor protein that may efficiently regulate the stability of CHIP's client substrates, by interfering with CHIP-mediated ERAD (Teng et al., 2015). Another report showed that CHIP overexpression prevented cell death, by pharmacologically induced RE stress in the hippocampus, and up-regulation p53 pro-apoptotic pathways (Cabral Miranda et al., 2014).

Besides its role in ubiquitinating misfolded substrates, CHIP has also been reported to interact with non-native and denatured proteins under conditions of stress (eg. heat) in an Hsp70 independent manner, in order to fold them. The molecular mechanism for this multifaceted role for CHIP is not completely understood but it has been suggested it can be due to conformational changes and oligomerization status (Rosser et al., 2007).

CHIP was also implicated in oxidative stress when it was reported that exogenous overexpression of CHIP in HT-22 cells in acute oxidative stress conditions impaired neuronal survival and led to a loss of proteasome activity; curiously an overload of polyubiquitinated proteins was offered as a cause for proteasome impairment (Stankowski et al., 2011). In a more recent study, CHIP exhibited Hsp70 dependent interaction and degradation of endonuclease G under normal but not in oxidative induced stress conditions. This reveals a new CHIP mediated protective mechanism against oxidative stress (Lee et al., 2013).

Additionally, CHIP has recently been suggested as a regulator of the autophagic flux as CHIP knockdown induced autophagosome formation due to an increase in the levels of PTEN and decreased AKT/mTOR activity (Guo et al., 2015)

Apart from its roles in mediating protein quality control under stress situations, CHIP is involved in the regulation of the Base Excision Repair (BER) pathway, responsible for processing simple lesions in DNA, by catalysing the ubiquitination of proteins that are not bound in repair complexes (Parsons et al., 2008). It also plays a role in the maturation of aggresomes, inclusion bodies rich in ubiquitin where misfolded proteins are sequestered (Sha et al., 2009)

As every coin has two sides, once CHIP’s functions and participation in physiological pathways came to light, it also became evident its possible influence in several disorders and pathologic processes.

One of the earliest examples of CHIP's role in human disease was reported in publications regarding Parkinson's disease, a neurodegenerative aggregation pathology. The first study focused on the involvement of CHIP in potentiating Parkin mediated ubiquitination of Pael-R, a receptor that accumulates in Lewy bodies which are a hallmark of Parkinson's disease. CHIP mediates the displacement of Parkin/Pael-R from Hsp70 allowing Parkin to ubiquitinate Pael-R (Imai et al., 2002).

Nowadays, CHIP related research in this area is focusing more on α-synuclein as it has been found that CHIP co-localizes with this intrinsically disordered protein and Hsp70 in Lewy bodies-like inclusions and decreases *in vitro* formation of inclusions in a model of α-synuclein aggregation. Besides, it was also suggested that CHIP was capable of promoting α-synuclein degradation via proteasome, by a TPR dependent mechanism, or through a U-box dependent lysosomal pathway. Additionally it has been shown CHIP's ability to selectively reduce the toxicity of α-synuclein stabilized oligomeric forms while having no effect on cytotoxic manifestations resulting from more transitory interactions of α-synuclein (Shin et al., 2005; Tetzlaff et al., 2008). More recently it was also demonstrated that CHIP can facilitate *in vivo* degradation of α-synuclein aggregates (Dimant et al., 2014).

CHIP has also been implicated in the ubiquitination and proteasomal degradation of LRRK2 (leucine-rich repeat kinase 2 gene), whose mutated form is the most common cause of familiar Parkinson's. This process can mitigated by Hsp90 (Ding and Goldberg, 2009).

Alzheimer's Disease (AD) is another neurodegenerative aggregation disorder with which CHIP has been associated. So far, deposition of extracellular amyloid beta (Aβ) and hyperphosphorylation of Tau protein are the strongest causal hypothesis for the development of this disease. CHIP is able to target proteosomal degradation of Tau through an Hsc70 dependent mechanism (Shimura et al., 2004) and then it was reported that CHIP up-regulation attenuated tau aggregation *in vivo* (Sahara et al., 2005). Later, CHIP complexed with Hsp90 was shown to distinguish and selectively degrade phosphorylated tau proteins (Dickey et al., 2007) while Zhang described CHIP's ability to degrade tau independently of its phosphorylation status (Zhang et al., 2008).

Another study highlighted a critical role for CHIP as new potential target in tauopathies as it showed that while Aβ accumulation decreases CHIP expression and increases tau levels, blocking Aβ accumulation restored CHIP levels, delaying the onset and development of tau pathology (Oddo et al., 2008). Interestingly, a more recent study portrayed CHIP as a suppressor of APP cleavage into Aβ, through ubiquitination of the responsible enzyme, β-secretase, which is activated by p53 inactivation. However, CHIP is also capable of stabilizing p53's DNA-binding conformation to inhibit its interaction with

β-secretase promoter thus regulating β-secretase levels both transcriptionally and at a post-translational level (Singh and Pati, 2015). Both these mechanisms suggest CHIP as a possible therapeutic target in AD.

The above mentioned are two of the most studied disorders nowadays however CHIP has also been found to participate in several other neurological disorders such as Huntington's disease, spino-cerebellar ataxia-1 and spinal and bulbar muscular atrophy by mediating ubiquitination and supressing aggregation of polyglutamine proteins including huntingtin, ataxin 1 and the androgen receptor (Miller et al., 2005; Al-Ramahi et al., 2006; Adachi et al., 2007); Inclusively it has been reported a new CHIP-mutant related ataxia (Casarejos et al., 2014). CHIP has also been implicated in ALS (Choi et al., 2004; Urushitani et al., 2004) and Lafora Disease (Rao et al., 2010).

Cancer is another pathology where CHIP seems to have an important role however it is not a direct one, considering contradictory concepts have been found.

Some evidence supports CHIP's involvement as a tumour suppressor as its levels have been shown to correlate negatively with tumour growth, metastasis (Kajiro et al., 2009), migration , angiogenesis (Wang et al., 2013; Sun et al., 2015) and increasing malignant grades (Patani et al., 2010). More recent work proposed CHIP's promoter hypermethylation as an underlying mechanism for CHIP's downregulation in various cancers (Gan et al., 2012). In addition, CHIP has been associated with decreased levels of several well-studied oncogenic proteins such as pAkt (Su et al., 2013), c-myc (Paul et al., 2013), HIF-1 (Bento et al., 2010; Ferreira et al., 2013) and EGFR (Wang et al., 2014a) in various cancers and a few more in breast cancer particularly, including histone acyltransferase SRC-3 (Kajiro et al., 2009), TNF receptor interactor TRAF2 and NF-κB (Jang et al., 2011), differentiation regulator PTK6 (Protein-Tyrosine Kinase 6) (Kang et al., 2012) and inflammatory cytokine MIF (macrophage inhibitory factor) (Schulz et al., 2012).

However it seems that for every study suggesting CHIP's tumour suppression influence there is evidence suggesting its oncogenic properties. CHIP-mediated ubiquitination and degradation of tumour suppressors such as FoxO1 in response to TNF signalling (Li et al., 2009), and of PTEN have been reported (Ahmed et al., 2012). Inclusively, a tissue microarray approach detected increased expression of CHIP in metastatic lymph nodes of oesophageal squamous cell carcinoma (Wen et al., 2013).

Considering cancers' diversity and sophistication along with CHIP's wide net of interactors and seemingly tight regulation it should not be a surprise if future studies find

this E3 ligase can in fact take on both the above mentioned roles, under different conditions.

It is likely that as the knowledge on CHIP's functions and mechanisms are further elucidated and research on physiologic and human disease pathways progresses, novel interactors and substrates for CHIP are revealed. In fact very recently a new study identified CHIP as an interactor of cellular prion protein, however physiological and pathologic implications of this finding are still being studied (Gimenez et al., 2015).

3.4. Targeting CHIP

The physiological significance of CHIP was definitely established when it was demonstrated that approximately 20% of CHIP null mice (CHIP-/-) died at embryonic stages and the remaining were incapable of surviving thermal stress (Dai et al., 2003).

Since then, and as it was described previously, CHIP's vital role in the regulation of varied biochemical phenomena, as well as CHIP's own regulation mechanisms, have been further elucidated. CHIP's physiological functions and its role in neurological disorders and cancer present this protein as a possible target for therapies; in most of these cases increase of CHIP's levels or activity can lead to a favourable outcome (Ishigaki et al., 2007; Cabral Miranda et al., 2014). Combinatory therapeutic strategies involving not only CHIP but also its interactors, like chaperones, might also prove to be useful when both parties are involved as occurs in several pathologies (Pratt et al., 2015).

As CHIP's intrinsic mechanistics, regulation and importance in disease continues to be investigated, new information will undoubtedly clear the way for modulation of its activity in order to better potentiate its aptitude as a therapeutic target.

II. AIM

Current knowledge of CHIP has drawn the image of a highly complex protein, apparently tightly regulated and involved in a plethora of cell processes, often seemingly inconsistent however it is clear that a lot is still left to be known.

The main aim of the present study was to develop and characterize single chain fragment variable antibodies (scFv) against the C-terminus of the Hsc70-Interacting protein (CHIP) by phage display technology with the long term goal of using them to image and modulate CHIP's activity.

The aim of the study will be achieved by the following approaches:

1. Production and Purification of His-tagged wild type CHIP;
2. Screening of a canine Phage scFv antibody library Phage Display Technology using His-tagged wild type CHIP and an untagged CHIP TPR mutant (K30A);
3. Selection and validation of scFv fragments that present the highest affinity for the targets used (WT CHIP and CHIP K30A);
4. Soluble expression and purification of the selected scFvs from *E.coli*;
5. Characterization of the purified scFvs using sequence analysis, high-throughput peptide and protein binding assays and gel electrophoresis techniques.
6. Establishment of an *in vitro* interaction assay between CHIP and its known substrate α-synuclein;
7. Determination of the influence of the obtained scFvs in the activity of CHIP using the aforementioned assay.

III. MATERIAL AND METHODS

1. Material

1.1. Proteins and Reaction kits

The following proteins, used in this study, were kindly offered by various members of the laboratory: CHIP mutant K30A and untagged WT CHIP (Jia Ning), p53 (Maria Gil) and α-synuclein (Jonas Gasparavičius). The E2 UbeH5α used in ubiquitination assays was produced in the laboratory by Fiona Lickiss. His_6-Ubiquitin E1 Enzyme (Ube1) and Ubiquitin were from Boston Biochem. Wild type His-tagged CHIP was produced and purified according to the protocol described in the 'Methods' section of this thesis. The kit QIAprep Spin Miniprep kit (QIAGEN) was used to isolate plasmid-DNA from *E.coli*.

1.2. Antibodies, Conjugates and Substrates

All the antibodies and conjugates used in this study, as well as their provenience are described in table 1.

Target	Class	Name	Provenience
CHIP	Mouse Monoclonal	3.1	Gifted by B. Vojtesek
α-Synuclein	Mouse Monoclonal	Purified Mouse Anti-α-Synuclein	BD Biosciences
p53	Mouse Monoclonal	DO1	Gifted by B. Vojtesek
M13 Phage	Monoclonal	Mouse Anti-M13 Phage/HRP	GE Healthcare
Mouse Immunoglobulins	Polyclonal	Rabbit Anti-Mouse Immunoglobulins/HRP	Dako
scFv	-	Protein A, HRP conjugate	Millipore

Table 1. Antibodies and conjugates.

ECL solutions I (100 mM Tris pH 8.5; 2.5 mM Luminol; 0.4 mM p-Coumaric acid; millipore water) and II (100 mM Tris pH 8.5; 0.02% (V/V) hydrogen peroxide; millipore water) used as a substrate for Western blotting and enzyme-linked immunosorbent assay were prepared in the laboratory.

1.3. Bacterial Strains

Escherichia coli strain BL21 (DE3) was used for expression of His-tagged wild type CHIP and for expression of soluble scFv-fragments; TG1 was used for generation of phage-displayed antibody libraries used in solid-phase panning and for expression of soluble scFv-fragments.

1.4. Equipment and Applications

Sonicator: MSE Soniprep 150 Plus ultrasonic disintegrator.

Centrifuges: 5810R and 5415R (Eppendorf); Sorval RC6 Plus rotor Fiberlite F21-8x50y (ThermoScientific).

Photometers and Microplate readers: Spectrophotometer Lambda Bio (Perkin Elmer); Fluoroskan Ascent™ FL Microplate Fluorometer and Luminometer (ThermoScientific); Spectrophotometer NanoDrop 2000c (Thermoscientific).

Gel electrophoresis equipment: Mini-PROTEAN Tetra Vertical Electrophoresis Cell (Biorad); Mini Trans-Blot cell (Biorad); PowerPack Basic Power Supply (Biorad).

Film Processor: SRX-101A Film processor (Konica Minolta).

Software: Windows 7 and Windows 10 OS (Microsoft); Microsoft Office and Excel 2013 (Microsoft); Chromas Lite.

2. Methods

2.1. Transformation of *E. coli* by heat shock

Aliquots (50 µl) of competent cells were thawed, gently mixed with plasmid DNA and incubated on ice for 30 minutes. Then the cells were exposed to a temperature of 42ºC for 1 minute followed by a 2 minutes' incubation on ice. Afterwards 1 mL of LB medium was added to the culture and incubated at 37ºC for 1 hour. A 150 µL fraction of the culture was plated onto a LB-Agar plate supplemented with the suitable antibiotics and incubated at 37ºC overnight.

2.2. His-tagged CHIP Production and Purification

Competent bacterial cells BL21(DE3) were transformed with pET15b-CHIP (His-CHIP, WT) construct as described above in "*Transformation of E. coli by heat-shock*". A colony was picked and incubated in LB supplemented with ampicillin overnight at 37ºC and 250 rpm. This culture was then used to seed 2 L of LB and incubated at 37ºC until OD600 reached ~0.8. Protein expression was induced with 0.5mM IPTG at 30ºC until OD600 reached 1.3. The cultures were then centrifuged at 6000 g for 20 minutes at 4ºC. The pellet was resuspended, sonicated and then centrifuged at 13000 rpm for 15 minutes at 4ºC. The supernatant was filtered and the protein was purified using its His tag through immobilised metal ion affinity chromatography with Ni^{2+}-NTA agarose beads (Qiagen) in a disposable column (Mobitec). Elution was performed with buffer containing 20 mM Tris (pH = 8), 150 mM NaCl and 300 mM Imidazole. To finalize, a desalting step was performed using Zeba Spin Desalting Columns (Pierce) and the final storage buffer was 20 mM Tris (pH = 8), 15 mM NaCl. Protein was quantified by A280 absorption on a NanoDrop Spectrophotometer and its purity evaluated with Coomassie stained SDS–PAGE gels.

2.3. SDS-PAGE

Polyacrylamide SDS gels of appropriate percentage (12% or 15%) were used for separation of protein samples. The samples were mixed with 2x SDS sample buffer (25% Glycerol, 5% SDS, 0.3 M Tris pH 6.8, bromophenol blue, 20% DTT, MilliQ water) in a ratio of 1:1, heated for 3 to 5 minutes at 95ºC and then allowed to return to room temperature before being loaded onto the gel along with prestained protein markers. The gels were run in Tris-Glycine-SDS running buffer at a constant voltage of 170 V until the dye front reached the end of the gel.

2.4. Coomassie Staining

Gels were submerged in Coomassie Blue stain (45% Methanol, 20% Glacial Acetic Acid; Brilliant Blue R-250 (ThermoFisher) for 1 hour. After discarding the Coomassie stain the gel was washed in destaining solution for 5 minutes, the destain was removed, fresh was added and left shaking until the protein bands could be easily distinguished in the gel. In order to accelerate destaining the destain solution was changed several times.

2.5. Biopanning

Microtiter wells (Costar) were coated overnight at 4 °C with 1 µg of His-CHIP and CHIP-K30A in 0.1 M bicarbonate buffer, pH 8.6. The wells were washed with sterile PBST

and to decrease nonspecific binding, 3% BSA in PBST was added for 1h at room temperature. Meanwhile a canine naïve phage library build from dog spleens was diluted in BSA and added to a blank well, as pre-clearing step. After 1h of incubation the phage library was transferred to the CHIP coated wells and incubated for 1h. The plate was extensively washed with sterile PBS-T and the bound phages were eluted in 100 µl triethylamine (100 nM), and neutralized with 22 µL of 1 M Tris/HCl, pH 7.4. Eluted phage were amplified by infection of fresh *E. coli* TG1 cells in the presence of helper phage M13KO7 (New England BioLabs) and kanamycin (50µg/mL). The phages were purified from the culture supernatant by PEG/NaCl (20% polyethylene glycol 6000, 2.5 M NaCl) precipitation and resuspended in PBS. The phage obtained were then further selected with two more rounds of biopanning and the binding ability of all three rounds was tested as described in *'Polyclonal Phage-ELISA'*.

2.6. Polyclonal phage-ELISA

Biopanning was monitored using polyclonal phage-ELISA. Wells were coated overnight with 1 µg His-CHIP and CHIP-K30A, washed five times with PBS-T and blocked with 3% BSA for 1h. Phages obtained from each round of panning were added to the corresponding wells. After one hour incubation at room temperature, the wells were washed and anti-M13 antibody conjugated to HRP was added to each well and incubated for one hour. The microtiter plate was then washed and electrochemical luminescence was quantified using a luminometer.

2.7. Monoclonal scFv Isolation

Biopanning rounds 2 and 3 were used for selection of monoclonal scFv antibodies. *E. coli* TG1 bacteria transformed with phagemids were plated on LB agar containing 100 µg/ml of ampicillin and grown overnight at 37ºC. Single colonies were picked and cultured in LB medium containing 100 µg/ml of ampicillin and 0.1% of Glucose and grown at 37ºC, constituting a starter culture. After 4h, 8 µL of the starter culture was used to inoculate 800 µL of LB supplemented with Ampicillin and Glucose and grown for 2h at 37ºC. A glycerol stock was made from the remaining starter culture. Protein production was induced with 1 mM of IPTG overnight at 30ºC. The cells were lysed through multiple freeze/thaw cycles and the plate was centrifuged for 10 minutes at 4000 g.

2.8. Soluble ScFv Binding Assay

Ninety six well microtiter plates were coated with the target proteins (His-CHIP and CHIP-K30A) in bicarbonate buffer pH 9.6 and left to incubate overnight at 4ºC. The plates

were washed five times in PBST and blocked with 3% BSA for 1h. Lysate containing scFv was added to the wells and incubated for 1h. The wells were washed and protein A conjugated to HRP was added. After 1h of incubation the microplate was washed and electrochemical luminescence was quantified using a luminometer (Labsystems Fluoroskan Ascent FL). The clones with the highest affinity were then further validated by probing against the target they were designed against, the other target and α-synuclein (as a negative control).

2.9. Isolation of plasmid-DNA from *E. coli*

Plasmid DNA from the clones with highest affinities were isolated from TG1 cells grown from the starter culture using QIAprep Spin Miniprep kit (QIAGEN), according to the manufacturer's protocols. Yield and quality of plasmid DNA was analysed using a NanoDrop spectrophotometer. The isolated plasmid DNA was stored at -20ºC.

2.10. ScFv clones Sequencing

A sample of each clone's plasmid DNA was sent for Sanger sequencing at Source BioSciences (BioCity Scotland, Lanarkshire) with the primer GIIIFOR (sequence: ACTTAAAAGACATACTCCAAAACG). Once received, DNA sequences were translated to protein sequences using the software ExPASy - Translate tool (Gasteiger et al., 2003) and aligned with Clustal Omega (Sievers et al., 2011).

2.11. Medium Scale scFv Production and Purification in TG1 cells

Selected scFv clones were picked from the starter culture and grown overnight in 5 ml of LB supplemented with 100 µg/ml of ampicillin and 0.1% Glucose at 37°C and 250 rpm. This culture was then used to seed 250 mL of LB (plus 100 µg/ml of ampicillin and 0.1% Glucose), which was cultured for approximately 4 h. Protein production was then induced with 1 mM IPTG overnight at 37°C and 250 rpm. Bacteria were harvested by centrifugation (4000 rpm, 4°C, 10 min), resuspended in 10 ml of PBS 1% Triton-X and incubated for 30 minutes at 4ºC in a rotating wheel. Lysis was achieved by sonication. Cell debris was removed by centrifugation (13000 rpm, 4°C, 10 min), and the supernatant was collected. Antibody fragments were purified using 500 µL of Protein A resin (Amintra). Soluble scFv concentration and purity was estimated by InstantBlue (Expedeon) stained SDS–PAGE gels.

2.12. Medium Scale scFv Production and Purification in BL21-DE3 cells

Competent bacterial cells BL21 (DE3) were transformed with scFv plasmids extracted as was described in *'Isolation of plasmid-DNA from E. coli'* using the heat shock method as described in *'Transformation of E. coli by heat shock'*. Single colonies were picked from the plate, inoculated into 100µL of LB medium supplemented with 100 µg/ml of ampicillin and incubated at 37ºC, in order to grow a starter culture. After 4h, 8 µL of the starter culture was used to inoculate 800 µL of LB medium with Ampicillin and grown for 2h at 37ºC. A glycerol stock was made from the remaining starter culture. Protein production was induced with 1 mM of IPTG overnight at 30ºC. The bacterial cells were lysed through multiple freeze/thaw cycles and centrifuged for 10 minutes at 4000 g. The lysate was used in a binding assay in order to determine if the bacterial cells' transformation had been successful. Afterwards the clones were picked from the starter culture and grown overnight at 37°C and 250 rpm in 5 mL of LB medium complemented with 100 µg/ml of ampicillin. This culture was then used to seed 250mL of fresh LB-Ampicillin, and grown until OD_{600}~0.6. ScFv antibodies production was then induced with 1 mM IPTG overnight at 37°C and 250 rpm. Bacteria were harvested by centrifugation (4000 rpm, 4°C, 10 min), resuspended in 10 ml of PBS 1% Triton-X and incubated for 30 minutes at 4ºC in a rotating wheel followed by sonication. Cell debris were removed by centrifugation (13000 rpm, 4°C, 10 min), and the supernatant was collected. Antibody fragments were purified using 40 mg of Protein A Sepharose CL-4B (GE Healthcare). Soluble scFv concentration and purity was estimated by Coomassie Brilliant Blue R-250 stained SDS–PAGE gels.

2.13. Binding Assays

Purified Protein (α-synuclein, His-CHIP, CHIP-K30A) was immobilized in microtitre plates in 0.1M NaHCO3 (pH 8.6) overnight at 4ºC. Following washes in PBS supplemented with 0.1%Tween, the wells were blocked with 3% BSA in PBS. A titration of the protein of interest was added for 1h at room temperature. Binding was detected using anti-α-synuclein or anti-CHIP 3.1 followed by HRP-tagged anti-mouse secondary or using ProteinA HRP-conjugate. Electrochemical luminescence was quantified using a luminometer.

2.14. Native Gel

Polyacrylamide gels of appropriate percentage (8%) were used for separation of protein samples. The samples were mixed with 2x Native sample buffer (25% Glycerol, 0.3M Tris pH 6.8, bromophenol blue, MilliQ water) in a ratio of 1:1, heated for 3 to 5 minutes

at 95ºC and then allowed to return to room temperature before being loaded onto the gel. The gels were run in Tris-Glycine running buffer at a constant voltage of 85V until the dye front reached the end of the gel.

2.15. Ubiquitination Assays

For *in vitro* ubiquitination assays, 0.1 µg purified α-synuclein was incubated with 3 µg of His-CHIP, 1 µM UbcH5α, 100 nM Ube1, 2 µg ubiquitin, and 3 mM ATP (Sigma), in reaction buffer (25 mM HEPES, 10 mM $MgCl_2$, H_2O, 0.5 mM DTT, 1 mM Benzamidine and, when mentioned 0.05% of Triton-X or n-Dodecyl-β-D-maltoside (ULTROL grade; Calbiochem)) for up to 60 minutes at 30ºC. If required, scFvs were added to the ubiquitination mix before the start of the reaction with CHIP (see legends for details). Samples were analysed by SDS-PAGE using 12% or 15% polyacrylamide gels followed by Western blot with anti-α-syn mouse monoclonal or anti-CHIP 3.1 mouse monoclonal and anti-mouse secondary.

2.16. Immunoblotting

Separated proteins were transferred from the SDS-PAGE gel to nitrocellulose membrane (0.2µm, Advantec). The transfer was carried out in Glycine/Tris/Methanol transfer buffer at a constant amperage of 400mV for 1h15. Membranes that were to be revealed with anti- α-synuclein antibody were incubated in 0.4% Paraformaldehyde (PFA) for 30 minutes and rinsed with MilliQ water (Millipore) water before blocking. Blocking is performed overnight with 5% (w/v) skimmed milk powder in PBS. After blocking, incubation with primary antibody diluted in blocking buffer was carried out for 1h at room temperature, followed by four 5 minutes washes with shaking in PBST. Anti-CHIP 3.1 (1:2000), anti- α-synuclein (1:2000) and anti p53 DO-I (1:1000) were used as primary antibodies and detected with secondary polyclonal anti-mouse antibody coupled to HRP (1:1000) diluted in blocking buffer incubated with the membrane for 40 minutes. After another set of four washes in PBST of 5 minutes with shaking, the blot was overlaid with a mix of ECL reagents I and II (1:1) for one minute, dried and exposed to x-ray film for the preferred period of time. The film was developed with a film processor.

IV. RESULTS

1. Expression and Purification of His-CHIP

In order to obtain CHIP for biopanning, scFv characterization and the enzyme assays, a plasmid encoding wild type Histidine tagged CHIP protein was expressed in *E. coli* BL21 (DE3) according to the already optimized protocol described above.

Previously to protein purification, bacterial culture samples collected before and after induction with IPTG were pelleted, resuspended in PBS, sonicated and the cell debris pelleted in order to collect whole protein extract. A fraction of whole protein extract was further centrifuged to obtain soluble protein extract. The extracts were then separated using an SDS-PAGE gel and stained with Coomassie Brilliant Blue to test the expression and confirm that CHIP had been produced successfully, before initiating the purification process.

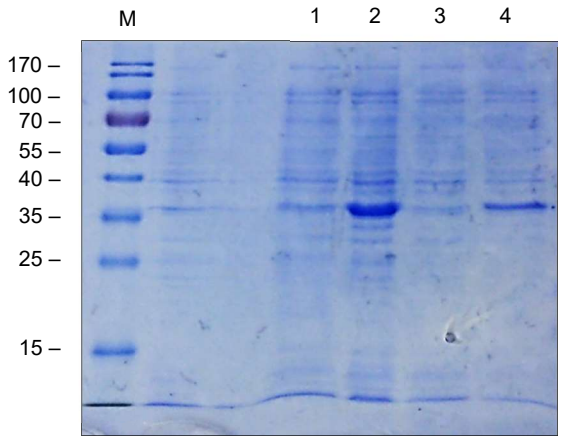

Figure 9. SDS-PAGE analysis of expression trail for CHIP protein.

Bacterial culture samples were prepared and resolved on 12% (w/v) SDS-PAGE gel and then stained with Coomassie brilliant blue. M: Molecular weight marker; 1: 10µL of Whole Protein Before IPTG fraction; 2: 10µL of Whole Protein After IPTG fraction; 3: 10µL Soluble Protein Before IPTG fraction; 4: 10 µL of Soluble Protein After IPTG fraction.

The expression trail confirms that a protein of approximately 35kDa, which is consistent with the expected molecular weight for CHIP, was successfully overproduced in an appreciable concentration, after induction with IPTG (Figure 9). CHIP was expected to be fully present on the soluble fraction, after induction with IPTG, but there is less of the 35 kD band in this fraction than in the whole protein fraction; this may be due to excessive centrifugation of the sample or the presence of other proteins with the same molecular weight as CHIP that are not present in the soluble fraction.

Following protein purification, concentration was evaluated on a Nanodrop spectrophotometer and an SDS-PAGE gel was run to assess the efficiency of the purification process and confirm the concentration of the purified protein, by comparison with BSA standards.

	M1	M2	Average
Concentration (mg/mL)	3.217	3.231	3.224
A260/A280	0.64	0.64	

Table 2. Determination of the Concentration of CHIP after purification by NanoDrop.

Two separate measurements were carried out, using the protein buffer to establish a baseline, and the values obtained were very similar and point towards a concentration around 3.2mg/mL. The 260/280 absorbance ratio is very close to the optimal value (0.6) which indicates there is no contamination with nucleic acids (table 2).

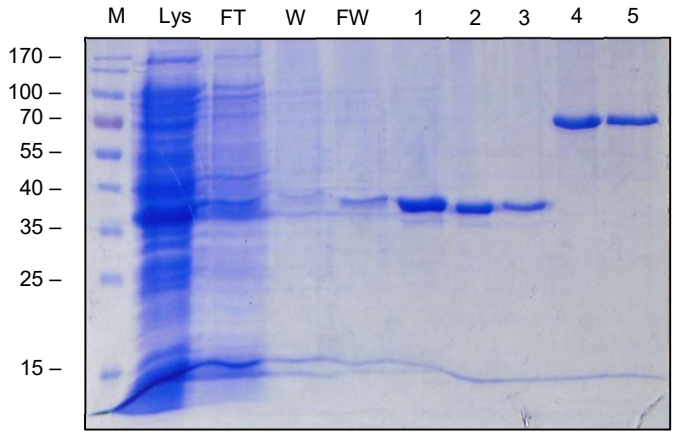

Figure 10. SDS-PAGE analysis of CHIP's affinity purification.

Affinity purified His-CHIP obtained from the expression system was resolved on 12% SDS-PAGE gel and posteriorly stained with Coomassie brilliant blue. M: Molecular Weight Marker; Lys: 10µL of Lysate; FT: 10µL of Flow Through, W: 10µL of washing fraction; FW: 10µL of Final washing fraction; 1: 1µL of His-CHIP; 2: 0.66µL of His-CHIP; 3: 0.33µL of His-CHIP; 4: 1 µL of 2mg/mL BSA standard; 5: 1µL of 1mg/mL BSA standard.

The SDS-PAGE gels shows that the purification was successful although some protein seems to have remained in the flow through and some was lost in the final wash (Figure 10). The comparison with the BSA standards is in agreement with the Nanodrop quantification since the purification yield seems to be higher than 2mg/mL. As such it will be considered that purified His-CHIP is at a concentration of 3.2mg/mL, as indicated by the Nanodrop.

2. ScFv development and selection

The phage library was subjected to three rounds of biopanning against 1ug of His-tagged CHIP and untagged CHIP K30A immobilized on the surface of a microtiter plate well. For each round of panning, the phages were pre-cleared on a blocked well to exclude phages binding to the blocking agent. After the biopanning rounds the goal is to have two phage libraries of single chain antibodies that bind to CHIP and to CHIP-K30A.

At the end of rounds 1 and 2, small fractions of each library were used in the following round and the remainder was stored for future analysis. After the biopanning, the three polyclonal rounds of each library were probed for binding against the target they had been selected against, the second target and uncoated wells. The results are presented in the graph below.

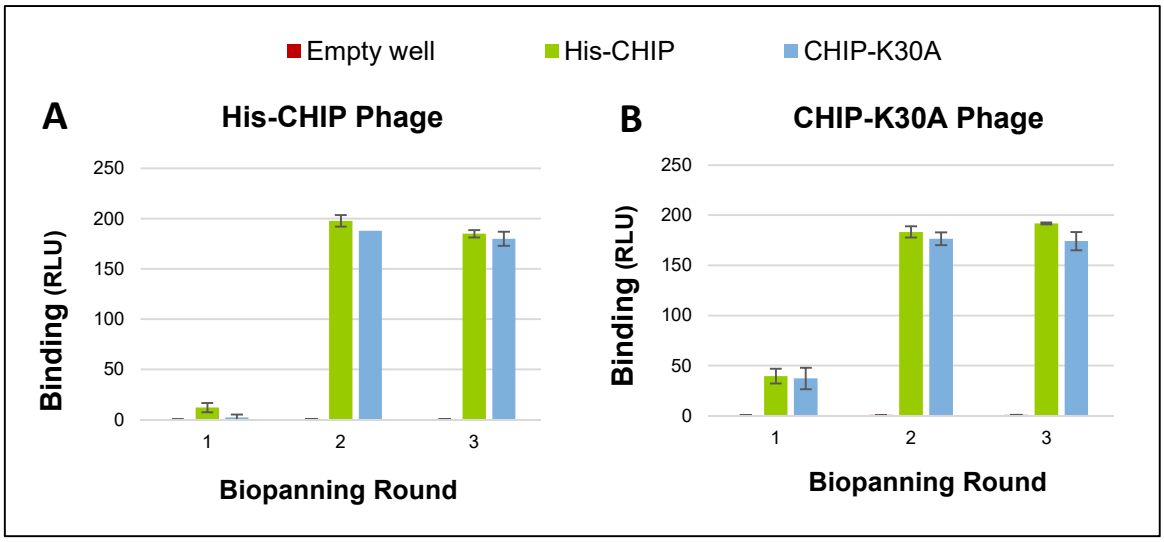

Figure 11. Enrichment of CHIP and CHIP-K30A binding phages through biopanning.

CHIP (A) or CHIP-K30A (B) phages obtained following each round of biopanning were tested against CHIP, CHIP-K30A and uncoated wells by Polyclonal Phage ELISA. Phages were detected with anti-M13 Phage polyclonal antibody conjugated with Horseradish peroxidase (HRP) and enhanced chemiluminescence. Binding is expressed in relative light units (RLU) and have been plotted as mean ± SD of duplicates.

The biopanning was successful as there was an increase in binding to the target following the first two rounds of panning (Figure 11). Since no substantial increase was obtained on the third round of panning, no more rounds were performed. The results also show that the polyclonal pools of phages show no specific affinity for CHIP or CHIP-K30A, binding indiscriminately to both targets despite having only been selected against one. This was to be expected as the difference between the two targets resides in the change of only one amino acid. Although this change produces structural alterations that may impact binding, at this stage, the phage libraries were polyclonal and as such there were

scFv antibodies with different binding affinities and probably capable of binding to different zones of the target proteins.

After the biopanning, dilutions of the second and third round of the CHIP and the CHIP-K30A phage libraries were used to infect *E. coli* TG1 and these were then plated out in agar-LB plates and grown overnight. Afterwards, 48 colonies from each library were randomly selected from both dilutions and grown in microtiter plates. Expression of soluble scFv-antibodies was induced by 1mM IPTG and rupturing of the bacterial cells was achieved through several freeze-thaw cycles. The supernatant obtained, after pelleting the cell debris, was used to test the scFv specificity in direct ELISA experiments against bacterially expressed CHIP or CHIP-K30A according to the target that had been used for the panning process and against α-synuclein as a negative control.

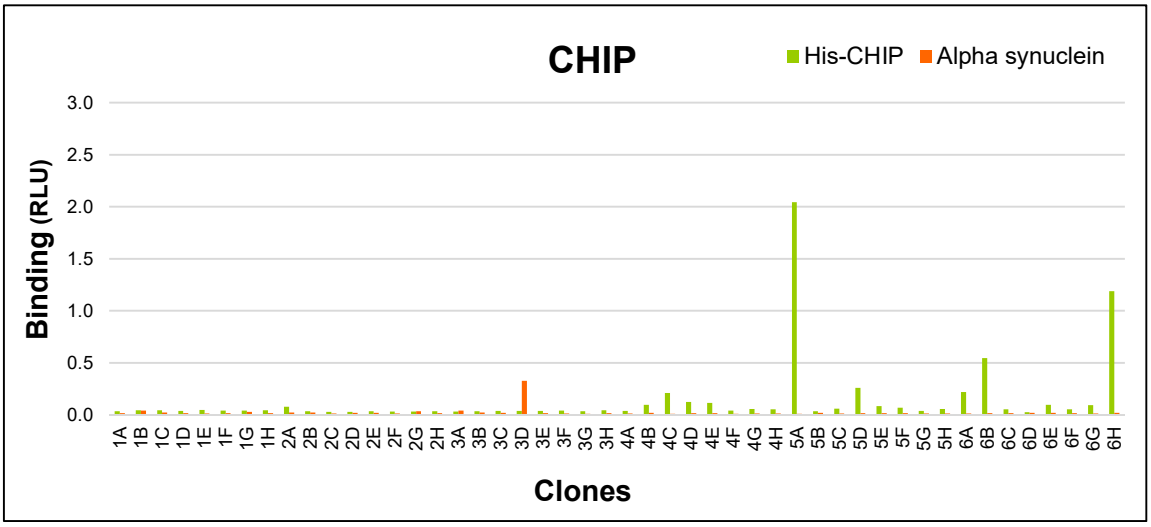

Figure 12. Screening of CHIP library selected clones in soluble scFv binding assay.

Binding activity of 48 randomly selected scFv-fragments after biopanning, against 0.1µg CHIP and 0.1µg alpha synuclein was revealed by direct ELISA. Bacterial supernatant was added and bound scFvs were detected with 1:1000 diluted ProteinA polyclonal antibody conjugated to horseradish peroxidase and enhanced chemiluminescence. The results are given in relative light units.

Overall the signal for binding to His-CHIP (Figure 12) was quite low and most of the clones selected did not present visible binding affinity for the target protein as the signal for CHIP coated wells was similar to the signal for wells coated with α-synuclein, the negative control. Inclusively there was one clone that appear to have a higher affinity for α-synuclein than CHIP.

As for the CHIP-K30A library (Figure 13), several clones seemed to bind to the target and there was one clone (11F) that presented a particularly high binding capacity in

comparison with the others, indicating that it might be a promising scFv antibody to take forward.

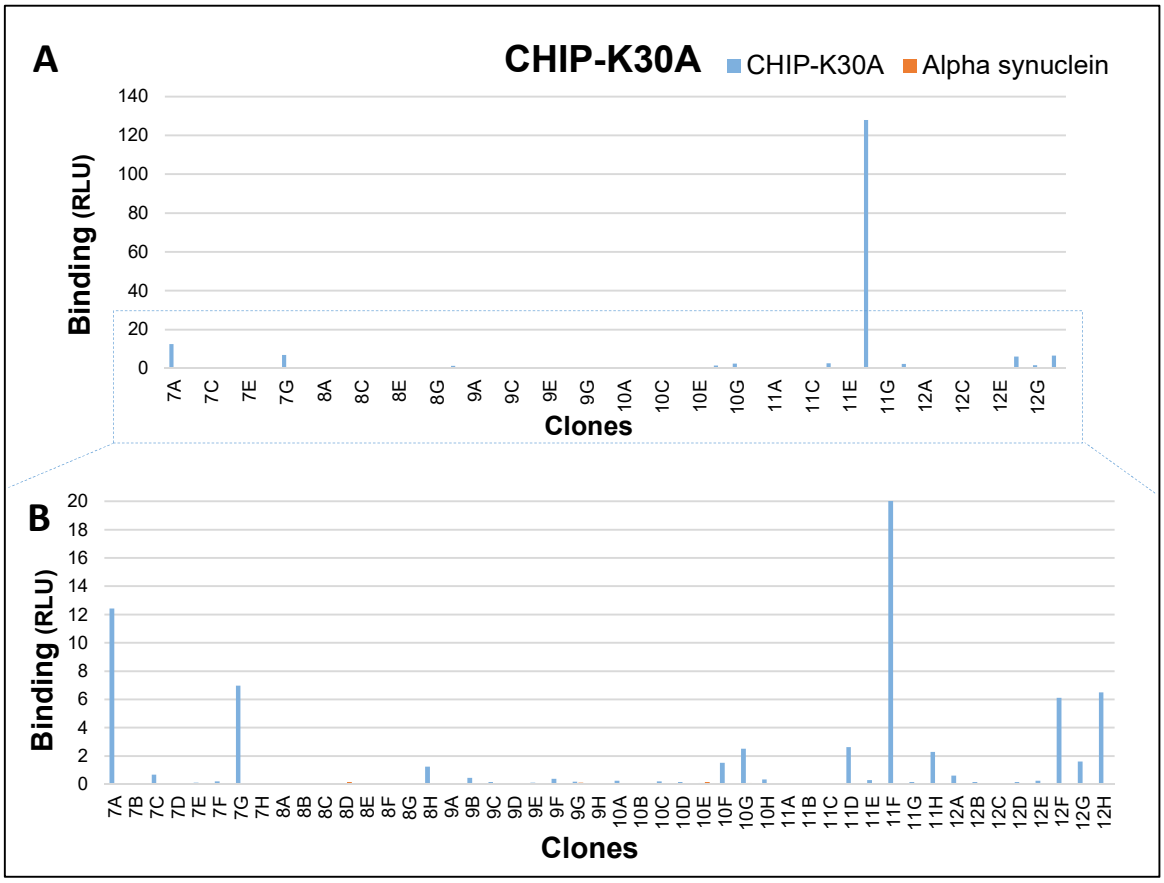

Figure 13. Screening of CHIP-K30A library selected clones in soluble binding assay.

(A) Binding activity of 48 randomly selected scFv-fragments after biopanning against 0.1µg CHIP-K30A and 0.1µg α-synuclein was revealed by direct ELISA. (B) Same as in (A) but with a smaller scale on the y axis to highlight other binders that, despite not being as strong binders as 11F, presented a considerable signal, clearly demarked from the negative control. The results are given in relative light units.

In this stage it is already possible to perceive the diversity of binding affinities present in the polyclonal pool of phages although it is likely that some of the differences observed may be due to different expression rates of different clones.

As these assays were performed without duplicates, the clones with the highest binding for each library were selected for further validation, in order to confirm the binding to the target used in the biopanning rounds and check for cross-reaction with the other target.

3. Sequencing analysis and validation of scFv

In order to further validate the scFv clones with the highest binding affinity, for the target from each library, the clones were probed against CHIP and CHIP-K30A, independently of which target was used to design them, and also against α-synuclein as a negative control, by direct ELISA. This would confirm that the generated scFv were capable of binding to the target and determine if any of them were specific for the wild type or the mutant CHIP.

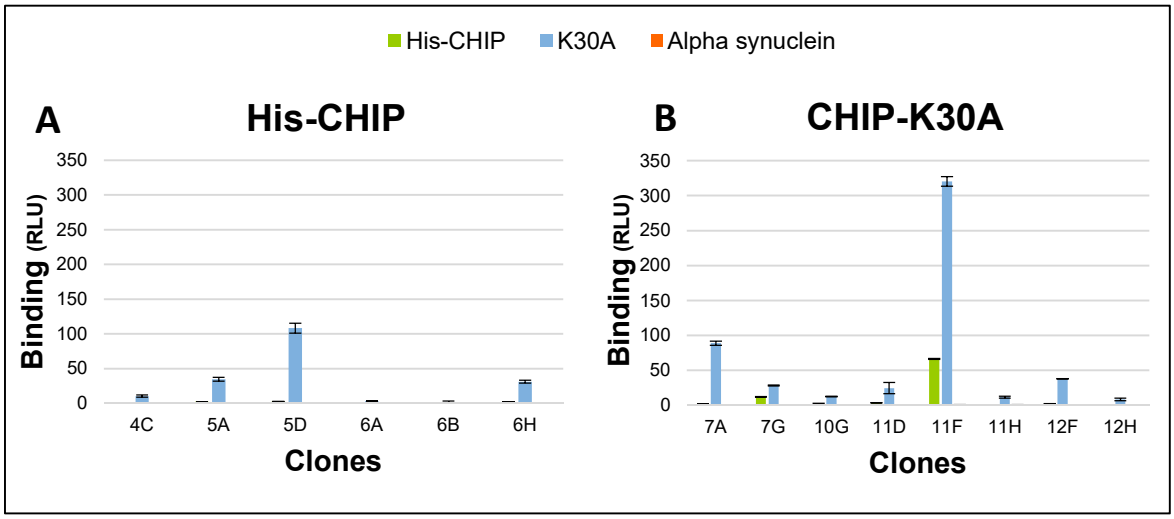

Figure 14. Validation of the scFv clones with highest affinity.

Binding activity of the 14 selected scFv-fragments with the highest binding from both His-CHIP (A) and CHIP-K30A (B) libraries against 0.1ug/mL WT CHIP, 0.1ug/mL CHIP-K30A and 0.1ug/mL alpha synuclein was revealed in soluble scFv binding assay. The results are given in relative light units and have been plotted as mean ± SD of duplicates.

All the selected scFv antibodies exhibit a higher binding affinity for the mutant CHIP-K30A than for wild type his-tagged CHIP, independently of the target they were selected for (Figure 14). This can be explained by the more stable conformation that the mutant adopts. The mutation decreases the degree of flexibility of the protein possibly decreasing the number of conformations it can adopt and resulting in a higher binding affinity.

As it is likely that some of these clones are actually the same, 12 of the 14 clones presented above were sent for sequencing so that it was possible to analyse their sequences and take forward only different clones. The clones 6A and 6B were excluded for presenting lower binding affinities.

In the 12 clones sent for sequencing, there were 8 different scFv antibodies. DNA sequences were translated to protein sequences using ExPASy - Translate tool and aligned with Clustal Omega software in order to be compared (Figure 15).

Figure 15. Alignment of the assumed amino acid sequences for the selected scFv clones with specificity for CHIP.

The singles chain sequences follow the direction 'heavy chain-Linker- Light chain' (V_H - L- V_L). The framework regions (red; FR), complementary determining regions (CDR) and linker (green; LINKER) are indicated. Within each CDR, different sequences are coloured differently. '*' (asterisk) indicates positions which have a single, fully conserved residue; ':' (colon) indicates conservation between groups of strongly similar properties, scoring >0.5 in the Gonnet PAM 250 matrix; '.' (period) indicates conservation between groups of weakly similar properties, scoring ≤ 0.5 in the Gonnet PAM 250 matrix.

As expected, generally, the framework regions show a high degree of similarity across all the sequences with most of the different amino acids having been exchanged by groups with similar properties. The CDRs in the light chain present the largest variety of sequences among the 8 clones, while in the heavy chain, CDR1 and CDR3 present only three different sequences each, among all the clones, and CDR2 has 6 different sequences.

Finally, the reactivity of the 8 selected clones was also analysed against untagged bacterially produced CHIP. This aimed to demonstrate the scFvs selected with His-CHIP (4C and 5D) were specific for epitopes in CHIP and not the histidine tag and that the scFvs were capable of binding to a form of CHIP without tags or mutations, that can alter the dynamics of the protein.

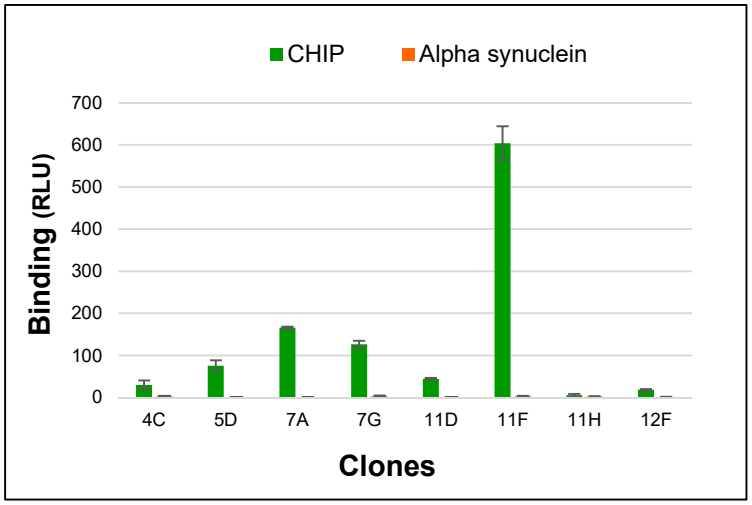

Figure 16. Reactivity of selected scFv clones against untagged CHIP.

A microtiter plate was coated with 0.1µg/mL of untagged CHIP and 0.1 µg/mL of α-synuclein and incubated overnight. The coating was washed off and the wells were blocked and periplasmic supernatant was added. Bound scFvs were detected with 1:1000 diluted ProteinA polyclonal antibody conjugated to horseradish peroxidase and enhanced chemiluminescence

All the clones displayed binding affinity for the untagged CHIP; in the case of 4C and 5D it also confirms that the scFv antibodies are specific for the CHIP protein and not for the histidine tag (Figure 16).

In summary, phage display technology allowed the selection and isolation of 8 single chain variable fragments specific for CHIP that bind to it with different degrees of reactivity which can be altered by small modifications in the protein as was shown by the different binding affinities observed for His-tagged CHIP and mutant K30A.

4. Soluble Expression and Purification of scFv clones

In order to overcome differences based on expression in microtiter plates and obtain purified scFvs that could then be used in other assays, the selected clones for each target were subjected to medium scale expression.

Initially the scFv clone that had shown the highest signal, 11F, was grown from the E.coli TG1 starter cultures generated at the time of the selection of monoclonals, in LB medium enriched with Ampicillin and 1% of Glucose. The addition of glucose, inhibitor of the lacZ promoter, was meant to repress the pIII fusion expression which is regulated by the lacZ promoter in the phage vector. Protein expression was induced by 1mM of IPTG overnight at 30ºC. Purification was accomplished using ProteinA beads and scFv were eluted from the beads with 0.2M Glycine pH 2. Five fractions were collected and immediately neutralised with 1M Tris pH 9.

The efficiency of the purification process was evaluated and the concentration of the fractions determined with SDS-PAGE gesl where samples of the lysate, flow through, washes, elution fractions and BSA standarts were run. The gels were stainned with InstantBlue since standard Comassie blue was not sensitive enough to detect the bands of eluted scFv (data not shown).

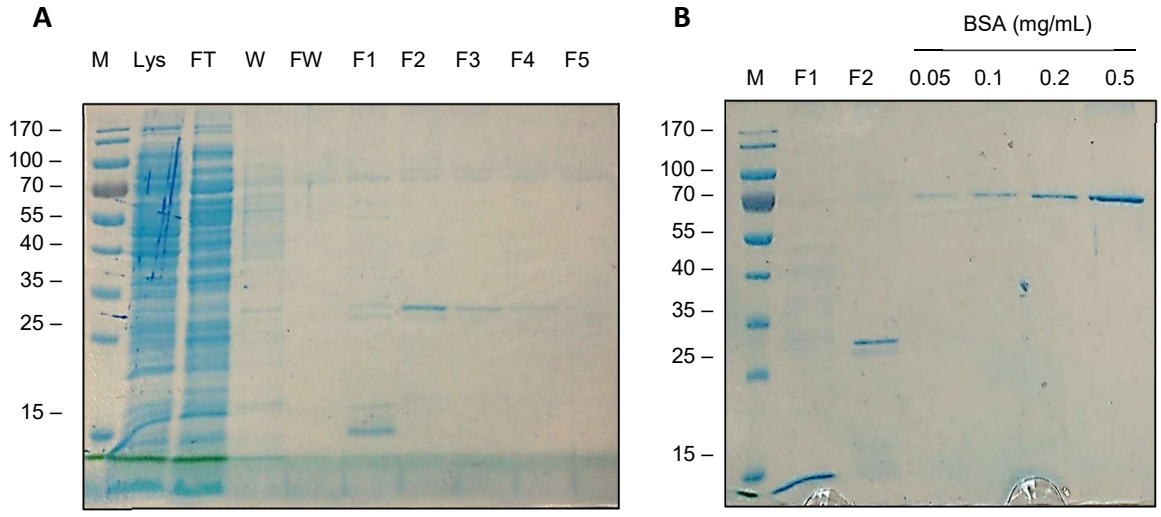

Figure 17. Soluble Expression, purification and quantification of scFv 11F in E. coli TG1.

Proteins were separated on 12% SDS-PAGE gel and stained with InstantBlue **(A) SDS page analysis of scFv 11F Purification.**. M: Marker; Lys: 10 µL of lysate; FT: 10 µL of flow through; W: 10 µL of washing fraction; FW: 10 µL of final washing fraction; F1, F2, F3, F4, F5: 10 µL of elution fractions. **(B) Quantification of scFv 11F.** F1, F2: 10 µL of elution fractions; BSA standards: 1µL of each BSA standard was loaded into the gel.

The production and purification process was successful but the yielded low concentrations of scFv (Figure 17A). The first elution fraction showed the presence of a 15kDa protein which is presumably a low affinity contaminant that elutes first from the column. It is possible to see bands of approximately 30kDa, in the elution fractions, which is, generally, the approximate molecular weight for scFv antibodies. The second elution fraction presents the highest concentrations of scFv; fraction 3 seems to have a very light band too but fractions 4 and 5 don't have any scFv. The concentration of fraction 2 was estimated, by SDS-PAGE with BSA standards, as approximately 0.02mg/mL. This fraction was further used in other assays.

As the production and purification did not yield a great amount of scFv, it was necessary to do so again. The second time, *E.coli* BL21-DE3 cells were used; these, unlike TG1, can read the amber stop codon upstream of the gene pIII sequence, resulting in expression of non-fused scFv. The bacterial cells were transformed with scFv plasmids using the heat shock method and starter cultures were grown.

Before proceeding with the production and purification of the scFv, the success of the BL21-DE3 cells transformation was assessed. For this, small bacterial cultures were grown and scFv production was induced with IPTG. The cells were lysed through multiple cycles of freeze/thaw and the lysate was used in a binding assay to determine if the cells were producing scFv.

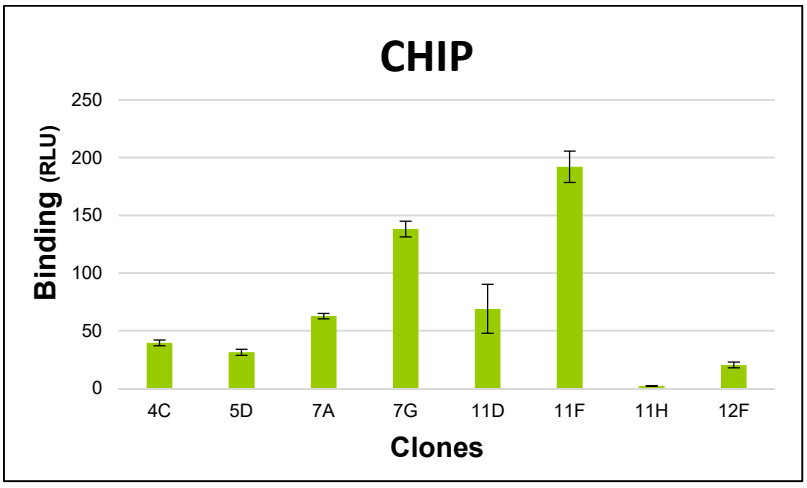

Figure 18. Transformation of E.coli BL21-DE3 with scFv plasmids.

Transformation of BL21-DE3 bacterial cells with scFv plasmids was assessed by inducing scFv production and detecting binding activity against 0.1ug/mL CHIP in a direct ELISA. Bacterial lysate was added and bound scFvs were detected with 1:1000 diluted ProteinA polyclonal antibody conjugated to horseradish peroxidase and enhanced chemiluminescence. Results are shown in RLU and were plotted as mean ± SD of triplicates.

The binding assay showed there was production of functional scFv antibodies capable of binding to His-CHIP (Figure 19); thus the transformation was successful and so the production and purification process was carried out.

A small culture was grown overnight from the starter culture and then diluted in 250mL of LB enriched with ampicillin. The OD was carefully monitored and scFv production was induced with 1mM IPTG once OD~0.6. The cultures were then incubated overnight at 30ºC.

Of the eight selected single chain fragments all were produced (data not shown) but only four were successfully purified from protein A beads. Five fractions of each scFv fragment were eluted with 0.2M Glycine and immediately neutralized with 1M Tris. Following the purification, the SDS-PAGE gel revealed the presence of a single band of approximately 30 kDa for scFvs 7A, 7G and 11F and the presence of a band of approximately 35 kDa for scFv 4C (Figure 19).

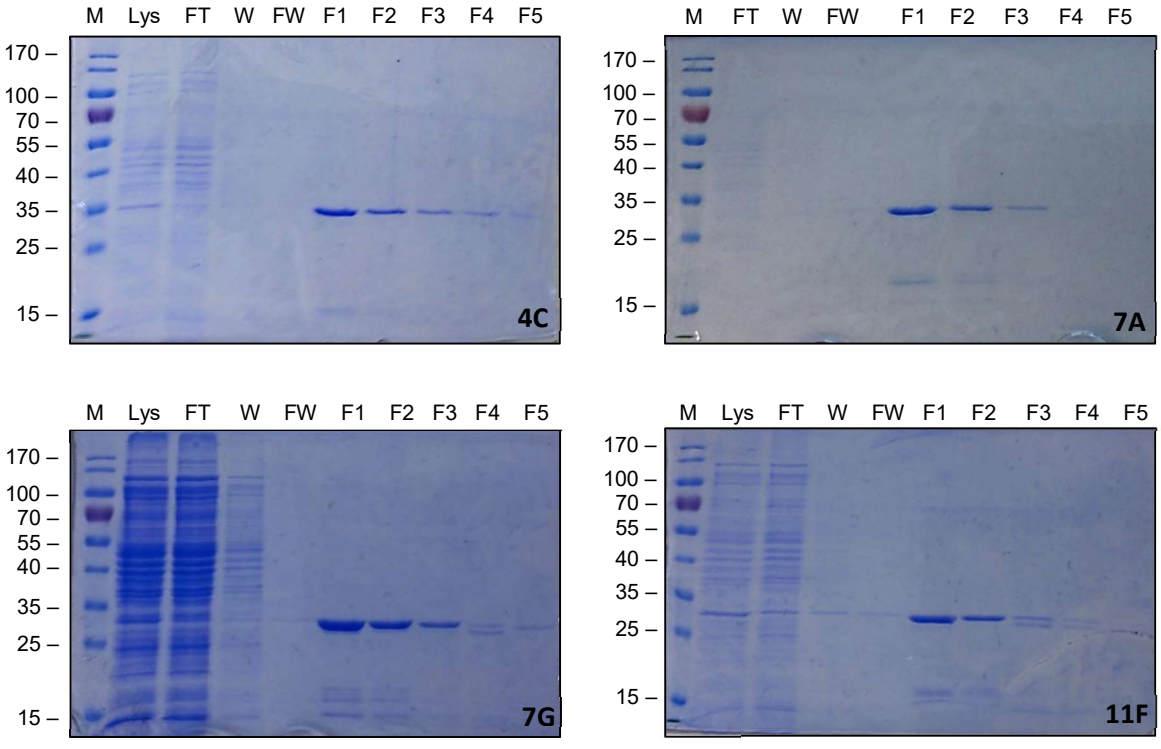

Figure 19. SDS-PAGE analysis of affinity purified scFvs 4C, 7A, 7G, 11F.

Selected scFvs (4C, 7A, 7G and 11F) were expressed in the E.coli strain BL21-DE3 upon induction with IPTG. Expressed scFvs were purified with Protein A beads. Proteins were separated on 12% SDS-PAGE gel and stained with Coomassie Blue stain. After an hour the gels were distained. M: Marker; Lys: 10 µL of lysate; FT: 10 µL of flow through; W: 10 µL of washing fraction; FW: 10 µL of final washing fraction; F1, F2, F3, F4, F5: 10 µL of elution fractions.

Afterwards, the scFv concentration was estimated through a Coomassie gel with BSA standards. The first fractions of 4C, 7A and 11F and the second fraction of 7G seem to have a concentration of approximately 0.1mg/mL and were chosen to be further used in subsequent assays. It is also possible to verify that 4C does indeed migrate slower than the remaining scFvs (Figure 20).

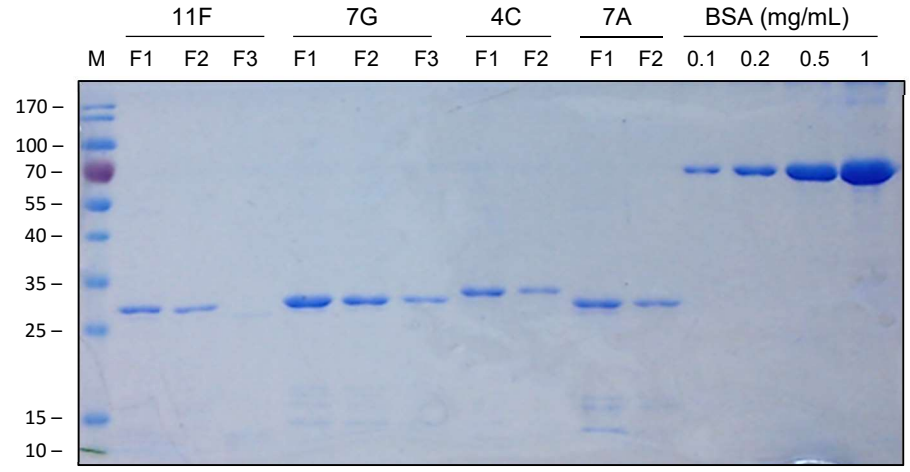

Figure 20. Quantification of purified scFv fractions.

Proteins were separated on 12% SDS-PAGE gel and stained with Coomassie Blue. M: Marker; F1, F2, F3: 10 µL of elution fractions; BSA standards: 1µL of each BSA standard was loaded into the gel.

5. Characterization of Purified scFv clones

In order to better characterize the purified scFv antibodies and to try to understand their behaviour several assays and analysis were conducted.

Initially, based on the scFv amino acid sequences, a set of biophysical and biochemical parameters were computed with the Expasy server's Protparam Tool and can be reviewed in the table 3.

The length of these four clones varies between 240 and 249 residues and the predicted molecular weight is around 26kDa. Considering figure 14 and comparing with this information, it is noticeable that all the scFvs run at a molecular weight slightly higher than anticipated. 7G presents the highest predicted molecular weight and in agreement with that runs slightly higher than 11F and 7A. However, 4C is the clone that migrates slower, even though it presents one of the lowest molecular weights. Analysing table 3 none of the parameters seems to suggest a reason as to why this would happen so it might be a structural problematic such as rigidity of a certain area or insufficient denaturation by SDS.

Primary Structure Comparison							
Clones	No. of residues	Molecular Weight	pI	Hidropathicity[1]	Aliphatic Index[2]	Instability Index[3]	Extinction Coeficient[4]
4C	240	25.65	5.56	-0.238	71	41	43110[a] / 42860[b]
7A	242	25.83	5.17	-0.253	68	32	44600[a] / 44350[b]
7G	249	26.19	6.72	-0.232	69	40	40130[a] / 39880[b]
11F	243	25.60	5.91	-0.262	68	40	45630[a] / 45380[b]

Table 3. Comparison of the Primary Structure of the purified scFv Antibodies.

These values were estimated using the ProtParam tool (http://www.expasy.org), based on the amino acidic structure of the scFv sequence. [1]Grand average of hydrophathicity (GRAVY) is calculated as the sum of hydropathy values of all the amino acids, divided by the number of residues in the sequence (Kyte and Doolittle, 1982) and ranges from -1.5 to 1.5. A more negative value implies a lower hydrophobicity overall. [2]Statistical index defined as the relative volume of a protein occupied by aliphatic side chains that can be considered a positive factor for the increase of thermostability of globular proteins (Ikai, 1980). [3]Statistical index based on the observation that there are certain dipeptides, the occurrence of which is significantly different in unstable proteins compared with those in stable ones (Guruprasad et al., 1990). A protein with an index under 40 is predicted stable whereas a value over 40 anticipates that the protein may be unstable. [4]It has been shown that it is possible to estimate the molar extinction coefficient of a protein from its amino acid sequence (Gill and von Hippel, 1989). Two values are produced, the first one (a) showing the computed values assuming that all cysteine residues appear as half cystines, and the second (b) assuming that all cysteine residues are reduced.

The clones 4C, 7G and 11F present borderline *in vitro* instability indexes but for 7A the value is lower than 40 suggesting that this scFv is more stable than the others. Additionally, the pI values (under 7) suggest that intracellularly the scFvs would adopt a negative charge and the negative GRAVY indicates hydrophilicity.

A direct ELISA was performed to examine the reactivity of the purified scFvs against His-CHIP and CHIP-K30A. To this end, the proteins were immobilized in microtiter plates and incubated with a titration of scFv.

In agreement with what had been described before, generally, all the clones are able to bind more strongly to the mutant than to wild type CHIP while presenting negligible binding for α-synuclein (Figure 21). Given the scFv ability to bind specifically to CHIP in ELISA, it is possible to conclude that all clones expressed functional scFvs.

All the clones display a rise in binding as the amount of scFv increases although there are different degrees of reactivity for the different clones. For the mutant CHIP-K30A, 4C is the weakest binder and 11F the strongest, as had already been suggested, whereas 7A and 7G present relatively similar reactivity. Regarding the wild type CHIP, 4C and 7A show the weakest binding and 7G and 11F the strongest.

It is also noteworthy that while the other clones show a great disparity between the reactivity against the mutant and wild type CHIP, 7G presents a only a small difference. While scFv 7A shows the greatest difference. This may suggest the scFvs bind to different epitopes more or less susceptible to changes in the conformation of CHIP.

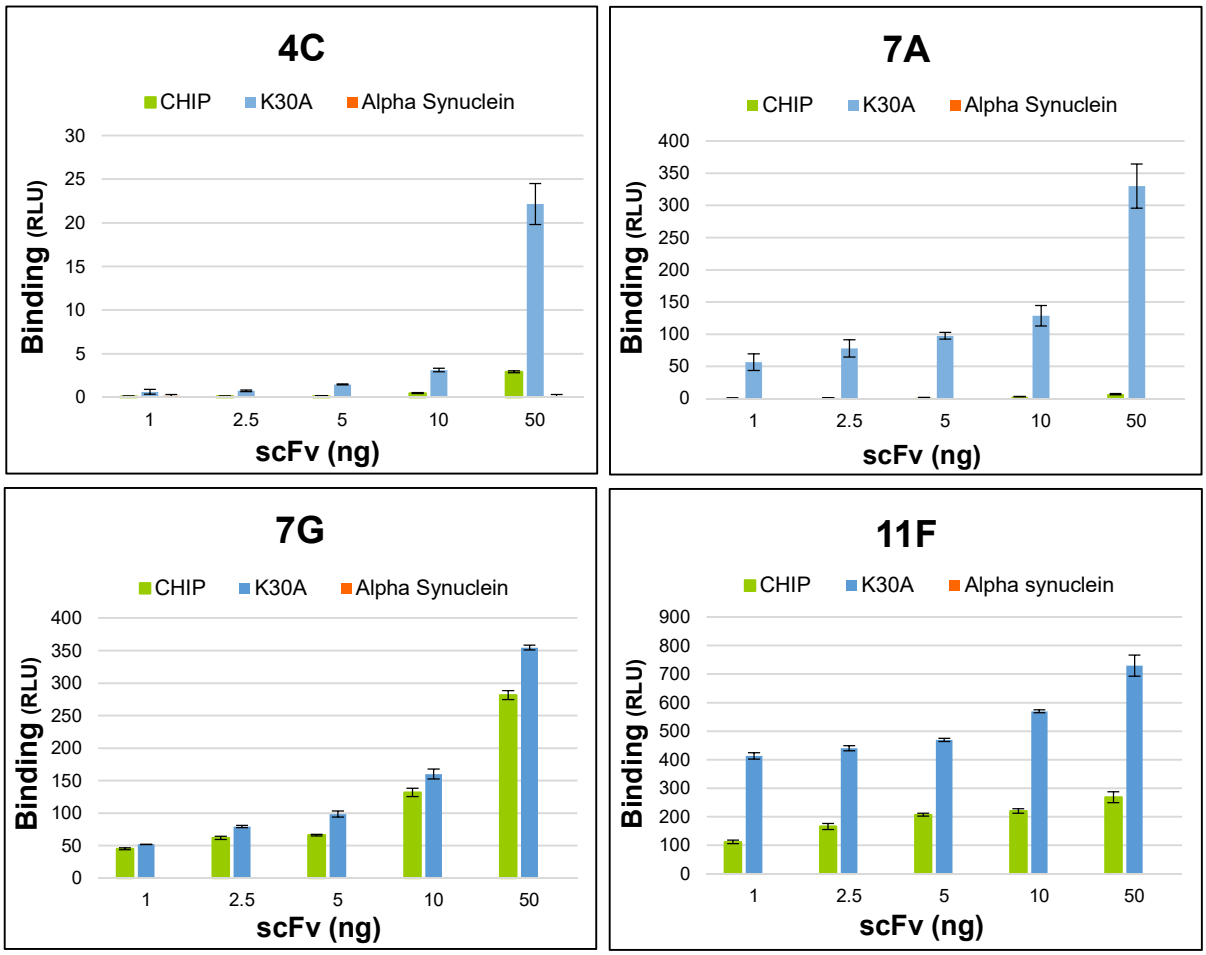

Figure 21. Binding of scFv purified from E.coli

50ng of His-CHIP, mutant CHIP-K30A and α-synuclein were coated on microtiter plate wells and a titration of the affinity purified scFv was added. Bound scFvs were detected by using Protein A HRP conjugate (1:1000). Results are displayed in RLU as mean ± SD of triplicates.The assay was run in the same plate and using the same reagents for all the scFvs in order to allow for a meaningful comparison between the binding affinities.

Considering the differences shown above together with the sequences of the scFv. ScFv 4C and 7A share most of the same heavy chain fragment, differing only in two amino acids in the CDR2 however they present a very different reactivity for CHIP. This suggests that either the bulk of the influence in binding resides on the light chain fragment or that the switch of two amino acids (threonine and Histidine) with bulkier side chains by two serines is enough to increase the binding to CHIP.

	Heavy Chain		
Clones	**CDR1**	**CDR2**	**CDR3**
4C	SYYMY	RITHDGSITYYADAVKG	TAI-------GSD
7A	SYYMY	RISSDGSTTYYADAVKG	TAI-------GSD
7G	SYTMS	AINSGGSSTKYTDAVKG	PAPRTAAPLNFDY
11F	SYYMY	RISSDGTDTFYADAVKG	SRVV------GAD
	** *	*. *: * *:*****	

	Light chain		
Clones	**CDR1**	**CDR2**	**CDR3**
4C	SGE--NLNKYYVR	KDTERPS	ESPVSTDTAAV
7A	SGRTNDIGIVGAS	SNGNRPS	QPFYTTFDSHV
7G	TGSSSNIGRGYVH	GISNRPS	SSWDSSLSAAV
11F	TGGNSNIGGNGVG	GDHYRPS	SSWDGSLGRHV
	:* . : .	***	. : *

Table 4. Comparative summary of CDRs' sequence from the purified scFv.

'*' (asterisk) indicates positions which have a single, fully conserved residue; ':' (colon) indicates conservation between groups of strongly similar properties, scoring >0.5 in the Gonnet PAM 250 matrix; '.' (period) indicates conservation between groups of weakly similar properties, scoring ≤ 0.5 in the Gonnet PAM 250 matrix. Matching amino acids are indicated in green.

An assay was also performed to evaluate the behaviour of the scFv in the presence of a CHIP titration. A titration of His-tagged CHIP was immobilized on a microtiter plate and incubated with scFv.

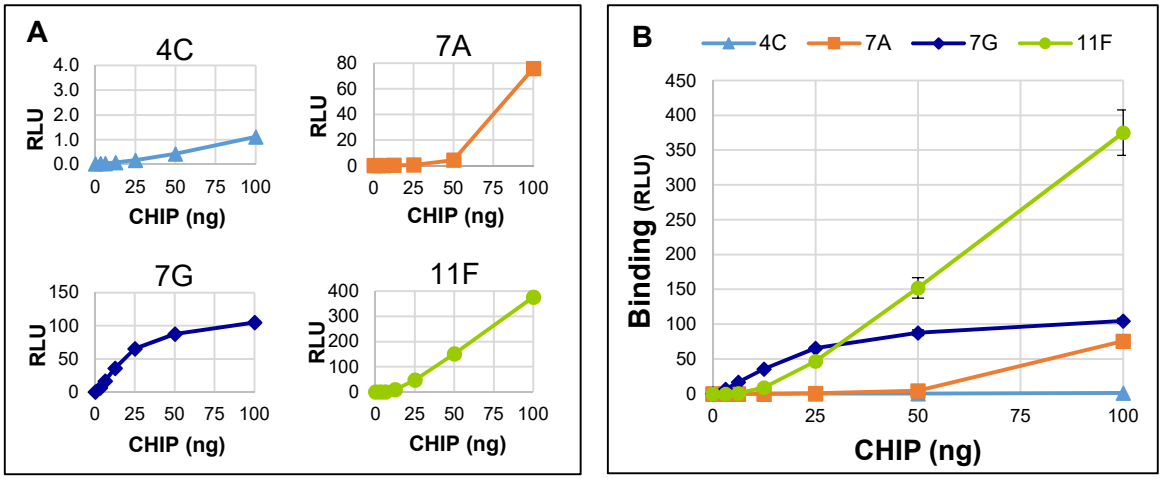

Figure 22. Reactivity of purified scFvs with CHIP Titration

(A) Binding Assay was performed by coating microtiter plates with a titration of His-CHIP (0-100ng) and 10ng of purified scFvs were added. Bound scFvs were detected by using Protein A HRP conjugate (1:1000). The assay was run in the same plate and using the same reagents for all the scFvs in order to allow for a meaningful comparison between the binding affinities. (B) Same as (A) but combined in the same graph. Results are displayed in RLU as mean ± SD of triplicates.

The four clones present very different binding patterns in the presence of a titration of CHIP but there are in agreement with what had been preciously observed with 11F

being the scFv with capacity to form more stable complexes, followed by 7G and 7A. While 4C appears to recognize the titration as small increments in signal can be observed, it still has low affinity for His-CHIP. 7A and 11F don't seem to distinguish very well between small concentrations of the protein but 7G presents continuously growing signal and appears to start to stabilize towards 100ng of CHIP.

Finally, in an attempt to gain some insight into how the scFv might influence CHIP's structure, the different scFv clones were incubated with His-CHIP and resolved in a Native-PAGE gel along with a sample of His-CHIP by itself and a control in the scFv buffer (Glycine and Tris).

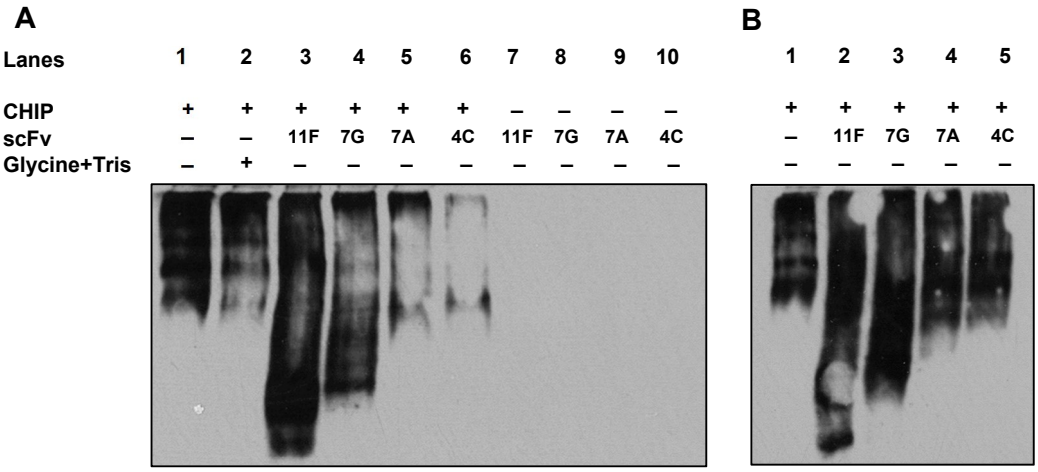

Figure 23. Native gel analysis of CHIP bound to scFv.

(A) His-tagged CHIP (3µg) was incubated by itself (lane 1), with 1µL of scFv buffer (lane 2) or with 0.1µg of scFvs (lanes 3-6) for 30 minutes at 30ºC. 0.1µg of scFv were also incubated on their own in the same conditions (lanes 7-10). Native sample buffer was added and the samples were run in 8% polyacrylamide gels. Detection was performed by Western Blot using anti-CHIP 3.1. **(B)** The experiment was repeated to clarify the impact of 7A and 4C on CHIP.

The results show a demarked increase in CHIP species that migrate faster on the native gel when scFv 11F and 7G are present while this doesn't happen with 7A and 4C. These results are independent of the scFv buffer as the pattern for this control is similar to the run of CHIP alone (Figure 23).This suggests that perhaps 11F and 7G are promoting the disassembly of CHIP, possibly by binding to an area essential for the association of the monomers.

6. CHIP interacts with α-Synuclein *in vitro*

Concurrently with the development and characterization of the scFvs, CHIP's *in vitro* activity on α-synuclein was studied in order to gain some insight into the possible dynamics of this interaction and to establish an assay that would allow the study of scFvs' influence in the activity of the E3 ligase CHIP.

A binding assay was performed with α-synuclein bound to the plate and CHIP in the soluble phase and in the alternative orientation.

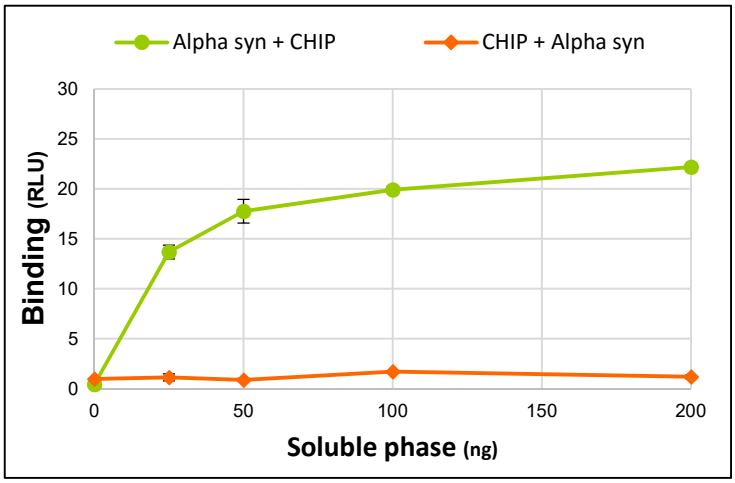

Figure 24. CHIP binds to α-synuclein *in vitro*.

0.1ug of purified His-CHIP (orange) or α-synuclein (green) was coated onto microtiter plates wells and a titration of α-synuclein (0-200ng) or His-CHIP (0 -200ng), respectively, was added. Bound CHIP was detected by using anti-CHIP 3.1 (1:1000) and α-synuclein with anti-α-synuclein (1:1000), both followed by anti-mouse (1:1000) and detected with ECL and the results are shown in RLU. The data is representative of two independent experiments and presented as mean ± SD of triplicates.

It is clear that CHIP is capable of binding to α-synuclein, in the conditions of the assay, but only when it is in the soluble phase (Figure 24). This suggests that either CHIP binds to the plate using the same interface used to bind to α-synuclein or that the binding to the plate restricts the flexibility of CHIP, forcing the protein to adopt a conformation that doesn't allow for binding to α-synuclein.

Afterwards, and given that CHIP is primarily an E3 ubiquitin ligase, it was studied CHIP's *in vitro* ubiquitination activity on α-synuclein.

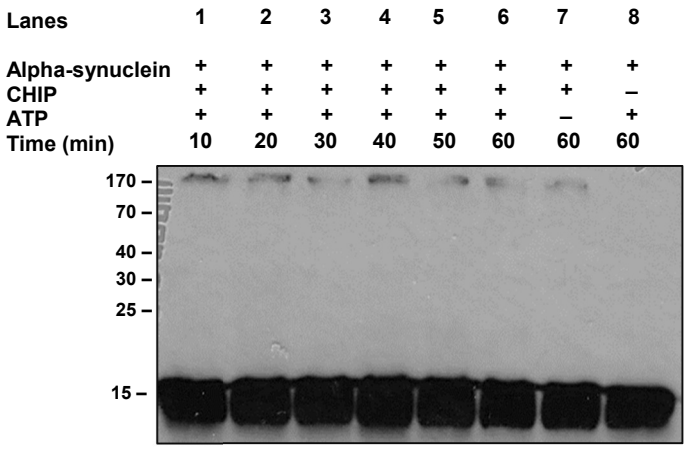

Figure 25. In vitro ubiquitination of α-synuclein by CHIP.

Immunoblot of in vitro ubiquitination reactions assembled using ATP, ubiquitin, Ube1, ubcH5α and **α**-synuclein and started with His-CHIP. The samples were incubated from 10 to 60 minutes at 30ºC and the reaction was stopped with the addition of sample buffer.

Several variations of the ubiquitination assay were tried but it was not possible to see any pattern that could correspond to ubiquitinated α-synuclein (Figure 25) even with long exposures.

There has been some controversy regarding endogenous α-synuclein detection in western blot as very different results have been obtained. However it has been proposed that crosslinking α-synuclein to the membrane using chemicals as paraformaldehyde (PFA), allows for a strong and clear detection (Newman et al., 2013). Even though this study is not being conducted with endogenous α-synuclein, a new assay was performed and this technique was attempted by incubating the blot in a low concentration of PFA, previous to blocking.

Interestingly, incubation with PFA, resulted in the appearance of bands of ubiquitinated α-synuclein, as can be seen in lanes 4-8 when compared with lanes 2 (control without E3) and 3 (control without ATP) (Figure 26).

The data shows that CHIP can efficiently bind and ubiquitinate α-synuclein *in vitro* and without the assistance of other cellular components such as Hsp70. It is noticeable the presence of a band just under 25kDa which is consistent with the expected molecular weight of monoubiquitinated α-synuclein (22.5 kDa; UB-α-syn). Above this band there are two more well defined bands and then a more diffuse pattern of multiple higher molecular weight forms which may be polyubiquitinated or multi-monoubiquitinated α-synuclein ($(UB)_n$-α-syn).

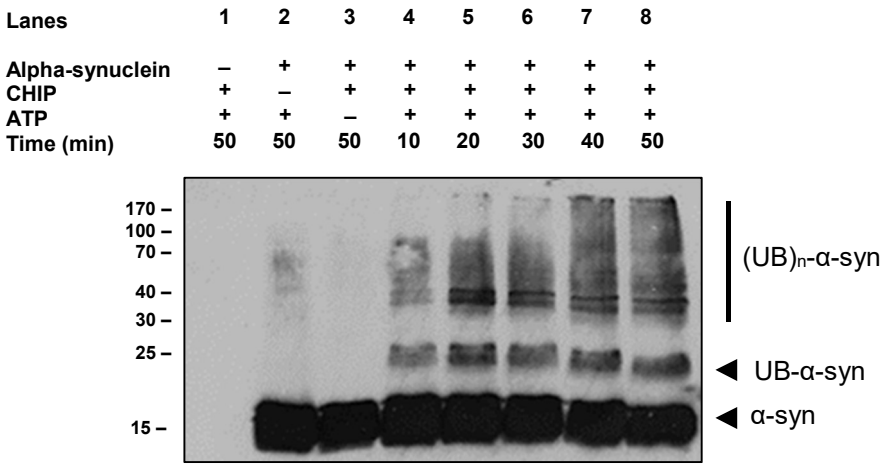

Figure 26. In vitro ubiquitination of α-synuclein by CHIP with PFA.

Immunoblot of in vitro ubiquitination reactions assembled using ATP, ubiquitin, Ube1, ubcH5α and alpha synuclein and started with His-CHIP. The samples were incubated from 10 to 50 minutes at 30ºC and the reaction was stopped with the addition of sample buffer. Between transferring and blocking a PFA 30 minute incubation step was added. The results are representative of two independent experiments.

In consequence of these results, a PFA incubation step was added to the standard Western blot protocol between the transferring and blocking steps for all membranes that would be incubated with anti-α-synuclein antibody.

Besides the incubation with PFA, the assay was also optimized regarding the presence of detergent in the reaction buffer, since the presence of some detergents (Chandra et al., 2003) has been shown to change α-synuclein's structure which could influence the ubiquitination reaction. Different concentrations of CHIP were also tested.

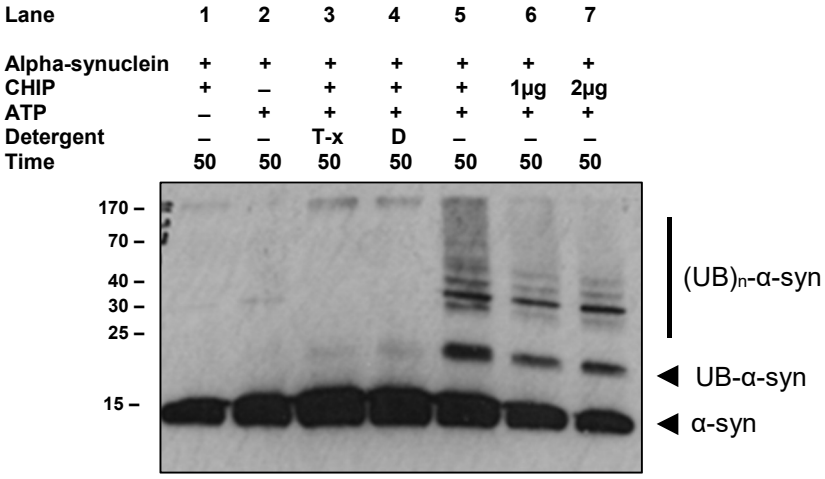

Figure 27. Optimization of *in vitro* CHIP/α-synuclein ubiquitination assay.

Immunoblot of in vitro ubiquitination reactions optimized for detergent presence and concentration of His-CHIP. The reactions were started with 3µg of His CHIP except when indicated. The samples were incubated for 50 minutes at 30ºC and the reaction was stopped with the addition of sample buffer. Two different detergents were used: Tríton-X (T-x) and n-Dodecyl-β-D-maltoside (D). The results are representative of two independent experiments.

The presence of detergent in the reaction buffer was a factor that had plenty of influence in the reaction, decreasing ubiquitination of α-synuclein by CHIP, as can be observed in lanes 3 and 4 (Figure 27) when compared with lane 5. In a previous assay (data not shown) CHIP's autoubiquitination was not affected by the presence of detergent suggesting this alteration is dependent on α-synuclein. It is possible that α-synuclein conformation is affected by the presence the detergents used influencing its binding to CHIP or CHIP's ability to ubiquitinate it. The following assays were performed without detergents in the reaction buffer.

Regarding CHIP's concentration it was decided to continue running the assays with 3µg of CHIP to guarantee that any changes in the ubiquitination patterns were not due to an insufficient amount of the E3 CHIP.

Afterwards, an ubiquitination assay was conducted using modified ubiquitin in which all the reactive lysines residues were mutated to arginine, rendering it unable to form poly-ubiquitin chains. Therefore the bands that appear will correspond only to monoubiquitinated and multi-monoubiquitinated α-synuclein.

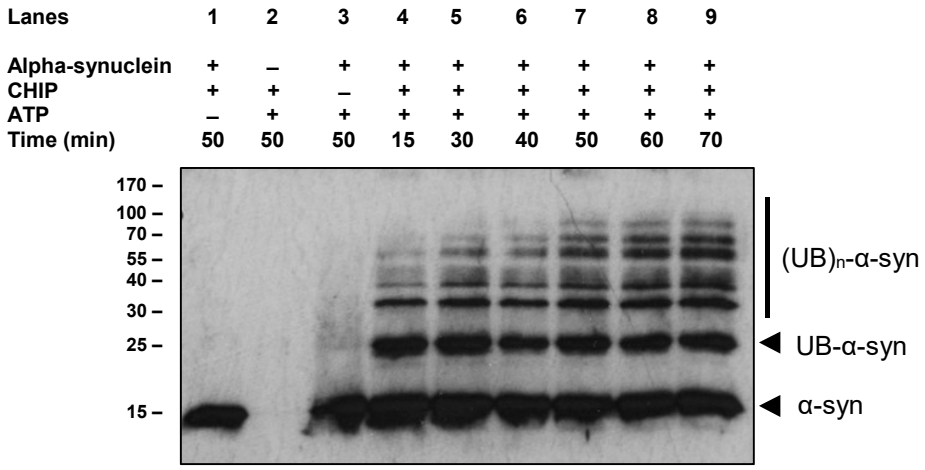

Figure 28. Time course ubiquitination assay with modified ubiquitin.

Immunoblot of in vitro ubiquitination reactions assembled using ATP, modified ubiquitin, Ube1, ubcH5α and **α**-synuclein and started with His-CHIP. The samples were incubated from 15 to 70 minutes at 30ºC and the reaction was stopped with the addition of sample buffer.

This assay (Figure 28) presents better defined bands, likely because there are less ubiquitinated forms of α-synuclein, due to the impossibility to form poly-ubiquitin chains, allowing for a clearer signal. This difference in the ubiquitination pattern obtained with the use of modified ubiquitin suggests that, *in vitro*, CHIP is not only capable of

monoubiquitinating α-synuclein in one and in multiple sites but can also insert poly-ubiquitin chains.

Finally, it was investigated whether the presence of α-synuclein had any effect on CHIP's *in vitro* activity, by looking at CHIP's autoubiquitination in the presence and absence of α-synuclein.

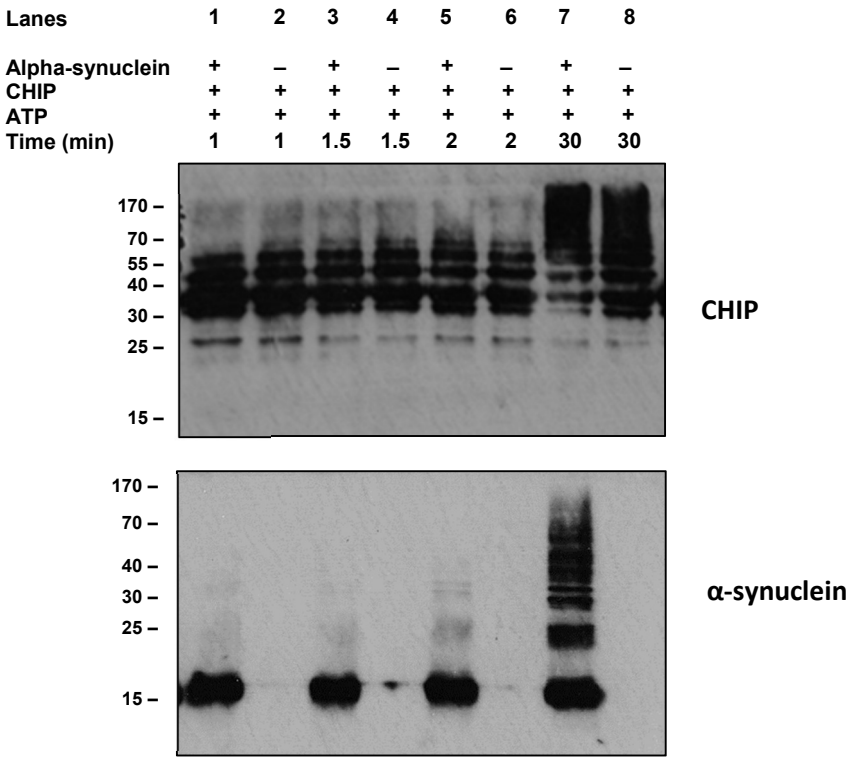

Figure 29. CHIP autoubiquitination in the presence and absence of α-synuclein.

Immunoblot of in vitro ubiquitination reactions assembled using ATP, ubiquitin, Ube1, ubcH5α and started with His-CHIP in the presence or absence of substrate (α-synuclein). Samples were incubated for 1 to 30 minutes at 30ºC and the reaction was stopped with the addition of sample buffer and run in 15% gels. CHIP and α-synuclein were detected with anti-CHIP 3.1 (1:2000) and anti-α-synuclein (1:2000), followed by anti-mouse (1:1000).

Since CHIP's autoubiquitination is a very swift process, the incubation times had to be reduced in order to make sure that both a decrease and an increase in activity could be detected should any occur. The data presented above shows that there is no visible difference between CHIP's autoubiquitination in the presence of α-synuclein and in its absence (Figure 29, compare lanes 1, 3 and 5 with lanes 2, 4 and 6) indicating that CHIP's autoubiquitination activity *in vitro* is not influenced by the presence of this substrate. In the future the assay should also be tried with a lower concentration of His-CHIP as the high immunoreactivity might be obscuring slighter differences.

7. Effect of scFvs in CHIP's ubiquitination activity *in vitro*

After establishing an optimized *in vitro* ubiquitination system and determining some of the particulars of the interaction between CHIP and α-synuclein in those conditions, this assay was used to study the effect of the purified scFvs in CHIP's *in vitro* activity. To this end, a titration of scFv was added to the assay and a control with only the scFv buffer, volume matched to the highest concentration in the scFv titration, was included.

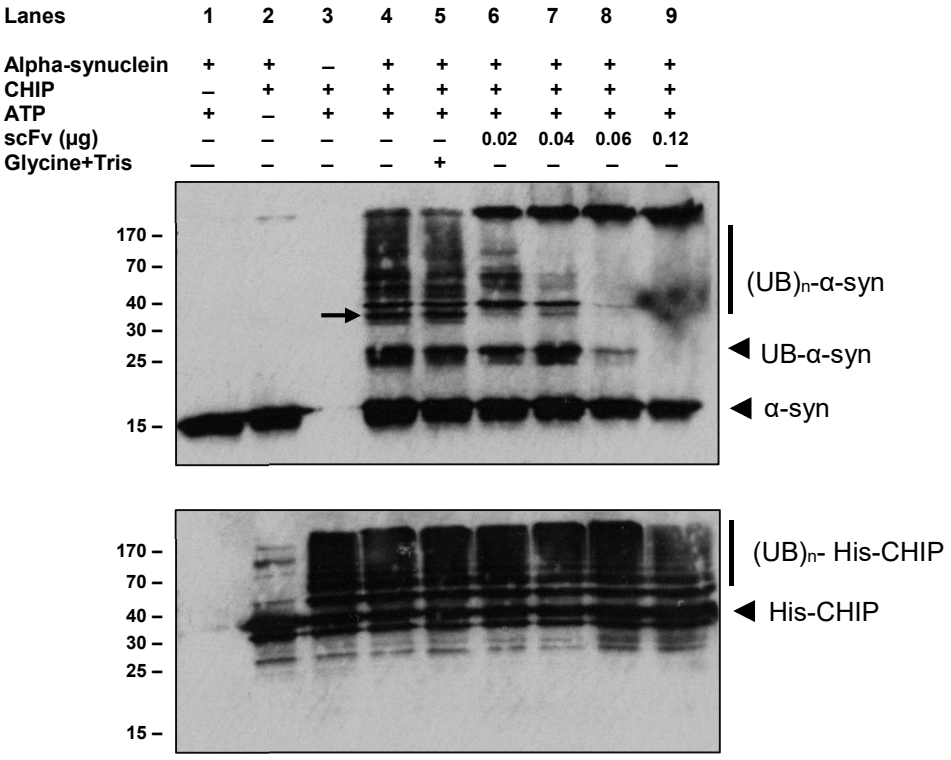

Figure 30. ScFv 11F (TG1) interferes with α-synuclein ubiquitination by CHIP.

Immunoblot of *in vitro* ubiquitination reactions assembled using ATP, ubiquitin, Ube1, ubcH5α and α-synuclein. A titration of scFv or scFv buffer was added when indicated immediately before the reaction was started with His-CHIP. Samples were incubated for 30 minutes at 30ºC and the reaction was stopped with the addition of sample buffer and run in 15% SDS-polyacrilamide gels. CHIP and α-synuclein were detected with anti-CHIP 3.1 (1:2000) and anti-α-synuclein (1:2000), followed by anti-mouse (1:1000).

Initial results with scFv 11F purified from TG1 cells showed that this clone was capable of inhibiting α-synuclein *in vitro* ubiquitination by CHIP (Figure 30) as is visible by comparing lane 5 (control with scFv buffer) with lanes 6-9. The ubiquitination bands of higher molecular weight are the first ones to be supressed followed by the first band of the upper pattern (marked with an arrow), possibly polyubiquitination bands. The bands corresponding to monoubiquitinated α-synuclein are the last ones to be inhibited by the binding of scFv 11F to CHIP.

It is also curious to note that the presence of the scFv 11F had no effect on CHIP's autoubiquitination suggesting that perhaps these two processes occur by different mechanisms.

An interesting finding was the increased signal of the bands present in the interface between the stacking and the resolving gels, in the lanes where scFv were present (lanes 6-9) when compared with lanes 2, 4 and 5. However they are not present in the absence of CHIP or α-synuclein (lanes 1 and 3, respectively). These bands had already appeared in several assays throughout this study (Figure 25, Figure 26 and Figure 27) and in others that were not included here and will be further investigated in the next chapter.

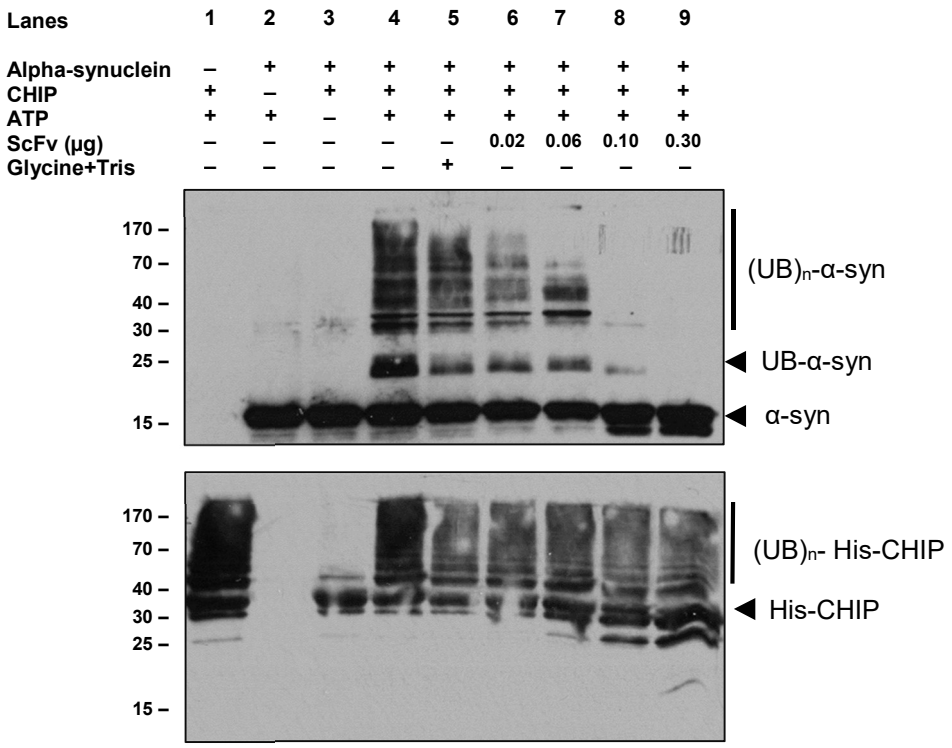

Figure 31. ScFv 11F (BL21-DE3) interferes with α-synuclein ubiquitination by CHIP.

Immunoblot of in vitro ubiquitination reactions assembled as described in Figure 33 but using the batch of scFv 11F obtained from E.coli BL21-DE3. Samples were incubated for 30 minutes at 30ºC and the reaction was stopped with the addition of sample buffer and run in 15% SDS-polyacrilamide gels. CHIP and α-synuclein were detected with anti-CHIP 3.1 (1:2000) and anti-α-synuclein (1:2000), followed bu anti-mouse (1:1000).

The influence of the scFv 11F, produced from BL21 (DE3) cells, in CHIP's ubiquitination of α-synuclein was also tested and confirmed the results obtained previously, as can be seen above (Figure 31) by comparing lanes 6-9 with lane 5 (control with scFv buffer)

The influence of the scFv 4C, 7A and 7G in CHIP's autoubiquitination and α-synuclein's ubiquitination was also tested and yielded mostly the same results as described for 11F (Figure 32 and 33). The only difference is that for these three clones with 0.3ug of scFv (Figure 32 and 33, lane 9) it is still possible to observe a band of monoubiquitinated α-synuclein, when for 11F this band is not present (Figure 31, lane 9). This may be related to the different affinities the clones present for CHIP with 11F being the clones that promotes the most stable binding to CHIP.

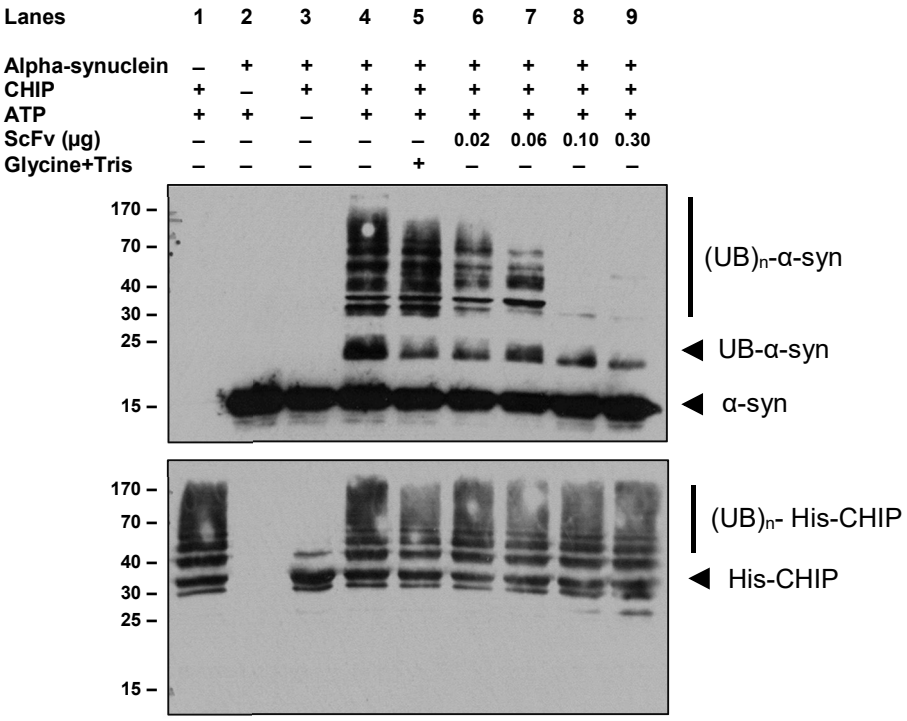

Figure 32. ScFv 4C interferes with α-synuclein ubiquitination by CHIP.

In vitro ubiquitination assay assembled as described above but using the scFv 4C. Samples were incubated for 30 minutes at 30ºC and the reaction was stopped with the addition of sample buffer and run in 15% SDS-polyacrilamide gels. CHIP and α-synuclein were detected with anti-CHIP 3.1 (1:2000) and anti-α-synuclein (1:2000), followed by anti-mouse (1:1000).

It is also interesting to notice that even though scFv 4C presented the lowest affinity for CHIP in the characterization assays (Figures 21 and 22), the results obtained in ubiquitination assay (Figure 32) were not very different from the results of scFv 7A and 7G (Figure 33) and scFv 11F (Figure 31). This suggests that perhaps the immobilization of CHIP to the plate hampers the binding of scFv 4C, maybe hampering its access to the epitope. However when both CHIP and scFv 4C are in solution this hindrance is removed and so the scFv reactivity towards CHIP increases.

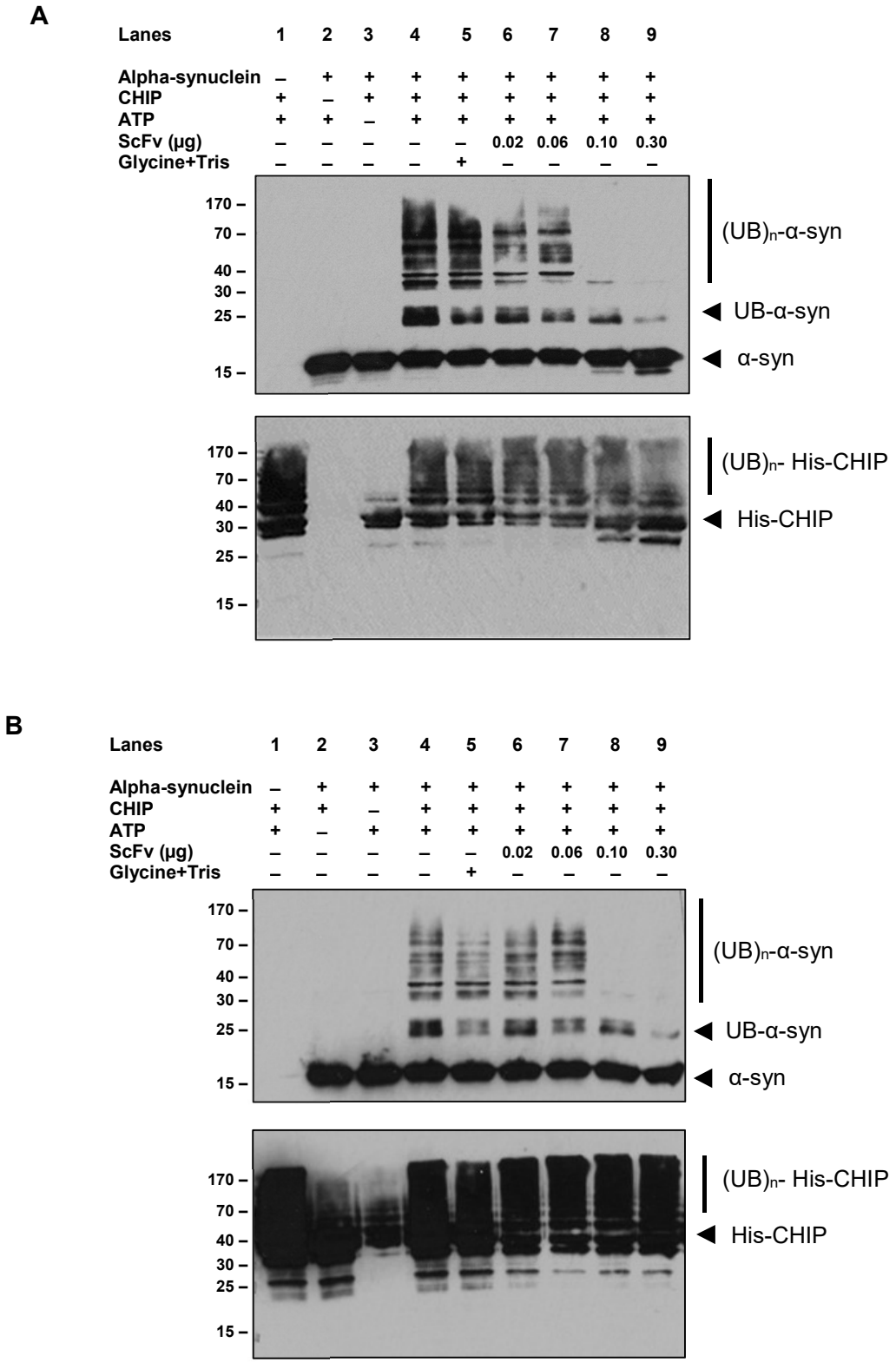

Figure 33. Impact of scFvs 7A and 7G CHIP's ubiquitination activity.

Western blots of in vitro ubiquitination assay assembled as described above but using the scFvs 7A (A) and 7G (B). Samples were incubated for 30 minutes at 30ºC and the reaction was stopped with the addition of sample buffer and run in 15% SDS-polyacrilamide gels. CHIP and α-synuclein were detected with anti-CHIP 3.1 (1:2000) and anti-α-synuclein (1:2000), followed by anti-mouse (1:1000).

As the purified scFvs interfered with ubiquitination of α-synuclein but not with CHIP's autoubiquitination, the assay was carried out using p53, another substrate of CHIP, to see if the scFv also prevented its ubiquitination by CHIP. The assay was carried out as the previous ones but using p53 instead of α-synuclein.

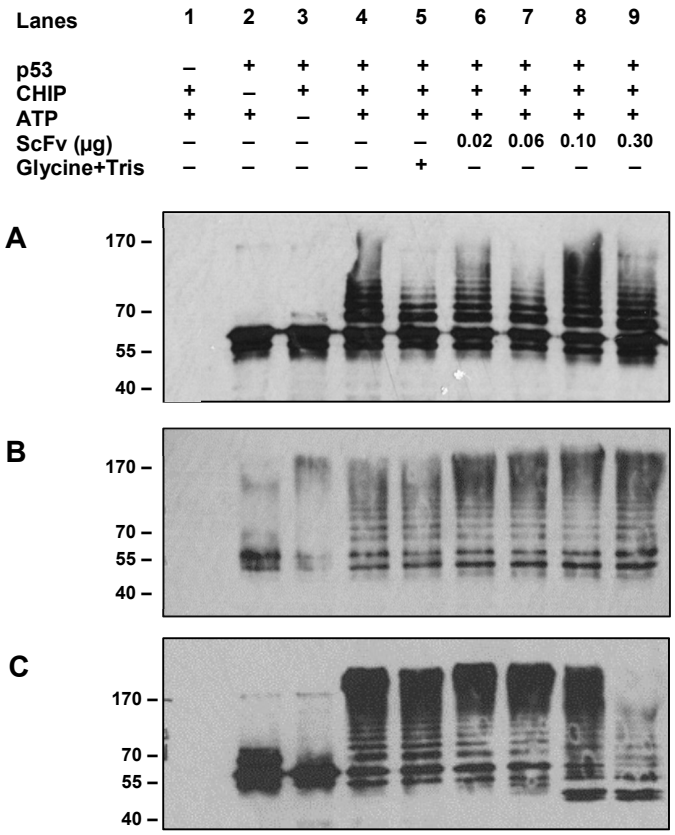

Figure 34. ScFvs effect in p53 *in vitro* ubiquitination by CHIP.

Immunoblot of in vitro ubiquitination reactions assembled using ATP, ubiquitin, Ube1, ubcH5α and p53. A titration of scFvs 4C (A), 7A (B) or 11F (C), or scFv buffer was added when indicated immediately before The reaction was started with His-CHIP. Samples were incubated for 30 minutes at 30ºC and the reaction was stopped with the addition of sample buffer and run in 12% SDS-polyacrilamide gels. P53 and CHIP were detected with anti-p53 DO1 (1:1000) and anti-CHIP 3.1 (1:2000) followed by anti-mouse (1:1000).

The results show that scFvs 4C and 7A have no effect on p53 ubiquitination by CHIP (Figure 34, compare lane 5 with lanes 6-9). When the assay is run with scFv 11F, it also seems to have no effect, even though the signal is not so strong in lane 9 compared with lanes 5-9; this is most likely related with the running of the gel or the transfer process.

Summarising, it is interesting to observe that the developed scFv seem to interfere only with *in vitro* α-synuclein ubiquitination by CHIP but not CHIP's autoubiquitination or p53's ubiquitination indicating that perhaps scFvs interferes with α-synuclein binding to CHIP or that these processes occur by different mechanisms.

8. CHIP appears to promote *in vitro* formation of gel-excluding α-synuclein bands

The presence of gel-excluding bands of α-synuclein was detected in several assays performed during this study (Figures 25-27) but they went mostly unnoticed until their presence was reinforced by the presence of the scFv 11F (Figure 30).

Although these bands are also present in some assays without the scFv, they're usually thinner and partly obscured due to the extension of the ubiquitination pattern that usually extends right up to the top of the resolving gel. In fact, before the results shown in figure 30, it was believed these bands were probably part of the ubiquitination pattern.

In order to gain some more insight into the conditions that led to the formation of these bands more assays were executed. This proved to be a difficult task due to the elusive nature of these bands and the fact that they aren't always detected however it was possible to answer some questions.

First, it was aimed to confirm that the bands were in fact α-synuclein bands and so the ubiquitination reactions were performed with and without α-synuclein.

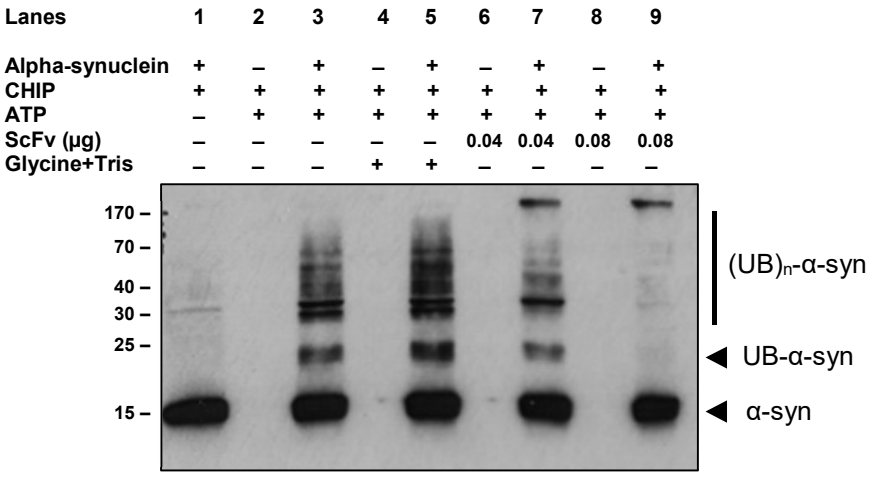

Figure 35. Gel-excluding bands dependence on α-synuclein.

Immunoblot of in vitro ubiquitination reactions assembled using ATP, ubiquitin, Ube1, ubcH5α and a titration of scFv or scFv buffer was added when indicated immediately before the reaction was started with His-CHIP. **α-**synuclein was added only when indicated. Samples were incubated for 30 minutes at 30ºC and the reaction was stopped with the addition of sample buffer and run in 15% SDS-polyacrilamide gels. α-synuclein was detected with anti-α-synuclein (1:2000), followed by anti-mouse (1:1000). The data is represenattive of two independent experiments.

The data above shows that the gel-excluded bands are in fact dependent on the presence of α-synuclein (Figure 35, compare lanes 6 and 8 with lanes 7 and 9). However

once again they are mostly present on the assays where scFv 11F was present, being detectable in lanes 3 and 5 only in longer exposures.

After establishing the bands contained α-synuclein, it was necessary to confirm that they were also dependent on the presence of CHIP, as they have never been present in the controls without the E3 ligase.

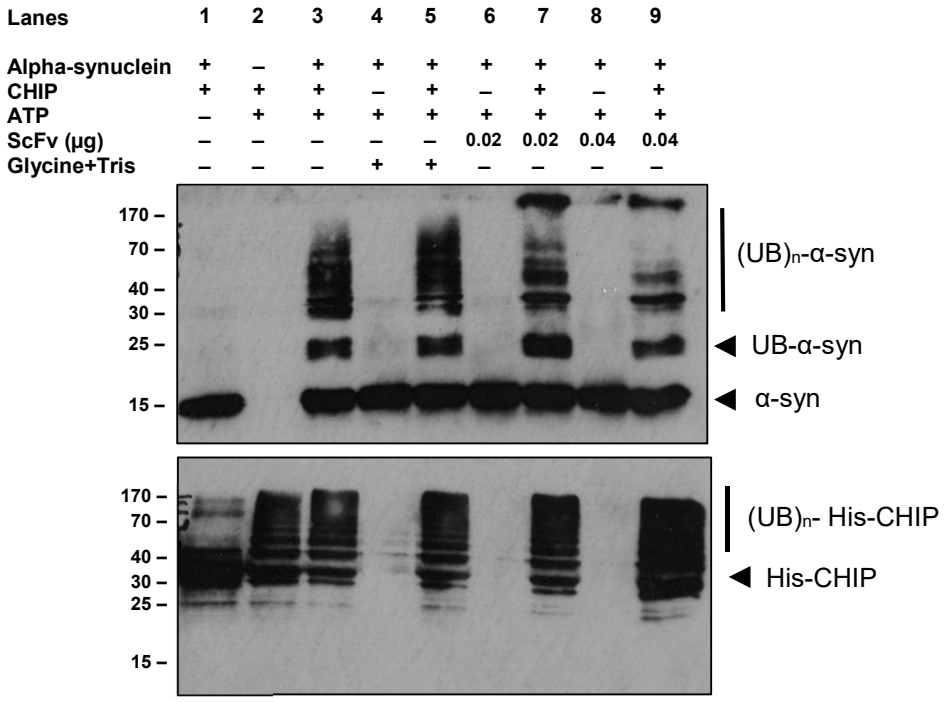

Figure 36. Identification of gel-excluding bands in the presence and absence of CHIP.

Immunoblot of in vitro ubiquitination reactions assembled using ATP, ubiquitin, Ube1, ubcH5α and α-synuclein. A titration of scFv or scFv buffer was added when indicated immediately before the reaction was started. His-CHIP was added only to lanes 1, 2, 3, 5, 7, and 9. Samples were incubated for 30 minutes at 30ºC and the reaction was stopped with the addition of sample buffer and run in 15% SDS-polyacrilamide gels. CHIP and α-synuclein were detected with anti-CHIP 3.1 (1:2000) and anti-α-synuclein (1:2000), followed by anti-mouse (1:1000).

Comparing lanes 6 and 8 with lanes 7 and 9 (Figure 36) demonstrates that the presence of the gel-excluded bands is dependent on the presence of CHIP, suggesting that, whatever is occurring, the process is catalysed by the E3 ligase. Once again the bands were only visible in the presence of scFv 11F.

Knowing that the bands are α-synuclein and CHIP-dependent it was relevant to exclude the bands' association to the ubiquitination process. This association was unlikely given that they seem to be stronger exactly when ubiquitination in inhibited by the scFv but to confirm the reactions were performed in the presence and absence of ATP.

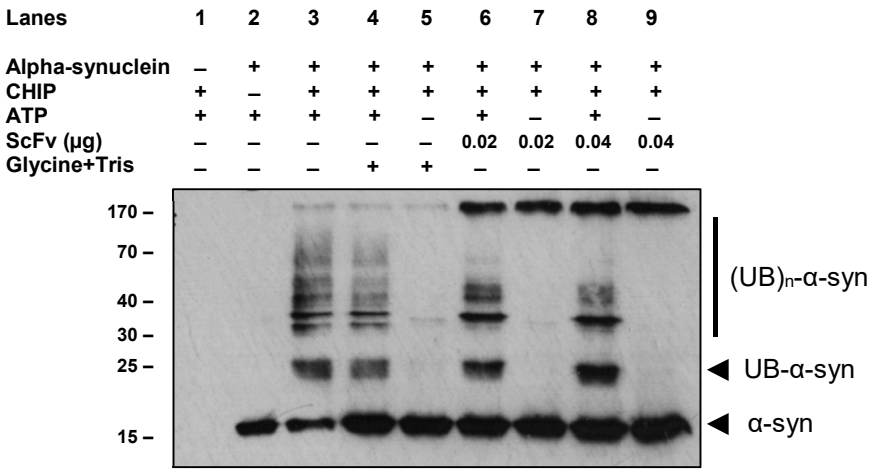

Figure 37. Association of gel-excluding bands to the ubiquitination reaction.

Immunoblot of in vitro ubiquitination reactions assembled using ubiquitin, Ube1, ubcH5α and α-synuclein. A titration of scFv or scFv buffer was added when indicated, immediately before the reaction was started with His-CHIP. ATP was included only in lanes 2-4, 6 and 8. Samples were incubated for 30 minutes at 30ºC and the reaction was stopped with the addition of sample buffer and run in 15% SDS-polyacrilamide gels. α-synuclein were detected with anti-α-synuclein (1:2000), followed by anti-mouse (1:1000). The results are representative of two independent experiments.

As described before, the band are missing from the controls without α-synuclein and CHIP (Figure 37, lanes 1 and 2); they can be detected in the regular ubiquitination reaction (lane 3) and in the control with the scFv buffer in the presence and absence of ATP (lanes 4 and 5) and are present with a stronger signal in the reactions to which scFv was added, both with and without ATP (lanes 6-9).

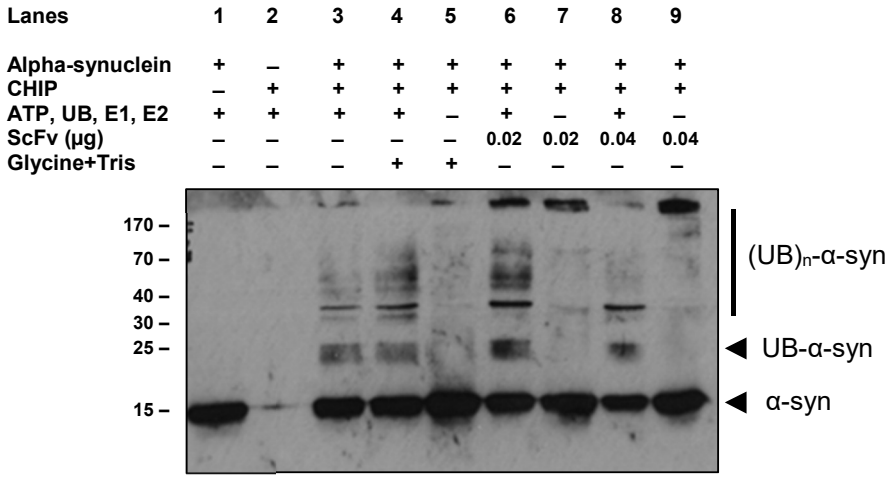

Figure 38. Dependence of gel-excluding bands on the presence of the ubiquitination assay components.

Immunoblot of in vitro ubiquitination reactions assembled with α-synuclein, His-CHIP and a titration of scFv 11F or scFv buffer when indicated. ATP, ubiquitin, Ube1 and ubcH5α was only added to reactions in lanes 1-4, 6 and 8. Samples were incubated for 30 minutes at 30ºC and the reaction was stopped with the addition of sample buffer and run in 15% SDS-polyacrilamide gels. α-synuclein was detected with anti-α-synuclein (1:2000), followed by anti-mouse (1:1000). The results are representative of three independent experiments.

Finally, it was studied whether the bands were still present if all the components of the ubiquitination system (ATP, ubiquitin, E1 and E2) were removed, leaving only α-synuclein and CHIP to interact in the reaction buffer, alongside scFv 11F.

The results show that the bands are still present when all the components of the ubiquitination system are removed from the reaction (Figure 38, lanes 7 and 9), effectively demonstrating that the bands are not associated with the ubiquitination process. The band appears to be missing in lane 8 but it more noticeable in higher exposures.

Taking all these results into consideration it is possible to say that CHIP is catalysing the development of non ubiquitinated α-synuclein forms that remain caught in the interface of the stacking and the resolving gel. Since the bands are usually stronger in the presence of the scFv it can be suggested that the lack of ability to ubiquitinate α-synuclein leads to an increase in the formation of these gel-excluded forms.

V. DISCUSSION

The C-terminus of the Hsc70-Interacting Protein is a complex and interesting protein intrinsically involved in the maintenance of the cellular proteome as it bridges the molecular chaperones network with the ubiquitin/proteasome system (Ballinger et al., 1999). This distinctive role places CHIP in the centre of a diverse array of biochemical phenomena, both in physiology and disease, motivating the search for a better understanding of its function and regulation in order to potentiate its use as a therapeutic target.

Overall, more than sixty substrates have already been described for CHIP and evidence, so far, has this peculiar protein involved in several, often contradictory, pathways. This observation is intimately related with one of the most prominent question in all CHIP-related research which involves substrate specificity. How does CHIP discriminate and correctly direct so many different substrates? Which specific details motivate these mechanisms? Recent studies involving facilitators of CHIP's activity, such as the chaperones (Soss et al., 2015), and exploring CHIP's intrinsic dynamics (Matsumura et al., 2013; Narayan et al., 2015) are opening the way for a better understanding of these concepts and the development of new strategies that can be applied in this endeavour are welcome.

At the same time, scFvs and its multimeric formats continue to emerge as powerful tools not just for detection and imaging but also as research instruments and therapeutic solutions. Initially these fragments were produced from hybridoma cell lines however that process was expensive and slow (McCafferty et al., 1990) so new technologies were developed. Phage display is, to date, the most used molecular display system to select scFvs and potentiated their use and development. Nowadays, the simple and inexpensive production process coupled with the small size and ease of tailoring and manipulation of these fragments puts them in the frontline for a growing range of applications (Monnier et al., 2013).

In this study, wild type His-tagged CHIP and mutant CHIP K30A were used to screen a canine scFv antibodies phage display library. Phage selection was carried out with the targets directly bound to microtiter plate wells as this method is easy to perform and has been widely successful (Winter et al., 1994). For both targets three rounds of panning were enough to successfully obtain polyclonal phage pools with increased specificity for CHIP as increasingly stringent washing conditions during panning eliminated non-specific and weak binders.

The resulting His-CHIP and CHIP-K30A libraries were used to grow randomly select clones and the functionality and affinity of the scFvs for the respective target were tested.

From this process 14 clones emerged as possible good binders with the clone 11F clearly appearing as a very strong candidate, even though the signals were subjected to expression bias.

These clones were then further validated and a higher binding affinity for the mutant CHIP-K30A was detected. This is in line with a recent publication that studied this mutant alongside wild type CHIP and found it lacking in motion and flexibility (Narayan et al., 2015). Considering the new ensemble model of allostery, that supports the presence of different structural species of one protein in solution at one time (Motlagh et al., 2014), it is reasonable to assume the mutant is limited when it comes to the conformations it can adopt in solution when compared with the wild type protein. This may potentiate the formation of more stable complexes with the scFv, resulting in a higher binding signal.

The most promising clones were sent for sequencing to ensure that only clones with different sequences would be taken forward and 8 different clones were obtained. As expected, the framework regions showed high similarity between the clones and the heavy chain CDRs were shared by several of the clones while the light chains were different for all. Finally the eight clones were shown to be able to bind to untagged CHIP, possibly a closer form to endogenous CHIP, with appreciable affinity.

Four of the above clones (4C, 7A, 7G and 11F) were successfully produced and purified from *E.coli and* characterized according to their binding to CHIP and the mutant. These clones, now free from expression bias, showed different binding affinities for the targets with 11F standing out as the strongest binder followed by 7G and 7A and lastly 4C. It was also interesting to notice that unlike the other clones 7G was capable of binding to both the mutant and wild type CHIP with similar affinity suggesting that it may bind to an epitope less susceptible to change in the different conformations CHIP may be able to adopt in solution. Conversely 7A shows the biggest difference in binding between the two forms while still being unspecific for either.

An attempt to identify the binding epitopes of the scFv through peptide binding assays with CHIP peptides was made but the results were inconclusive or irreproducible (data not shown). So in order to gain some insight into the binding interfaces of the scFv with CHIP the complexes were analysed in a native gel. Curiously the binding of 11F and 7G gave CHIP a higher mobility on the gel and lower bands were observed. This raises the possibility the scFv can interfere with the assembly of CHIP monomers, inhibiting dimerization, and reinforces the supposition that these scFvs may bind to different epitopes

ScFvs have been shown to interfere and modulate the activity of proteins both *in vitro* an *in vivo* (Moller et al., 2010; Basu et al., 2012), alter intracellular location of the

targets (Bai et al., 2003) or disrupt interactions protein-protein (Visintin et al., 2008). All these strategies can be used not only in the development of therapies but also to help study the functions of the scFvs' targets or the importance of different protein domains.

The main goal of this study was to select scFv antibodies that would not only allow the detection of CHIP and could be used in imaging solutions but also that could modulate the activity of this E3 ligase.

To this end, an *in vitro* ubiquitination assay was established as a model that would allow the study of the scFvs impact on the activity of CHIP. The chosen substrate was α-synuclein, a 15kDa protein whose physiological functions still haven't been completely elucidated but whose aggregates have been associated with Parkinson's disease (Polymeropoulos et al., 1996). Alpha-synuclein undergoes CHIP-mediated degradation *in vivo* (Dimant et al., 2014) and has been found to co-localize with CHIP and Hsp70 in Lewy bodies (Spillantini et al., 1997) revealing itself as relevant substrate.

The addition of a PFA incubation step in the conventional western blot procedure was necessary to stop ubiquitinated α-synuclein species from washing away. It has been shown that the use of small concentrations of PFA prevents the washing off of endogenous α-synuclein monomers from the blotting membranes (Newman et al., 2013). In this case, the monomers were very immunoreactive and the absent bands were the ubiquitinated forms. It is possible that the binding of the ubiquitinated α-synuclein to the membrane is more unstable, causing the species to be washed off during the numerous washing steps of the Western blot procedure.

The presence of detergents such as Tríton-X seemed to decrease ubiquitination of α-synuclein by CHIP. Alpha-synuclein is usually considered an intrinsically disordered protein however, in the presence of lipids and detergents, it has been shown to adopt a more helical structure at the N-terminal region (Chandra et al., 2003). Perhaps the detergent-induced helical structure of α-synuclein decreased ubiquitination by CHIP by altering the stability of the binding between the two proteins.

This study demonstrated that direct binding of CHIP to α-synuclein was sufficient to signal mono-, poly- and multi-monoubiquitination without additional cellular components, such as Hsp70. This observation agrees with several studies in which direct interaction of CHIP with its substrates has been reported (McDonough et al., 2009; Shang et al., 2009; Narayan et al., 2011).

Upon inclusion of a titration of scFvs in the assay, it was revealed that the four clones appear to inhibit α-synuclein ubiquitination by CHIP, in a concentration dependent manner, however there was no decrease in CHIP's autoubiquitination. Additionally, the assay was performed with p53, another known substrate of CHIP, and it was shown the ubiquitination had not been affected by the scFvs either. This would suggest that either

the scFv fragments are blocking the binding site of α-synuclein in CHIP, and both p53 and CHIP itself bind to another domain, or the scFvs are producing changes in CHIP that stop it from ubiquitinating α-synuclein while p53 ubiquitination and CHIP's autoubiquitination occur by a different mechanism and are not affected. However, the fact that 11F and 7G induce an apparent monomerization of CHIP also needs to be considered along with the observation that this held no effect on CHIP and p53 *in vitro* ubiquitination. This could be a very relevant finding seeing as dimerization has been considered a requirement for CHIP's activity as an E3 ligase (Nikolay et al., 2004).

It is also curious that the four scFvs seem to produce the same effect in CHIP's activity although they seem to provoke different alterations in CHIP itself. Since these molecular mechanisms haven't been well explored and the binding interfaces of these substrates to CHIP as well as the epitopes of the scFvs are still to be determined it is not yet possible to draw a more conclusive interpretation of these results.

An interesting observation of this study was the appearance of gel-excluding bands on western blots revealed with anti-α-synuclein. It was shown these bands were α-synuclein and CHIP dependent but not dependent on the ubiquitination reaction. In some blots these bands were enhanced in the presence of scFv 11F. So it seems that CHIP is capable of producing other alterations on α-synuclein besides ubiquitination. Inclusively, this activity seems to be stimulated once the ubiquitination is blocked.

One of the possible explanations is that CHIP is promoting the formation of α-synuclein aggregates. This might seem a bit unlikely as CHIP is an important enzyme involved in the maintenance of the proteome integrity and its main functions are assisting chaperones in the folding of misfolded or unfolded proteins or directing them to the ubiquitin/proteasome pathway. However this would not be the first contradictory role CHIP would have as it has been shown to function as both a tumour suppressor (Bento et al., 2010; Su et al., 2013; Wang et al., 2014b) and an oncogene (Li et al., 2009; Ahmed et al., 2012). In fact CHIP has been shown to promote aggregation of ataxin-1 by a TPR-dependent mechanism. While CHIP's primary role towards ataxin-1 is to mediate its ubiquitination, this modification along with the innate tendency of misfolded ataxin-1 to aggregate promotes the accumulation of detergent insoluble aggregates, when CHIP is overexpressed (Choi et al., 2007). This ubiquitination dependent aggregation has already been shown for tau (Petrucelli et al., 2004) and nNOS (Peng et al., 2004) and was ameliorated by overexpression of Hsc/Hsp70. The only detail against this theory is the fact that in this study α-synuclein was not ubiquitinated.

Another possible explanation could be that CHIP is folding α-synuclein. Although CHIP is better known for its role as a co-chaperone, it has been reported it also possesses intrinsic chaperone activity. This hypothesis was first suggested when overexpression of

CHIP in cultured cells was shown to enhance refolding of stress damaged proteins (Kampinga et al., 2003). Later another study investigated whether CHIP had the ability to function as an autonomous molecular chaperone and found that CHIP has intrinsic chaperone activity, enhanced by heat stress, which enables it to bind to non native substrates through the TPR domain (Rosser et al., 2007). CHIP's chaperoning activity has also been demonstrated for wild type p53 both *in vitro* and *in vivo* (Tripathi et al., 2007). Considering that α-synuclein is usually intrinsically disordered it is plausible that CHIP would attempt to fold it, especially when ubiquitination is inhibited, providing an alternate pathway to respond to cellular stress.

Broadening the range of strategies available to study a system always opens the door for new possibilities. In this project, Phage Display has proven to be a very suitable method to successfully select high affinity scFv binders for WT CHIP and the mutant K30A. These scFv were characterized as having different affinities for the targets which can be useful for different future applications. The scFvs' specificity for CHIP allows their use for detection and prospective imaging techniques while their capacity to modulate CHIP's activity opens the doors for the possible application of these biological tools in therapeutics.

CHIP is a protein tightly wrapped in layers of regulation and its activity is dependent on different molecular mechanisms still largely unidentified. Before the jump to therapeutic applications can find solid ground there is still a lot to be known about this protein and the processes it is involved in, especially considering the opposite roles it can take on. Until regulation and mechanistics of those roles are clarified it would be easy to interfere with more than one pathway simultaneously.

This project has also shown that scFvs can be a useful tool to gain new insight into possible differences in CHIP's molecular mechanisms, substrate selection and regulation of less known functions. Once the epitopes of the selected single chains are mapped more conclusions can be drawn from this study, as the information will shed light into some of differences observed and possibly open new research paths.

Future perspectives include the characterization of the scFv with endogenous CHIP and expression in mammalian cells to assess the intracellular functionality of the scFvs. Another possibility is the development of imaging applications probably involving fluorescence-based techniques. Additionally these scFvs can be used to keep studying CHIP's intrinsic mechanics and new scFvs can be developed against specific domains of the protein.

VI. REFERENCES

Aagaard L, Rossi JJ. RNAi therapeutics: principles, prospects and challenges. Adv Drug Deliv Rev. 2007;59:75-86.

Adachi H, Waza M, Tokui K, Katsuno M, Minamiyama M, Tanaka F, et al. CHIP overexpression reduces mutant androgen receptor protein and ameliorates phenotypes of the spinal and bulbar muscular atrophy transgenic mouse model. J Neurosci. 2007;27:5115-26.

Ahmed SF, Deb S, Paul I, Chatterjee A, Mandal T, Chatterjee U, et al. The chaperone-assisted E3 ligase C terminus of Hsc70-interacting protein (CHIP) targets PTEN for proteasomal degradation. J Biol Chem. 2012;287:15996-6006.

Al-Ramahi I, Lam YC, Chen HK, de Gouyon B, Zhang M, Perez AM, et al. CHIP protects from the neurotoxicity of expanded and wild-type ataxin-1 and promotes their ubiquitination and degradation. J Biol Chem. 2006;281:26714-24.

Alberti S, Bohse K, Arndt V, Schmitz A, Hohfeld J. The cochaperone HspBP1 inhibits the CHIP ubiquitin ligase and stimulates the maturation of the cystic fibrosis transmembrane conductance regulator. Mol Biol Cell. 2004;15:4003-10.

Aravind L, Koonin EV. The U box is a modified RING finger - a common domain in ubiquitination. Curr Biol. 2000;10:R132-4.

Argos P. An investigation of oligopeptides linking domains in protein tertiary structures and possible candidates for general gene fusion. J Mol Biol. 1990;211:943-58.

Arndt V, Daniel C, Nastainczyk W, Alberti S, Hohfeld J. BAG-2 acts as an inhibitor of the chaperone-associated ubiquitin ligase CHIP. Mol Biol Cell. 2005;16:5891-900.

Azzazy HM, Highsmith WE, Jr. Phage display technology: clinical applications and recent innovations. Clin Biochem. 2002;35:425-45.

Bai J, Sui J, Zhu RY, Tallarico AS, Gennari F, Zhang D, et al. Inhibition of Tat-mediated transactivation and HIV-1 replication by human anti-hCyclinT1 intrabodies. J Biol Chem. 2003;278:1433-42.

Ballinger CA, Connell P, Wu Y, Hu Z, Thompson LJ, Yin L-Y, et al. Identification of CHIP, a Novel Tetratricopeptide Repeat-Containing Protein That Interacts with Heat Shock Proteins and Negatively Regulates Chaperone Functions. Mol Cell Biol. 1999;19:4535-45.

Barbas CF, 3rd, Bain JD, Hoekstra DM, Lerner RA. Semisynthetic combinatorial antibody libraries: a chemical solution to the diversity problem. Proc Natl Acad Sci U S A. 1992;89:4457-61.

Basu B, Correa de Sampaio P, Mohammed H, Fogarasi M, Corrie P, Watkins NA, et al. Inhibition of MT1-MMP activity using functional antibody fragments selected against its hemopexin domain. Int J Biochem Cell Biol. 2012;44:393-403.

Bento CF, Fernandes R, Ramalho J, Marques C, Shang F, Taylor A, et al. The chaperone-dependent ubiquitin ligase CHIP targets HIF-1alpha for degradation in the presence of methylglyoxal. PLoS One. 2010;5:e15062.

Bird RE, Hardman KD, Jacobson JW, Johnson S, Kaufman BM, Lee SM, et al. Single-chain antigen-binding proteins. Science. 1988;242:423-6.

Boder ET, Wittrup KD. Yeast surface display for screening combinatorial polypeptide libraries. Nat Biotechnol. 1997;15:553-7.

Bradbury AR, Sidhu S, Dubel S, McCafferty J. Beyond natural antibodies: the power of in vitro display technologies. Nat Biotechnol. 2011;29:245-54.

Burritt JB, Bond CW, Doss KW, Jesaitis AJ. Filamentous phage display of oligopeptide libraries. Anal Biochem. 1996;238:1-13.

Burton DR, Barbas CF, 3rd, Persson MA, Koenig S, Chanock RM, Lerner RA. A large array of human monoclonal antibodies to type 1 human immunodeficiency virus from combinatorial libraries of asymptomatic seropositive individuals. Proc Natl Acad Sci U S A. 1991;88:10134-7.

Cabral Miranda F, Adao-Novaes J, Hauswirth WW, Linden R, Petrs-Silva H, Chiarini LB. CHIP, a carboxy terminus HSP-70 interacting protein, prevents cell death induced by endoplasmic reticulum stress in the central nervous system. Front Cell Neurosci. 2014;8:438.

Casarejos MJ, Perucho J, López-Sendón JL, García de Yébenes J, Bettencourt C, Gómez A, et al. Trehalose Improves Human Fibroblast Deficits in a New CHIP-Mutation Related Ataxia. PLoS ONE. 2014;9:e106931.

Cattepoel S, Hanenberg M, Kulic L, Nitsch RM. Chronic intranasal treatment with an anti-Abeta(30-42) scFv antibody ameliorates amyloid pathology in a transgenic mouse model of Alzheimer's disease. PLoS One. 2011;6:e18296.

Chames P, Van Regenmortel M, Weiss E, Baty D. Therapeutic antibodies: successes, limitations and hopes for the future. Br J Pharmacol. 2009;157:220-33.

Chandra S, Chen X, Rizo J, Jahn R, Südhof TC. A Broken α-Helix in Folded α-Synuclein. J Biol Chem. 2003;278:15313-8.

Chaudhary VK, Queen C, Junghans RP, Waldmann TA, FitzGerald DJ, Pastan I. A recombinant immunotoxin consisting of two antibody variable domains fused to Pseudomonas exotoxin. Nature. 1989;339:394-7.

Choi JS, Cho S, Park SG, Park BC, Lee DH. Co-chaperone CHIP associates with mutant Cu/Zn-superoxide dismutase proteins linked to familial amyotrophic lateral sclerosis and promotes their degradation by proteasomes. Biochem Biophys Res Commun. 2004;321:574-83.

Choi JY, Ryu JH, Kim HS, Park SG, Bae KH, Kang S, et al. Co-chaperone CHIP promotes aggregation of ataxin-1. Mol Cell Neurosci. 2007;34:69-79.

Choo AB, Dunn RD, Broady KW, Raison RL. Soluble expression of a functional recombinant cytolytic immunotoxin in insect cells. Protein Expr Purif. 2002;24:338-47.

Clackson T, Hoogenboom HR, Griffiths AD, Winter G. Making antibody fragments using phage display libraries. Nature. 1991;352:624-8.

Clague MJ, Liu H, Urbe S. Governance of endocytic trafficking and signaling by reversible ubiquitylation. Dev Cell. 2012;23:457-67.

Cloutier SM, Couty S, Terskikh A, Marguerat L, Crivelli V, Pugnieres M, et al. Streptabody, a high avidity molecule made by tetramerization of in vivo biotinylated, phage display-selected scFv fragments on streptavidin. Mol Immunol. 2000;37:1067-77.

Coloma MJ, Morrison SL. Design and production of novel tetravalent bispecific antibodies. Nat Biotechnol. 1997;15:159-63.

Connell P, Ballinger CA, Jiang J, Wu Y, Thompson LJ, Hohfeld J, et al. The co-chaperone CHIP regulates protein triage decisions mediated by heat-shock proteins. Nat Cell Biol. 2001;3:93-6.

Crissman JW, Smith GP. Gene-III protein of filamentous phages: evidence for a carboxyl-terminal domain with a role in morphogenesis. Virology. 1984;132:445-55.

Dai Q, Qian SB, Li HH, McDonough H, Borchers C, Huang D, et al. Regulation of the cytoplasmic quality control protein degradation pathway by BAG2. J Biol Chem. 2005;280:38673-81.

Dai Q, Zhang C, Wu Y, McDonough H, Whaley RA, Godfrey V, et al. CHIP activates HSF1 and confers protection against apoptosis and cellular stress. EMBO J. 2003;22:5446-58.

Das AK, Cohen PW, Barford D. The structure of the tetratricopeptide repeats of protein phosphatase 5: implications for TPR-mediated protein-protein interactions. EMBO J. 1998;17:1192-9.

de Wildt RM, Mundy CR, Gorick BD, Tomlinson IM. Antibody arrays for high-throughput screening of antibody-antigen interactions. Nat Biotechnol. 2000;18:989-94.

Demand J, Alberti S, Patterson C, Hohfeld J. Cooperation of a ubiquitin domain protein and an E3 ubiquitin ligase during chaperone/proteasome coupling. Curr Biol. 2001;11:1569-77.

Dephoure N, Zhou C, Villen J, Beausoleil SA, Bakalarski CE, Elledge SJ, et al. A quantitative atlas of mitotic phosphorylation. Proc Natl Acad Sci U S A. 2008;105:10762-7.

Desplancq D, King DJ, Lawson AD, Mountain A. Multimerization behaviour of single chain Fv variants for the tumour-binding antibody B72.3. Protein Eng. 1994;7:1027-33.

Di Lullo E, Haton C, Le Poupon C, Volovitch M, Joliot A, Thomas JL, et al. Paracrine Pax6 activity regulates oligodendrocyte precursor cell migration in the chick embryonic neural tube. Development. 2011;138:4991-5001.

Dickey CA, Kamal A, Lundgren K, Klosak N, Bailey RM, Dunmore J, et al. The high-affinity HSP90-CHIP complex recognizes and selectively degrades phosphorylated tau client proteins. J Clin Invest. 2007;117:648-58.

Diez P, Jara-Acevedo R, Gonzalez-Gonzalez M, Casado-Vela J, Dasilva N, Lecrevisse Q, et al. High-throughgput phage-display screening in array format. Enzyme Microb Technol. 2015;79-80:34-41.

Dikshit P, Jana NR. The co-chaperone CHIP is induced in various stresses and confers protection to cells. Biochem Biophys Res Commun. 2007;357:761-5.

Dimant H, Zhu L, Kibuuka LN, Fan Z, Hyman BT, McLean PJ. Direct visualization of CHIP-mediated degradation of alpha-synuclein in vivo: implications for PD therapeutics. PLoS One. 2014;9:e92098.

Dimova NV, Hathaway NA, Lee BH, Kirkpatrick DS, Berkowitz ML, Gygi SP, et al. APC/C-mediated multiple monoubiquitylation provides an alternative degradation signal for cyclin B1. Nat Cell Biol. 2012;14:168-76.

Ding X, Goldberg MS. Regulation of LRRK2 stability by the E3 ubiquitin ligase CHIP. PLoS One. 2009;4:e5949.

Dolezal O, De Gori R, Walter M, Doughty L, Hattarki M, Hudson PJ, et al. Single-chain Fv multimers of the anti-neuraminidase antibody NC10: the residue at position 15 in the

V(L) domain of the scFv-0 (V(L)-V(H)) molecule is primarily responsible for formation of a tetramer-trimer equilibrium. Protein Eng. 2003;16:47-56.

Donnelly BF, Needham PG, Snyder AC, Roy A, Khadem S, Brodsky JL, et al. Hsp70 and Hsp90 multichaperone complexes sequentially regulate thiazide-sensitive cotransporter endoplasmic reticulum-associated degradation and biogenesis. J Biol Chem. 2013;288:13124-35.

Droste P, Frenzel A, Steinwand M, Pelat T, Thullier P, Hust M, et al. Structural differences of amyloid-beta fibrils revealed by antibodies from phage display. BMC Biotechnol. 2015;15:57.

Du C, Chan WC, McKeithan TW, Nickerson KW. Surface display of recombinant proteins on Bacillus thuringiensis spores. Appl Environ Microbiol. 2005;71:3337-41.

Ferreira JV, Fofo H, Bejarano E, Bento CF, Ramalho JS, Girao H, et al. STUB1/CHIP is required for HIF1A degradation by chaperone-mediated autophagy. Autophagy. 2013;9:1349-66.

Fitch JC, Rollins S, Matis L, Alford B, Aranki S, Collard CD, et al. Pharmacology and biological efficacy of a recombinant, humanized, single-chain antibody C5 complement inhibitor in patients undergoing coronary artery bypass graft surgery with cardiopulmonary bypass. Circulation. 1999;100:2499-506.

Forrer P, Jung S, Pluckthun A. Beyond binding: using phage display to select for structure, folding and enzymatic activity in proteins. Curr Opin Struct Biol. 1999;9:514-20.

Francisco JA, Campbell R, Iverson BL, Georgiou G. Production and fluorescence-activated cell sorting of Escherichia coli expressing a functional antibody fragment on the external surface. Proc Natl Acad Sci U S A. 1993;90:10444-8.

Galeffi P, Lombardi A, Pietraforte I, Novelli F, Di Donato M, Sperandei M, et al. Functional expression of a single-chain antibody to ErbB-2 in plants and cell-free systems. J Transl Med. 2006;4:39.

Gan L, Liu DB, Lu HF, Long GX, Mei Q, Hu GY, et al. Decreased expression of the carboxyl terminus of heat shock cognate 70 interacting protein in human gastric cancer and its clinical significance. Oncol Rep. 2012;28:1392-8.

Gasteiger E, Gattiker A, Hoogland C, Ivanyi I, Appel RD, Bairoch A. ExPASy: The proteomics server for in-depth protein knowledge and analysis. Nucleic Acids Res. 2003;31:3784-8.

Gill SC, von Hippel PH. Calculation of protein extinction coefficients from amino acid sequence data. Anal Biochem. 1989;182:319-26.

Gimenez AP, Richter LM, Atherino MC, Beirao BC, Favaro C, Jr., Costa MD, et al. Identification of novel putative-binding proteins for cellular prion protein and a specific interaction with the STIP1 homology and U-Box-containing protein 1. Prion. 2015:1-12.

Goel A, Colcher D, Baranowska-Kortylewicz J, Augustine S, Booth BJ, Pavlinkova G, et al. Genetically engineered tetravalent single-chain Fv of the pancarcinoma monoclonal antibody CC49: improved biodistribution and potential for therapeutic application. Cancer Res. 2000;60:6964-71.

Goletz S, Christensen PA, Kristensen P, Blohm D, Tomlinson I, Winter G, et al. Selection of large diversities of antiidiotypic antibody fragments by phage display. J Mol Biol. 2002;315:1087-97.

Goshorn S, Sanderson J, Axworthy D, Lin Y, Hylarides M, Schultz J. Preclinical evaluation of a humanized NR-LU-10 antibody-streptavidin fusion protein for pretargeted cancer therapy. Cancer Biother Radiopharm. 2001;16:109-23.

Graf C, Stankiewicz M, Nikolay R, Mayer MP. Insights into the conformational dynamics of the E3 ubiquitin ligase CHIP in complex with chaperones and E2 enzymes. Biochemistry. 2010;49:2121-9.

Griffiths AD, Malmqvist M, Marks JD, Bye JM, Embleton MJ, McCafferty J, et al. Human anti-self antibodies with high specificity from phage display libraries. EMBO J. 1993;12:725-34.

Guo D, Ying Z, Wang H, Chen D, Gao F, Ren H, et al. Regulation of autophagic flux by CHIP. Neurosci Bull. 2015;31:469-79.

Guo J, Ren F, Wang Y, Li S, Gao Z, Wang X, et al. miR-764-5p promotes osteoblast differentiation through inhibition of CHIP/STUB1 expression. J Bone Miner Res. 2012;27:1607-18.

Guo JQ, Chen L, Ai HW, Jing JN, Zhou JY, Zhang CY, et al. A novel fusion protein of IP10-scFv retains antibody specificity and chemokine function. Biochem Biophys Res Commun. 2004;320:506-13.

Guruprasad K, Reddy BV, Pandit MW. Correlation between stability of a protein and its dipeptide composition: a novel approach for predicting in vivo stability of a protein from its primary sequence. Protein Eng. 1990;4:155-61.

Halin C, Rondini S, Nilsson F, Berndt A, Kosmehl H, Zardi L, et al. Enhancement of the antitumor activity of interleukin-12 by targeted delivery to neovasculature. Nat Biotechnol. 2002;20:264-9.

Hanes J, Pluckthun A. In vitro selection and evolution of functional proteins by using ribosome display. Proc Natl Acad Sci U S A. 1997;94:4937-42.

Hassan R, Sharon E, Thomas A, Zhang J, Ling A, Miettinen M, et al. Phase 1 study of the antimesothelin immunotoxin SS1P in combination with pemetrexed and cisplatin for front-line therapy of pleural mesothelioma and correlation of tumor response with serum mesothelin, megakaryocyte potentiating factor, and cancer antigen 125. Cancer. 2014;120:3311-9.

Ho M, Nagata S, Pastan I. Isolation of anti-CD22 Fv with high affinity by Fv display on human cells. Proc Natl Acad Sci U S A. 2006;103:9637-42.

Hoet RM, Cohen EH, Kent RB, Rookey K, Schoonbroodt S, Hogan S, et al. Generation of high-affinity human antibodies by combining donor-derived and synthetic complementarity-determining-region diversity. Nat Biotechnol. 2005;23:344-8.

Holliger P, Hudson PJ. Engineered antibody fragments and the rise of single domains. Nat Biotechnol. 2005;23:1126-36.

Holliger P, Prospero T, Winter G. "Diabodies": small bivalent and bispecific antibody fragments. Proc Natl Acad Sci U S A. 1993;90:6444-8.

Hoogenboom HR, de Bruine AP, Hufton SE, Hoet RM, Arends JW, Roovers RC. Antibody phage display technology and its applications. Immunotechnology. 1998;4:1-20.

Hoogenboom HR, Winter G. By-passing immunisation. Human antibodies from synthetic repertoires of germline VH gene segments rearranged in vitro. J Mol Biol. 1992;227:381-8.

Hornsby M, Paduch M, Miersch S, Saaf A, Matsuguchi T, Lee B, et al. A High Throughput Platform for Recombinant Antibodies to Folded Proteins. Mol Cell Proteomics. 2015.

Hu S, Shively L, Raubitschek A, Sherman M, Williams LE, Wong JY, et al. Minibody: A novel engineered anti-carcinoembryonic antigen antibody fragment (single-chain Fv-CH3) which exhibits rapid, high-level targeting of xenografts. Cancer Res. 1996;56:3055-61.

Humphrey W, Dalke A, Schulten K. VMD: visual molecular dynamics. J Mol Graph. 1996;14:33-8, 27-8.

Huston JS, Levinson D, Mudgett-Hunter M, Tai MS, Novotny J, Margolies MN, et al. Protein engineering of antibody binding sites: recovery of specific activity in an anti-digoxin single-chain Fv analogue produced in Escherichia coli. Proc Natl Acad Sci U S A. 1988;85:5879-83.

Ikai A. Thermostability and aliphatic index of globular proteins. J Biochem. 1980;88:1895-8.

Iliades P, Kortt AA, Hudson PJ. Triabodies: single chain Fv fragments without a linker form trivalent trimers. FEBS Lett. 1997;409:437-41.

Imai Y, Soda M, Hatakeyama S, Akagi T, Hashikawa T, Nakayama KI, et al. CHIP is associated with Parkin, a gene responsible for familial Parkinson's disease, and enhances its ubiquitin ligase activity. Mol Cell. 2002;10:55-67.

Inbar D, Hochman J, Givol D. Localization of antibody-combining sites within the variable portions of heavy and light chains. Proc Natl Acad Sci U S A. 1972;69:2659-62.

Ishigaki S, Niwa J, Yamada S, Takahashi M, Ito T, Sone J, et al. Dorfin-CHIP chimeric proteins potently ubiquitylate and degrade familial ALS-related mutant SOD1 proteins and reduce their cellular toxicity. Neurobiol Dis. 2007;25:331-41.

Jacobin MJ, Laroche-Traineau J, Little M, Keller A, Peter K, Welschof M, et al. Human IgG monoclonal anti-alpha(IIb)beta(3)-binding fragments derived from immunized donors using phage display. J Immunol. 2002;168:2035-45.

Jang KW, Lee KH, Kim SH, Jin T, Choi EY, Jeon HJ, et al. Ubiquitin ligase CHIP induces TRAF2 proteasomal degradation and NF-kappaB inactivation to regulate breast cancer cell invasion. J Cell Biochem. 2011;112:3612-20.

Jiang J, Ballinger CA, Wu Y, Dai Q, Cyr DM, Hohfeld J, et al. CHIP is a U-box-dependent E3 ubiquitin ligase: identification of Hsc70 as a target for ubiquitylation. J Biol Chem. 2001;276:42938-44.

Kajiro M, Hirota R, Nakajima Y, Kawanowa K, So-ma K, Ito I, et al. The ubiquitin ligase CHIP acts as an upstream regulator of oncogenic pathways. Nat Cell Biol. 2009;11:312-9.

Kakimoto K, Onoue K. Characterization of the Fv fragment isolated from a human immunoglobulin M. J Immunol. 1974;112:1373-82.

Kallberg M, Wang H, Wang S, Peng J, Wang Z, Lu H, et al. Template-based protein structure modeling using the RaptorX web server. Nat Protoc. 2012;7:1511-22.

Kampinga HH, Kanon B, Salomons FA, Kabakov AE, Patterson C. Overexpression of the cochaperone CHIP enhances Hsp70-dependent folding activity in mammalian cells. Mol Cell Biol. 2003;23:4948-58.

Kanazaki K, Sano K, Makino A, Shimizu Y, Yamauchi F, Ogawa S, et al. Development of anti-HER2 fragment antibody conjugated to iron oxide nanoparticles for in vivo HER2-targeted photoacoustic tumor imaging. Nanomedicine. 2015.

Kang SA, Cho HS, Yoon JB, Chung IK, Lee ST. Hsp90 rescues PTK6 from proteasomal degradation in breast cancer cells. Biochem J. 2012;447:313-20.

Kim C, Yun N, Lee J, Youdim MB, Ju C, Kim WK, et al. Phosphorylation of CHIP at Ser20 by Cdk5 promotes tAIF-mediated neuronal death. Cell Death Differ. 2015.

Kim HT, Kim KP, Uchiki T, Gygi SP, Goldberg AL. S5a promotes protein degradation by blocking synthesis of nondegradable forked ubiquitin chains. EMBO J. 2009;28:1867-77.

Kim W, Bennett EJ, Huttlin EL, Guo A, Li J, Possemato A, et al. Systematic and quantitative assessment of the ubiquitin-modified proteome. Mol Cell. 2011;44:325-40.

Kipriyanov SM, Breitling F, Little M, Dubel S. Single-chain antibody streptavidin fusions: tetrameric bifunctional scFv-complexes with biotin binding activity and enhanced affinity to antigen. Hum Antibodies Hybridomas. 1995;6:93-101.

Kipriyanov SM, Little M, Kropshofer H, Breitling F, Gotter S, Dubel S. Affinity enhancement of a recombinant antibody: formation of complexes with multiple valency by a single-chain Fv fragment-core streptavidin fusion. Protein Eng. 1996;9:203-11.

Knappik A, Ge L, Honegger A, Pack P, Fischer M, Wellnhofer G, et al. Fully synthetic human combinatorial antibody libraries (HuCAL) based on modular consensus frameworks and CDRs randomized with trinucleotides. J Mol Biol. 2000;296:57-86.

Kreitman RJ, Tallman MS, Robak T, Coutre S, Wilson WH, Stetler-Stevenson M, et al. Phase I trial of anti-CD22 recombinant immunotoxin moxetumomab pasudotox (CAT-8015 or HA22) in patients with hairy cell leukemia. J Clin Oncol. 2012;30:1822-8.

Kuan CT, Reist CJ, Foulon CF, Lorimer IA, Archer G, Pegram CN, et al. 125I-labeled anti-epidermal growth factor receptor-vIII single-chain Fv exhibits specific and high-level targeting of glioma xenografts. Clin Cancer Res. 1999;5:1539-49.

Kyte J, Doolittle RF. A simple method for displaying the hydropathic character of a protein. J Mol Biol. 1982;157:105-32.

Landre V, Pion E, Narayan V, Xirodimas DP, Ball KL. DNA-binding regulates site-specific ubiquitination of IRF-1. Biochem J. 2013;449:707-17.

Laukkanen ML, Alfthan K, Keinanen K. Functional immunoliposomes harboring a biosynthetically lipid-tagged single-chain antibody. Biochemistry. 1994;33:11664-70.

Lee JS, Seo TW, Yi JH, Shin KS, Yoo SJ. CHIP has a protective role against oxidative stress-induced cell death through specific regulation of endonuclease G. Cell Death Dis. 2013;4:e666.

Lees MJ, Peet DJ, Whitelaw ML. Defining the role for XAP2 in stabilization of the dioxin receptor. J Biol Chem. 2003;278:35878-88.

Li F, Xie P, Fan Y, Zhang H, Zheng L, Gu D, et al. C terminus of Hsc70-interacting protein promotes smooth muscle cell proliferation and survival through ubiquitin-mediated degradation of FoxO1. J Biol Chem. 2009;284:20090-8.

Li SL, Liang SJ, Guo N, Wu AM, Fujita-Yamaguchi Y. Single-chain antibodies against human insulin-like growth factor I receptor: expression, purification, and effect on tumor growth. Cancer Immunol Immunother. 2000;49:243-52.

Lim MK, Kawamura T, Ohsawa Y, Ohtsubo M, Asakawa S, Takayanagi A, et al. Parkin interacts with LIM Kinase 1 and reduces its cofilin-phosphorylation activity via ubiquitination. Exp Cell Res. 2007;313:2858-74.

Lin LC, Putnam FW. Cold pepsin digestion: a novel method to produce the Fv fragment from human immunoglobulin M. Proc Natl Acad Sci U S A. 1978;75:2649-53.

Lin Y, Pagel JM, Axworthy D, Pantelias A, Hedin N, Press OW. A genetically engineered anti-CD45 single-chain antibody-streptavidin fusion protein for pretargeted radioimmunotherapy of hematologic malignancies. Cancer Res. 2006;66:3884-92.

Linsley PS. New look at an old costimulator. Nat Immunol. 2005;6:231-2.

Liu M, Wang X, Yin C, Zhang Z, Lin Q, Zhen Y, et al. Targeting TNF-alpha with a tetravalent mini-antibody TNF-TeAb. Biochem J. 2007;406:237-46.

Liu W, Onda M, Lee B, Kreitman RJ, Hassan R, Xiang L, et al. Recombinant immunotoxin engineered for low immunogenicity and antigenicity by identifying and silencing human B-cell epitopes. Proc Natl Acad Sci U S A. 2012;109:11782-7.

Lunder M, Bratkovic T, Urleb U, Kreft S, Strukelj B. Ultrasound in phage display: a new approach to nonspecific elution. BioTechniques. 2008;44:893-900.

Marks JD, Hoogenboom HR, Bonnert TP, McCafferty J, Griffiths AD, Winter G. By-passing immunization. Human antibodies from V-gene libraries displayed on phage. J Mol Biol. 1991;222:581-97.

Matsumura Y, Sakai J, Skach WR. Endoplasmic reticulum protein quality control is determined by cooperative interactions between Hsp/c70 protein and the CHIP E3 ligase. J Biol Chem. 2013;288:31069-79.

May C, Sapra P, Gerber HP. Advances in bispecific biotherapeutics for the treatment of cancer. Biochem Pharmacol. 2012;84:1105-12.

Mayer A, Chester KA, Flynn AA, Begent RH. Taking engineered anti-CEA antibodies to the clinic. J Immunol Methods. 1999;231:261-73.

Maynard J, Georgiou G. Antibody engineering. Annu Rev Biomed Eng. 2000;2:339-76.

McCafferty J, Griffiths AD, Winter G, Chiswell DJ. Phage antibodies: filamentous phage displaying antibody variable domains. Nature. 1990;348:552-4.

McDonough H, Charles PC, Hilliard EG, Qian SB, Min JN, Portbury A, et al. Stress-dependent Daxx-CHIP interaction suppresses the p53 apoptotic program. J Biol Chem. 2009;284:20649-59.

McDonough H, Patterson C. CHIP: a link between the chaperone and proteasome systems. Cell Stress Chaperones. 2003;8:303-8.

McWhirter JR, Kretz-Rommel A, Saven A, Maruyama T, Potter KN, Mockridge CI, et al. Antibodies selected from combinatorial libraries block a tumor antigen that plays a key role in immunomodulation. Proc Natl Acad Sci U S A. 2006;103:1041-6.

Meacham GC, Patterson C, Zhang W, Younger JM, Cyr DM. The Hsc70 co-chaperone CHIP targets immature CFTR for proteasomal degradation. Nat Cell Biol. 2001;3:100-5.

Mead DA, Kemper B. Chimeric single-stranded DNA phage-plasmid cloning vectors. Biotechnology. 1988;10:85-102.

Merk H, Stiege W, Tsumoto K, Kumagai I, Erdmann VA. Cell-free expression of two single-chain monoclonal antibodies against lysozyme: effect of domain arrangement on the expression. J Biochem. 1999;125:328-33.

Miller VM, Nelson RF, Gouvion CM, Williams A, Rodriguez-Lebron E, Harper SQ, et al. CHIP suppresses polyglutamine aggregation and toxicity in vitro and in vivo. J Neurosci. 2005;25:9152-61.

Moller A, Pion E, Narayan V, Ball KL. Intracellular activation of interferon regulatory factor-1 by nanobodies to the multifunctional (Mf1) domain. J Biol Chem. 2010;285:38348-61.

Monnier P, Vigouroux R, Tassew N. In Vivo Applications of Single Chain Fv (Variable Domain) (scFv) Fragments. Antibodies. 2013;2:193.

Motlagh HN, Wrabl JO, Li J, Hilser VJ. The ensemble nature of allostery. Nature. 2014;508:331-9.

Murphy K, Travers P, Walport M, Janeway C. Janeway's immunobiology. New York: Garland Science; 2012.

Nakamura T, Peng KW, Vongpunsawad S, Harvey M, Mizuguchi H, Hayakawa T, et al. Antibody-targeted cell fusion. Nat Biotechnol. 2004;22:331-6.

Narayan V, Landre V, Ning J, Hernychova L, Muller P, Verma C, et al. Protein:protein Interactions Modulate the Docking-Dependent E3-Ubiquitin Ligase Activity of CHIP. Mol Cell Proteomics. 2015.

Narayan V, Pion E, Landre V, Muller P, Ball KL. Docking-dependent Ubiquitination of the Interferon Regulatory Factor-1 Tumor Suppressor Protein by the Ubiquitin Ligase CHIP. J Biol Chem. 2011;286:607-19.

Neri D, Momo M, Prospero T, Winter G. High-affinity antigen binding by chelating recombinant antibodies (CRAbs). J Mol Biol. 1995;246:367-73.

Newman AJ, Selkoe D, Dettmer U. A new method for quantitative immunoblotting of endogenous alpha-synuclein. PLoS One. 2013;8:e81314.

Nie L, Wu H, Sun XH. Ubiquitination and degradation of Tal1/SCL are induced by notch signaling and depend on Skp2 and CHIP. J Biol Chem. 2008;283:684-92.

Niesen J, Stein C, Brehm H, Hehmann-Titt G, Fendel R, Melmer G, et al. Novel EGFR-specific immunotoxins based on panitumumab and cetuximab show in vitro and ex vivo activity against different tumor entities. J Cancer Res Clin Oncol. 2015.

Nikolay R, Wiederkehr T, Rist W, Kramer G, Mayer MP, Bukau B. Dimerization of the Human E3 Ligase CHIP via a Coiled-coil Domain Is Essential for Its Activity. J Biol Chem. 2004;279:2673-8.

Nisonoff A, Wissler FC, Lipman LN, Woernley DL. Separation of univalent fragments from the bivalent rabbit antibody molecule by reduction of disulfide bonds. Arch Biochem Biophys. 1960;89:230-44.

O'Connell D, Becerril B, Roy-Burman A, Daws M, Marks JD. Phage versus phagemid libraries for generation of human monoclonal antibodies. J Mol Biol. 2002;321:49-56.

Oddo S, Caccamo A, Tseng B, Cheng D, Vasilevko V, Cribbs DH, et al. Blocking Abeta42 accumulation delays the onset and progression of tau pathology via the C terminus of heat shock protein70-interacting protein: a mechanistic link between Abeta and tau pathology. J Neurosci. 2008;28:12163-75.

Oldenburg KR, Loganathan D, Goldstein IJ, Schultz PG, Gallop MA. Peptide ligands for a sugar-binding protein isolated from a random peptide library. Proc Natl Acad Sci U S A. 1992;89:5393-7.

Pack P, Pluckthun A. Miniantibodies: use of amphipathic helices to produce functional, flexibly linked dimeric FV fragments with high avidity in Escherichia coli. Biochemistry. 1992;31:1579-84.

Parashar V, Jeffrey PD, Neiditch MB. Conformational change-induced repeat domain expansion regulates Rap phosphatase quorum-sensing signal receptors. PLoS Biol. 2013;11:e1001512.

Parmley SF, Smith GP. Antibody-selectable filamentous fd phage vectors: affinity purification of target genes. Gene. 1988;73:305-18.

Parsons JL, Tait PS, Finch D, Dianova, II, Allinson SL, Dianov GL. CHIP-mediated degradation and DNA damage-dependent stabilization regulate base excision repair proteins. Mol Cell. 2008;29:477-87.

Passmore LA, Barford D. Getting into position: the catalytic mechanisms of protein ubiquitylation. Biochem J. 2004;379:513-25.

Patani N, Jiang W, Newbold R, Mokbel K. Prognostic implications of carboxyl-terminus of Hsc70 interacting protein and lysyl-oxidase expression in human breast cancer. J Carcinog. 2010;9:9.

Paul I, Ahmed SF, Bhowmik A, Deb S, Ghosh MK. The ubiquitin ligase CHIP regulates c-Myc stability and transcriptional activity. Oncogene. 2013;32:1284-95.

Peng HM, Morishima Y, Jenkins GJ, Dunbar AY, Lau M, Patterson C, et al. Ubiquitylation of neuronal nitric-oxide synthase by CHIP, a chaperone-dependent E3 ligase. J Biol Chem. 2004;279:52970-7.

Petrucelli L, Dickson D, Kehoe K, Taylor J, Snyder H, Grover A, et al. CHIP and Hsp70 regulate tau ubiquitination, degradation and aggregation. Hum Mol Genet. 2004;13:703-14.

Polymeropoulos MH, Higgins JJ, Golbe LI, Johnson WG, Ide SE, Di Iorio G, et al. Mapping of a gene for Parkinson's disease to chromosome 4q21-q23. Science. 1996;274:1197-9.

Porter RR. The hydrolysis of rabbit y-globulin and antibodies with crystalline papain. Biochem J. 1959;73:119-26.

Prassler J, Thiel S, Pracht C, Polzer A, Peters S, Bauer M, et al. HuCAL PLATINUM, a synthetic Fab library optimized for sequence diversity and superior performance in mammalian expression systems. J Mol Biol. 2011;413:261-78.

Pratt WB, Gestwicki JE, Osawa Y, Lieberman AP. Targeting Hsp90/Hsp70-based protein quality control for treatment of adult onset neurodegenerative diseases. Annu Rev Pharmacol Toxicol. 2015;55:353-71.

Ramaekers CH, Wouters BG. Regulatory functions of ubiquitin in diverse DNA damage responses. Curr Mol Med. 2011;11:152-69.

Ramanathan HN, Ye Y. Cellular strategies for making monoubiquitin signals. Crit Rev Biochem Mol Biol. 2012;47:17-28.

Rao SN, Sharma J, Maity R, Jana NR. Co-chaperone CHIP stabilizes aggregate-prone malin, a ubiquitin ligase mutated in Lafora disease. J Biol Chem. 2010;285:1404-13.

Rauchenberger R, Borges E, Thomassen-Wolf E, Rom E, Adar R, Yaniv Y, et al. Human combinatorial Fab library yielding specific and functional antibodies against the human fibroblast growth factor receptor 3. J Biol Chem. 2003;278:38194-205.

Reth M, Imanishi-Kari T, Rajewsky K. Analysis of the repertoire of anti-(4-hydroxy-3-nitrophenyl)acetyl (NP) antibodies in C 57 BL/6 mice by cell fusion. II. Characterization of idiotopes by monoclonal anti-idiotope antibodies. Eur J Immunol. 1979;9:1004-13.

Rheinnecker M, Hardt C, Ilag LL, Kufer P, Gruber R, Hoess A, et al. Multivalent antibody fragments with high functional affinity for a tumor-associated carbohydrate antigen. J Immunol. 1996;157:2989-97.

Robert R, Wark KL. Engineered antibody approaches for Alzheimer's disease immunotherapy. Arch Biochem Biophys. 2012;526:132-8.

Rossant CJ, Carroll D, Huang L, Elvin J, Neal F, Walker E, et al. Phage display and hybridoma generation of antibodies to human CXCR2 yields antibodies with distinct mechanisms and epitopes. MAbs. 2014;6:1425-38.

Rosser MF, Washburn E, Muchowski PJ, Patterson C, Cyr DM. Chaperone functions of the E3 ubiquitin ligase CHIP. J Biol Chem. 2007;282:22267-77.

Rothe C, Urlinger S, Lohning C, Prassler J, Stark Y, Jager U, et al. The human combinatorial antibody library HuCAL GOLD combines diversification of all six CDRs according to the natural immune system with a novel display method for efficient selection of high-affinity antibodies. J Mol Biol. 2008;376:1182-200.

Ruckova E, Muller P, Nenutil R, Vojtesek B. Alterations of the Hsp70/Hsp90 chaperone and the HOP/CHIP co-chaperone system in cancer. Cell Mol Biol Lett. 2012;17:446-58.

Ryan DA, Mastrangelo MA, Narrow WC, Sullivan MA, Federoff HJ, Bowers WJ. Abeta-directed single-chain antibody delivery via a serotype-1 AAV vector improves learning behavior and pathology in Alzheimer's disease mice. Mol Ther. 2010;18:1471-81.

Sahara N, Murayama M, Mizoroki T, Urushitani M, Imai Y, Takahashi R, et al. In vivo evidence of CHIP up-regulation attenuating tau aggregation. J Neurochem. 2005;94:1254-63.

Scaglione KM, Zavodszky E, Todi SV, Patury S, Xu P, Rodriguez-Lebron E, et al. Ube2w and ataxin-3 coordinately regulate the ubiquitin ligase CHIP. Mol Cell. 2011;43:599-612.

Schmukle AC, Walczak H. No one can whistle a symphony alone - how different ubiquitin linkages cooperate to orchestrate NF-kappaB activity. J Cell Sci. 2012;125:549-59.

Schofield DJ, Pope AR, Clementel V, Buckell J, Chapple S, Clarke KF, et al. Application of phage display to high throughput antibody generation and characterization. Genome Biol. 2007;8:R254.

Schultz J, Lin Y, Sanderson J, Zuo Y, Stone D, Mallett R, et al. A tetravalent single-chain antibody-streptavidin fusion protein for pretargeted lymphoma therapy. Cancer Res. 2000;60:6663-9.

Schulz R, Marchenko ND, Holembowski L, Fingerle-Rowson G, Pesic M, Zender L, et al. Inhibiting the HSP90 chaperone destabilizes macrophage migration inhibitory factor and thereby inhibits breast tumor progression. J Exp Med. 2012;209:275-89.

Sen J, Beychok S. Proteolytic dissection of a hapten binding site. Proteins. 1986;1:256-62.

Sha Y, Pandit L, Zeng S, Eissa NT. A critical role for CHIP in the aggresome pathway. Mol Cell Biol. 2009;29:116-28.

Shabek N, Herman-Bachinsky Y, Buchsbaum S, Lewinson O, Haj-Yahya M, Hejjaoui M, et al. The size of the proteasomal substrate determines whether its degradation will be mediated by mono- or polyubiquitylation. Mol Cell. 2012;48:87-97.

Shang Y, Zhao X, Xu X, Xin H, Li X, Zhai Y, et al. CHIP functions an E3 ubiquitin ligase of Runx1. Biochem Biophys Res Commun. 2009;386:242-6.

Sharma SK, Pedley RB, Bhatia J, Boxer GM, El-Emir E, Qureshi U, et al. Sustained tumor regression of human colorectal cancer xenografts using a multifunctional mannosylated fusion protein in antibody-directed enzyme prodrug therapy. Clin Cancer Res. 2005;11:814-25.

Sharon J, Givol D. Preparation of Fv fragment from the mouse myeloma XRPC-25 immunoglobulin possessing anti-dinitrophenyl activity. Biochemistry. 1976;15:1591-4.

Sheridan C. Amgen's bispecific antibody puffs across finish line. Nat Biotechnol. 2015;33:219-21.

Shimamoto S, Kubota Y, Yamaguchi F, Tokumitsu H, Kobayashi R. Ca2+/S100 proteins act as upstream regulators of the chaperone-associated ubiquitin ligase CHIP (C terminus of Hsc70-interacting protein). J Biol Chem. 2013;288:7158-68.

Shimura H, Schwartz D, Gygi SP, Kosik KS. CHIP-Hsc70 complex ubiquitinates phosphorylated tau and enhances cell survival. J Biol Chem. 2004;279:4869-76.

Shin Y, Klucken J, Patterson C, Hyman BT, McLean PJ. The Co-chaperone Carboxyl Terminus of Hsp70-interacting Protein (CHIP) Mediates -Synuclein Degradation Decisions between Proteasomal and Lysosomal Pathways. J Biol Chem. 2005;280:23727-34.

Sievers F, Wilm A, Dineen D, Gibson TJ, Karplus K, Li W, et al. Fast, scalable generation of high-quality protein multiple sequence alignments using Clustal Omega. Mol Syst Biol. 2011;7:539.

Singh AK, Pati U. CHIP stabilizes amyloid precursor protein via proteasomal degradation and p53-mediated trans-repression of beta-secretase. Aging Cell. 2015;14:595-604.

Skerra A, Pluckthun A. Assembly of a functional immunoglobulin Fv fragment in Escherichia coli. Science. 1988;240:1038-41.

Smith GP. Filamentous fusion phage: novel expression vectors that display cloned antigens on the virion surface. Science. 1985;228:1315-7.

Smith GP, Petrenko VA. Phage Display. Chem Rev. 1997;97:391-410.

Soss SE, Rose KL, Hill S, Jouan S, Chazin WJ. Biochemical and Proteomic Analysis of Ubiquitination of Hsc70 and Hsp70 by the E3 Ligase CHIP. PLoS One. 2015;10:e0128240.

Soss SE, Yue Y, Dhe-Paganon S, Chazin WJ. E2 conjugating enzyme selectivity and requirements for function of the E3 ubiquitin ligase CHIP. J Biol Chem. 2011;286:21277-86.

Spillantini MG, Schmidt ML, Lee VM, Trojanowski JQ, Jakes R, Goedert M. Alpha-synuclein in Lewy bodies. Nature. 1997;388:839-40.

Stankowski JN, Zeiger SL, Cohen EL, DeFranco DB, Cai J, McLaughlin B. C-terminus of heat shock cognate 70 interacting protein increases following stroke and impairs survival against acute oxidative stress. Antioxid Redox Signal. 2011;14:1787-801.

Su CH, Lan KH, Li CP, Chao Y, Lin HC, Lee SD, et al. Phosphorylation accelerates geldanamycin-induced Akt degradation. Arch Biochem Biophys. 2013;536:6-11.

Sun C, Li HL, Chen HR, Shi ML, Liu QH, Pan ZQ, et al. Decreased expression of CHIP leads to increased angiogenesis via VEGF-VEGFR2 pathway and poor prognosis in human renal cell carcinoma. Sci Rep. 2015;5:9774.

Teeling JL, French RR, Cragg MS, van den Brakel J, Pluyter M, Huang H, et al. Characterization of new human CD20 monoclonal antibodies with potent cytolytic activity against non-Hodgkin lymphomas. Blood. 2004;104:1793-800.

Teng Y, Rezvani K, De Biasi M. UBXN2A regulates nicotinic receptor degradation by modulating the E3 ligase activity of CHIP. Biochem Pharmacol. 2015.

Tetzlaff JE, Putcha P, Outeiro TF, Ivanov A, Berezovska O, Hyman BT, et al. CHIP Targets Toxic -Synuclein Oligomers for Degradation. J Biol Chem. 2008;283:17962-8.

Thammasit P, Sangboonruang S, Suwanpairoj S, Khamaikawin W, Intasai N, Kasinrerk W, et al. Intracellular Acidosis Promotes Mitochondrial Apoptosis Pathway: Role of EMMPRIN Down-regulation via Specific Single-chain Fv Intrabody. J Cancer. 2015;6:276-86.

Tian H, Davidowitz E, Lopez P, He P, Schulz P, Moe J, et al. Isolation and characterization of antibody fragments selective for toxic oligomeric tau. Neurobiol Aging. 2015;36:1342-55.

Tripathi V, Ali A, Bhat R, Pati U. CHIP chaperones wild type p53 tumor suppressor protein. J Biol Chem. 2007;282:28441-54.

Urushitani M, Kurisu J, Tateno M, Hatakeyama S, Nakayama K, Kato S, et al. CHIP promotes proteasomal degradation of familial ALS-linked mutant SOD1 by ubiquitinating Hsp/Hsc70. J Neurochem. 2004;90:231-44.

Vaughan TJ, Williams AJ, Pritchard K, Osbourn JK, Pope AR, Earnshaw JC, et al. Human antibodies with sub-nanomolar affinities isolated from a large non-immunized phage display library. Nat Biotechnol. 1996;14:309-14.

Vieira J, Messing J. Production of single-stranded plasmid DNA. Methods Enzymol. 1987;153:3-11.

Vigor KL, Kyrtatos PG, Minogue S, Al-Jamal KT, Kogelberg H, Tolner B, et al. Nanoparticles functionalized with recombinant single chain Fv antibody fragments (scFv) for the magnetic resonance imaging of cancer cells. Biomaterials. 2010;31:1307-15.

Visintin M, Melchionna T, Cannistraci I, Cattaneo A. In vivo selection of intrabodies specifically targeting protein-protein interactions: a general platform for an "undruggable" class of disease targets. J Biotechnol. 2008;135:1-15.

Wang S, Wu X, Zhang J, Chen Y, Xu J, Xia X, et al. CHIP functions as a novel suppressor of tumour angiogenesis with prognostic significance in human gastric cancer. Gut. 2013;62:496-508.

Wang T, Yang J, Xu J, Li J, Cao Z, Zhou L, et al. CHIP is a novel tumor suppressor in pancreatic cancer and inhibits tumor growth through targeting EGFR. Oncotarget. 2014a;5:1969-86.

Wang WW, Das D, McQuarrie SA, Suresh MR. Design of a bifunctional fusion protein for ovarian cancer drug delivery: single-chain anti-CA125 core-streptavidin fusion protein. Eur J Pharm Biopharm. 2007;65:398-405.

Wang Y, Dossey AM, Froude JW, 2nd, Lubitz S, Tzur D, Semenchenko V, et al. PSA fluoroimmunoassays using anti-PSA ScFv and quantum-dot conjugates. Nanomedicine (Lond). 2008;3:475-83.

Wang Y, Ren F, Wang Y, Feng Y, Wang D, Jia B, et al. CHIP/Stub1 functions as a tumor suppressor and represses NF-kappaB-mediated signaling in colorectal cancer. Carcinogenesis. 2014b;35:983-91.

Wang YJ, Gao CY, Yang M, Liu XH, Sun Y, Pollard A, et al. Intramuscular delivery of a single chain antibody gene prevents brain Abeta deposition and cognitive impairment in a mouse model of Alzheimer's disease. Brain Behav Immun. 2010;24:1281-93.

Ward RL, Clark MA, Lees J, Hawkins NJ. Retrieval of human antibodies from phage-display libraries using enzymatic cleavage. J Immunol Methods. 1996;189:73-82.

Weisser NE, Almquist KC, Hall JC. A rAb screening method for improving the probability of identifying peptide mimotopes of carbohydrate antigens. Vaccine. 2007;25:4611-22.

Wen J, Luo KJ, Hu Y, Yang H, Fu JH. Metastatic lymph node CHIP expression is a potential prognostic marker for resected esophageal squamous cell carcinoma patients. Ann Surg Oncol. 2013;20:1668-75.

Whitlow M, Bell BA, Feng SL, Filpula D, Hardman KD, Hubert SL, et al. An improved linker for single-chain Fv with reduced aggregation and enhanced proteolytic stability. Protein Eng. 1993;6:989-95.

Wickliffe KE, Williamson A, Meyer HJ, Kelly A, Rape M. K11-linked ubiquitin chains as novel regulators of cell division. Trends Cell Biol. 2011;21:656-63.

Winter G, Griffiths AD, Hawkins RE, Hoogenboom HR. Making antibodies by phage display technology. Annu Rev Immunol. 1994;12:433-55.

Woo CH, Le NT, Shishido T, Chang E, Lee H, Heo KS, et al. Novel role of C terminus of Hsc70-interacting protein (CHIP) ubiquitin ligase on inhibiting cardiac apoptosis and dysfunction via regulating ERK5-mediated degradation of inducible cAMP early repressor. FASEB J. 2010;24:4917-28.

Wu J, Fu J, Zhang M, Liu D. Blinatumomab: a bispecific T cell engager (BiTE) antibody against CD19/CD3 for refractory acute lymphoid leukemia. J Hematol Oncol. 2015;8:104.

Xiao L, Chen D, Hu P, Wu J, Liu W, Zhao Y, et al. The c-Abl-MST1 signaling pathway mediates oxidative stress-induced neuronal cell death. J Neurosci. 2011;31:9611-9.

Xu P, Duong DM, Seyfried NT, Cheng D, Xie Y, Robert J, et al. Quantitative proteomics reveals the function of unconventional ubiquitin chains in proteasomal degradation. Cell. 2009;137:133-45.

Xu W, Liu L, Brown NJ, Christian S, Hornby D. Quantum dot-conjugated anti-GRP78 scFv inhibits cancer growth in mice. Molecules. 2012;17:796-808.

Xu Z, Kohli E, Devlin KI, Bold M, Nix JC, Misra S. Interactions between the quality control ubiquitin ligase CHIP and ubiquitin conjugating enzymes. BMC Struct Biol. 2008;8:26.

Yang J, Pattanayak A, Song M, Kou J, Taguchi H, Paul S, et al. Muscle-directed anti-Abeta single-chain antibody delivery via AAV1 reduces cerebral Abeta load in an Alzheimer's disease mouse model. J Mol Neurosci. 2013;49:277-88.

Zdobnova TA, Stremovskiy OA, Lebedenko EN, Deyev SM. Self-assembling complexes of quantum dots and scFv antibodies for cancer cell targeting and imaging. PLoS One. 2012;7:e48248.

Zhang M, Windheim M, Roe SM, Peggie M, Cohen P, Prodromou C, et al. Chaperoned Ubiquitylation-Crystal Structures of the Chip U Box E3 Ubiquitin Ligase and a Chip-Ubc13-Uev1A Complex. MolCell. 2005;20:525-null.

Zhang YJ, Xu YF, Liu XH, Li D, Yin J, Liu YH, et al. Carboxyl terminus of heat-shock cognate 70-interacting protein degrades tau regardless its phosphorylation status without affecting the spatial memory of the rats. J Neural Transm. 2008;115:483-91.

Zhao M, Wang SW, Wang YJ, Zhang R, Li YN, Su YJ, et al. Pan-amyloid oligomer specific scFv antibody attenuates memory deficits and brain amyloid burden in mice with Alzheimer's disease. Curr Alzheimer Res. 2014;11:69-78.